



Enhancement of Compound Extreme Event Forecasting by Integrating Machine Learning and Physical-based Approaches

File Number : PDF/2023/003673

Submitted By : Mr. Gaurav Tripathi
[SERB Qualified Unique Identification Document: SQUID-1992-GT-4682]
Submission Date : 10-Aug-2023

PROPOSAL DETAILS

(PDF/2023/003673)

Principal Investigator	Mentor & Host Institution
Mr. Gaurav Tripathi richytripathi@gmail.com Assistant Professor(Department of Civil Engineering) Contact No : +918521617151 Date of Birth : 15-Jul-1992 Name of Father/Spouse : Dileep Kumar Tripathi	Manabendra Saharia msaharia@live.com Assistant Professor(Civil Engineering) Indian Institute of Technology Delhi Hauz khas, new delhi, New delhi, Delhi-110016 Contact No. : +19405955219 Registrar Email : registrar@admin.iitd.ac.in No. of PHD Scholars : 09 No. Post-Doctoral Fellow : 00

Details of Post Doctorate

Ph.D. (Geoinformatics) [Not yet Awarded. Thesis Submitted On : 14-Sep-2022]

Flood Inundation characterization through Remote Sensing for flood risk mapping and monitoring in parts of North Bihar, India

Research Supervisor/Guide & Institution :

Prof A C Pandey
Dr B R Parida
Central University of Jharkhand

Brief details of Thesis work :

This study was intended to examine and analyse flooding events based on the primary and secondary data collected with objectives such as (i) to characterize flood inundation through remote sensing for flood risk mapping, (ii) to investigate temporal flood inundation through a comparative study of optical and microwave remote sensing data, (iii) to characterize floodwater depth and sediment load using microwave remote sensing data, (iv) to analyse flood frequency based on rainfall variability with different return periods, and (v) to delineate the flood zoning over parts of North Bihar, and to delineate flood Hazard, Vulnerability and Risk using geospatial data.

Technical Details :

Research Area : Earth & Atmospheric Sciences (Earth & Atmospheric Sciences)

Project Summary :

The changing patterns of extreme hydrological and meteorological phenomena, such as floods and droughts, present significant challenges to society and science. Accurately predicting and modelling these phenomena is crucial for effective disaster management, designing climate change adaptation strategies, and sustainable water resources management. The coupled effects of climate change with concurrent rapid landscape changes, such as forest disturbance, increase uncertainty in hydrological predictions. Climate change has brought heavier rainfall incidents and lasted longer than in previous seasons. Millions of people across the nation (India) have been affected by floods caused by monsoon rains. Ganga-Brahmaputra-Meghna Basin (GBM) is considered a study area which is the joint third largest river system in the world (tied with the Río Orinoco, Venezuela) in terms of its mean annual discharge after the Amazon and Congo, also known as the Jamuna in Bangladesh. According to the World Bank report, the Lower Ganges subbasin is severely affected due to being a densely populated region. However, the Brahmaputra River basin is comparatively prone to severe flooding due to high discharge rates caused by annual precipitation (rain and seasonal snow) and snowmelt from its highly glaciated upper basin encompassing the Eastern Himalaya and parts of the Southern Tibetan Plateau. The river and its tributaries provide critical societal, ecological, cultural, and economic services to more than 60 million people in Bangladesh, North-eastern India, Bhutan, and Tibet, China. Although the GBM provides these important benefits, it is also a frequent cause of human suffering from flooding in Northeast India (primarily in Assam), Nepal, and Bangladesh. Long-duration (more than 10-days) floods that cause widespread disruptions are most common during the monsoon season in GBM. The proposed research project explores the potential and limitations of using Machine Learning (ML) models coupled with physical-based approaches using satellite (optical and microwave remote sensing satellite data) and data from automated hydro-meteorological sensor networks. Flood and drought modelling will be performed on different spatial and temporal scales, using the network of experimental catchments in montane catchments, from event-scale to long-term perspective based on distributed hydrological models such as WRF-Hydro, WATFLOOD, Distributed Basin Simulator (DBSIM) model, etc. Simulations will focus on extreme hydrological phenomena in montane basins, experiencing effects of climate warming, forest disturbance, or land use change, being a sensible indicator of hydrological change. Different ML algorithms will be employed, such as SVM, ANN, CNN, LSTM, or DL, along with the physical-based approaches such as XAJ-DCH, TOPKAPI, Sacramento model, MCQRNN, etc., to improve flood forecasting scenarios in the basin.

Objectives :

This research aims to integrate and expand our capabilities to forecast compound extreme weather events, like floods and droughts, by combining machine learning algorithms with traditional physical-based models and exploiting new datasets and methodological advances. The comprehensive objectives of this research are: 1. Development and Evaluation of an Integrated Framework 2. Exploration and Comparison of Machine Learning Models: The research seeks to understand and compare the performance of various machine learning models, including Hybrid models like SVR-RSM, in extreme weather event forecasting. The focus will be on their ability to accurately model trans-critical flows at catchment and sub-catchment levels and predict drought indices. 3. Understanding Compound Extreme Events and their Impact: A deep-dive analysis will be performed to understand compound extreme events, occurrence patterns, related risk factors, and potential impacts. This will involve statistical characterization of discharge, catchment rainfall, and other meteorological parameters and exploring their connection to the occurrence of floods and droughts. 4. Validation of the Model and Performance Evaluation 5. Development of a Decision Support System 6. Open-Source Contribution

Keywords :

Deep Neural Network, Compound Extreme Event, Flood Forecasting, Hybrid Modelling, Machine Learning, Physically based Model

Expected Output and Outcome of the proposal :

The outcome of this research project will be a pioneering hybrid model that marries machine learning (ML) techniques, such as Artificial Neural Networks (ANNs), Long Short-Term Memory (LSTM), Support Vector Machines (SVM), and Multilayer Perceptron (MLP) with physical models such as Xin'anjiang, TOPKAPI, and Sacramento. This model's primary function will be to predict compound extreme events, and its flexibility will allow it to be adapted to other regions with similar hydrological concerns. By merging ML methodologies and physical models, we aim to substantially improve the flood forecasting's accuracy and prediction lead time. This advanced flood forecasting model will empower disaster management authorities to take preventive action, reducing the impact of floods and safeguarding at-risk communities. Here are the key anticipated results from this project: 1. Rainfall Frequency Graph 2. Integrated Flood Forecasting System 3. High-Resolution Basin DEM 4. Temporal Floodwater Maps: We will use Deep Learning (DL) algorithms to create past, present, and future floodwater maps. 5. Temporal Soil Moisture Data 6. Drought Scenario for the GBM Basin 7. Hybrid Approach-based Flood Forecast 8. Integrated Flood Forecasting System 9. Decision Support System 10. Research Publications With these outputs and outcomes, we aim to enhance the accuracy and efficiency of predicting extreme weather events and also offer a valuable resource for disaster management and mitigation.

Reference Details :

S.No	Reference Details
1	Prof Arvind Chandra Pandey, Dean School of Natural Resource Management, Professor at the Department of Geoinformatics, Central University of Jharkhand, Ranchi [+91955492100] arvind.pandey@cuj.ac.in
2	Dr Bikash Ranjan Parida, Assistant Professor, Department of Geoinformatics, Central University of Jharkhand, Ranchi [+91955492100] bikash.parida@cuj.ac.in

Work Methodology and Research Plan

The work methodology aligns with the primary objectives to develop a hybrid forecasting model that integrates Machine Learning (ML) algorithms with physical-based approaches for predicting compound extreme events, such as floods and droughts, in the **Ganga-Brahmaputra-Meghna Basin** (GBM).

XAJ-DCH model (Xin'anjiang Digital CHannel model) will be used here to **simulate channel flow routing** based on river cross-section data, and **cross-section data can be generated using HEC-RAS/ VIC model**. The diffusion wave method is characterized by its comparatively higher computational efficiency when compared to other complex hydraulic routing methods. Given the diverse topography of the study region, this method becomes a suitable choice for areas with gently sloping terrain due to its inclusion of the water surface slope term in the equation, which effectively accounts for backwater effects. **Due to the uneven distribution of gauge stations in the GBM basin, flood prediction in these regions a physically based distributed hydrological model 'TOPKAPI' will be used.** This model is built upon investigating rainfall-runoff relationships and encompasses multiple modules, including evapotranspiration, snowmelt, soil flow, surface runoff, river runoff, and groundwater. ML successfully assimilates recent hydro-meteorological observations to improve near-term daily forecasts. In some cases, machine learning can ingest near-real-time data without the need for backwards methods like data assimilation since any data stream can be fed directly into the model as input as long as some samples from each input data stream are available during training. So, there are several ML models (ANNs, LSTM, neuro-fuzzy, adaptive neuro-fuzzy inference systems (ANFIS), support vector machines (SVM), wavelet neural networks (WNN), and multilayer perceptron (MLP)) that can be used and compared.

Hybrid forecasts leverage the strengths of both physical models, such as NWPs or climate model predictions, which excel at predicting and explaining large-scale phenomena, and data-driven models, which also efficiently estimate event characteristics from observed data and effectively account for bias or anomalies in data.

Workflow of the research plan is as follows:

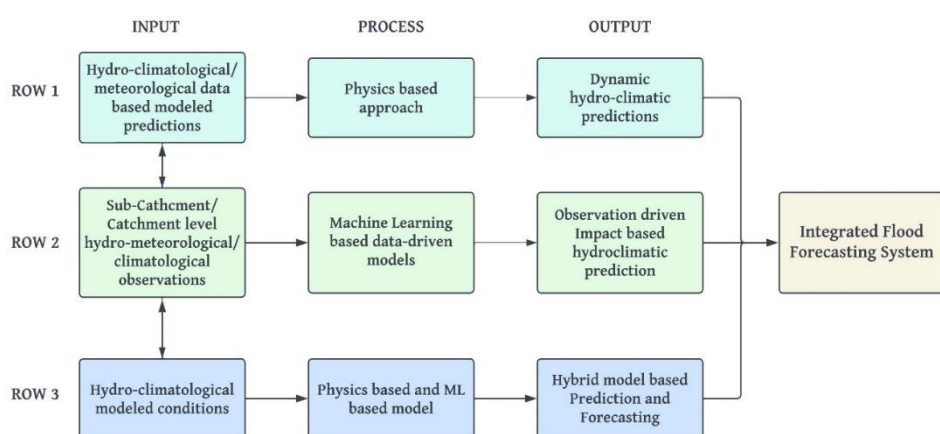


Figure 1. Showing hybrid hydroclimate forecasting and prediction. "Hydroclimate" refers to a range of variables defined in the text, including streamflow. Row 1 indicates the traditional dynamical hydroclimate predictions, Row 2 is data-driven, and Row 3 represents hybrid predictions, combining dynamical and data-driven approaches.

The Project's outcomes will contribute to better climate change adaptation strategies in the GBM basin. The ability to predict and understand extreme hydrological phenomena under changing

climate conditions will enable policymakers to develop more effective sustainable water resources management and disaster preparedness strategies. The research will serve SDG 13, "Climate Action," by developing adaptive capabilities to extreme events. By enhancing flood forecasting and reducing overall risk in the GBM basin, the project will build resilience and achieve SDG targets related to climate change and disaster risk reduction.

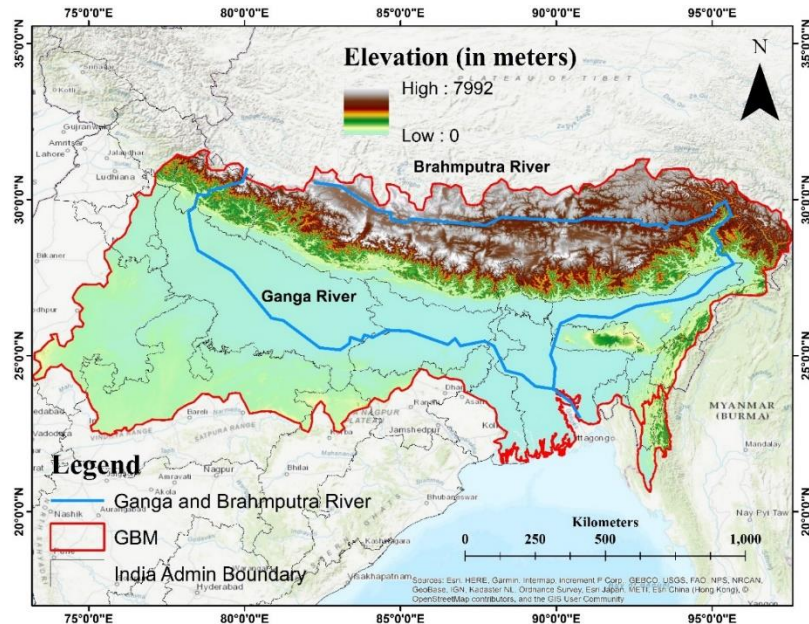


Figure 2. Showing the geographical spread of the Ganga, Brahmaputra, and Meghna Basin

Research Questions are:

- How can the integration of machine learning (ML) algorithms, such as SVM, ANN, CNN, LSTM, and DL, with physics-based models like XAJ-DCH and TOPKAPI, improve the accuracy of flood prediction and real-time forecasting in the GBM?
- What are the key hydro-climatological parameters (e.g., rainfall, temperature, soil characteristics, land use) that significantly influence flood occurrence and how can these parameters be effectively incorporated into the hybrid modelling approach to enhance flood prediction precision?
- How do El Niño and La Niña events, along with other climatic factors, interact with the complex weather patterns in the GBM Basin, and how can a hybrid modelling strategy effectively capture these interactions to predict compound extreme events, such as floods caused by monsoon rains?
- What are the spatial and temporal scales at which flood, and drought modelling should be performed in montane catchments within the GBM Basin to provide accurate predictions and insights into the effects of climate warming, forest disturbance, and land use change on hydrological processes?
- In what ways can the advanced flood forecasting system, developed through the hybrid modelling approach, contribute to improved water resource management and aid disaster managers in making informed decisions to minimize economic and social losses during extreme hydrological events in the GBM Basin and South Asian region?

Research Plan:

Year 1

Stage 1 (0-6 months): In this stage, the integration of collected observation data and hydro climatological modelled outputs have been proposed to get dynamic predictions. Refers to the Row 1 (Fig. 1)

It is proposed to the:

- Estimation of rainfall frequency based on CMIP5 GCMs, RCMs and statistically downscaled NEX-GDDP precipitation data.
- Generation of high-resolution DEM
- Creation of historical flood inundation database using deep learning models.
- Statistical characterization of discharge, catchment rainfall, and other meteorological parameters and its connection to the occurrence of flood as well as drought.
- Generation of high-resolution soil moisture data for the basin.

Stage 2 (7-12 months): Refers to the Row 2 (Fig. 1)

It is proposed to:

- Model trans critical flows: applied to catchments and sub catchments level.
- Analyse and predict drought indices using Hybrid models i.e., SVR-RSM.

Year 2

Stage 3 (13-18 months): Refers to the Row 3 (Fig. 1)

It is proposed to:

- Develop and apply physical based/ hybrid forecasting models ((semi-)automatic modelling processes) for impact-based flood forecasting.
- Improve flood forecasting accuracy by exploiting new datasets and the latest methodological advances in statistics, data science, and climate modelling.

Stage 4 (19-24 months):

- Develop an 'Integrated Flood Forecasting' system as a Decision Support System to minimize risk factor and support decision makers.
- Project report preparation and Journal Article publication.

References:

1. Zou, Y.; Rasch, P.; Wang, H. *Hybridizing Machine Learning and Physically-Based Earth System Models to Improve Prediction of Multivariate Extreme Events (AI Exploration of Wildland Fire Prediction)*; 2021; pp. AI4ESP--1155, 1769718.
2. Khalequzzaman, Md.; Masud, B.; Islam, Z.; Alam, S.; Mostafa Ali, Md. Future Floods in the Brahmaputra River Basin Based on Multi-Model Ensemble of CMIP6 Projections. In *Floods in the Ganga–Brahmaputra–Meghna Delta*; Islam, A., Shit, P.K., Datta, D.K., Islam, M.S., Roy, S., Ghosh, S., Das, B.C., Eds.; Springer Geography; Springer International Publishing: Cham, 2023; pp. 385–402 ISBN 978-3-031-21085-3.
3. Kong, X.; Li, Z.; Liu, Z. Flood Prediction in Ungauged Basins by Physical-Based TOPKAPI Model. *Adv. Meteorol.* **2019**, 2019, 1–16, doi:10.1155/2019/4795853.
4. Rao, M.P.; Cook, E.R.; Cook, B.I.; D'Arrigo, R.D.; Palmer, J.G.; Lall, U.; Woodhouse, C.A.; Buckley, B.M.; Uriarte, M.; Bishop, D.A.; et al. Seven Centuries of Reconstructed Brahmaputra River Discharge Demonstrate Underestimated High Discharge and Flood Hazard Frequency. *Nat. Commun.* **2020**, 11, 6017, doi:10.1038/s41467-020-19795-6.
5. Roushangar, K.; Ghasempour, R.; Kirca, V.S.O.; Demirel, M.C. Hybrid Point and Interval Prediction Approaches for Drought Modeling Using Ground-Based and Remote Sensing Data. *Hydrol. Res.* **2021**, 52, 1469–1489, doi:10.2166/nh.2021.028.
6. Slater, L.J.; Arnal, L.; Boucher, M.-A.; Chang, A.Y.-Y.; Moulds, S.; Murphy, C.; Nearing, G.; Shalev, G.; Shen, C.; Speight, L.; et al. Hybrid Forecasting: Blending Climate Predictions with AI Models. *Hydrol. Earth Syst. Sci.* **2023**, 27, 1865–1889, doi:10.5194/hess-27-1865-2023.
7. Zang, S.; Li, Z.; Zhang, K.; Yao, C.; Liu, Z.; Wang, J.; Huang, Y.; Wang, S. Improving the Flood Prediction Capability of the Xin'anjiang Model by Formulating a New Physics-Based Routing Framework and a Key Routing Parameter Estimation Method. *J. Hydrol.* **2021**, 603, 126867, doi:10.1016/j.jhydrol.2021.126867.
8. Priya, S.; Young, W.; Hopson, T.; Avasthi, A. Flood Risk Assessment and Forecasting for the Ganges-Brahmaputra-Meghna River Basins; Washington, DC, 2017.

BIO-DATA

- 1. Name and full correspondence address:** Gaurav Tripathi and Correspondence address: OBC Colony Flat no 397, 2nd Floor, Jagatpura, Jaipur, 302017
- 2. Email(s) and contact number(s):** richytripathi@gmail.com, gauravtripathi3135gt@gmail.com and 8521617151, 8840160324
- 3. Institution:** Pursuing PhD (Thesis Submitted) from Central University of Jharkhand and working as an Assistant Professor at Suresh Gyan Vihar University, Jaipur.
- 4. Date of Birth:** 15th July 1992
- 5. Gender (M/F/T):** Male
- 6. Category Gen/SC/ST/OBC:** GEN (EWS)
- 7. Whether differently abled (Yes/No):** No

8. Academic Qualification (Undergraduate Onwards):

Sl. No.	Degree	Passing	Subjects Undertaken	Institution/University	Marks/ CGPA
1	Ph.D.	2023	Geoinformatics	Central University of Jharkhand, Ranchi	9 CGPA (in course work exam)
2	PGD	2016	Geo-information Science & Earth Observation with specialization in 'Geo-informatics'	IIRS & Faculty of ITC, University of TWENTE	62%
3	M.Sc.	2015	Geoinformatics	Central University of Jharkhand, Ranchi	84%
4	B.C.A.	2013	Computer Application	R.S.M.T., MGKVP, Varanasi	74%

9. PhD thesis title, Guide's Name, Institute/Organization/University, Year of Award:

PhD Thesis title "Flood Inundation characterization through Remote Sensing for flood risk mapping and monitoring in parts of North Bihar, India"

Supervisor: Prof. Arvind Chandra Pandey

Co-Supervisor: Dr Bikash Ranjan Parida

Year of Award: Not awarded yet, waiting for the defense, it is likely to be held in August 2023

10. Work experience (in chronological order):

Sl. No.	Position held	Name of the Institute	From	To	Pay Scale
1	Assistant Professor	Suresh Gyan Vihar University, Jaipur	16/09/2023	Till date	AGP 6000/- Pay Level 10
2	Project Associate-1	Central University of Jharkhand, Ranchi	11/06/2018	08/11/2020	25,000/p.m.+HRA (DST JRF/SRF scale)
3	Trainee GIS Executive	RAMTech Software Solutions Pvt. Ltd.	16/07/2015	16/09/2015	10,500/p.m.
4	Trainee GIS	BSES Rajdhani Power Limited, Delhi	12/06/2015	15/06/2015	NIL

11. Professional Recognition/ Award/ Prize/ Certificate, Fellowship received by the applicant:

Sl. No.	Name of Award	Awarding Agency	Year
1	3 rd position in 3-Minute Thesis competition	AAFT University, Chhattisgarh	2023
2	3rd Prize winner in a Data Basin Survey	Conservation Biology Institute, Washington	2022

12. Publications (List of papers published in SCI Journals, in year wise descending order):

Sl. No.	Author	Title	Name of Journal	Volume	Page	Year
1	Upadhyay, R.K., Tripathi, G., Đurin, B., Šamanović, S., Cetl, V., Kishore, N., Sharma, M., Singh, S.K., Kanga, S., Wasim, M.	Groundwater Potential Zone Mapping in the Ghaggar River Basin, North-West India, Using Integrated Remote Sensing and GIS Techniques	Water	15	961	2023
2	Nigam Ritwik, Tripathi Gaurav, Priya Tannu, Luis Alvarinho J., Vaz Eric, Kumar Shashikant, Shakya Achala, Damásio Bruno, and Kotha Mahender	Did Covid-19 lockdown positively affected urban environment and UN-Sustainable Development Goals?	PLoS One	17	-	2022
3	Tripathi, Gaurav, Pandey Arvind Chandra, Parida, Bikash Ranjan	Flood Hazard and Risk Zonation in North Bihar Using Satellite-Derived Historical Flood Events and Socio-Economic Data	Sustainability	14	1472	2022
4	Parida Bikash Ranjan, Tripathi Gaurav, Pandey Arvind Chandra, and Kumar Amit	Estimating Floodwater depth using SAR-derived Flood inundation maps and Geomorphic model in Kosi River Basin (India)	Geocarto International	37	4336-4360	2021
5	Tripathi Gaurav, Pandey Arvind Chandra, Parida Bikash Ranjan, and Kumar Amit	Flood Inundation Mapping and Impact Assessment Using Multi-Temporal Optical and SAR Satellite Data: A Case Study of 2017 Flood in Darbhanga District, Bihar, India	Water Resource Management	34	1871 – 1892	2020

6	Tripathi Gaurav; Parida Bikash Ranjan, and Pandey Arvind Chandra	Spatio-Temporal Rainfall Variability and Flood Prognosis Analysis Using Satellite Data Over North Bihar during the August 2017 Flood Event	Hydrology	6	38	2019
---	--	--	-----------	---	----	------

13. Detail of patents:

Sl. No.	Patent Title	Name of Applicants	Patent Number	Award Date	Agency/ Country	Status
1	A virtual interfacing system to train farmers for smart farming and a method thereof	Achala Shakya, Ashish Kumar, Gaurav Tripathi, Satyasundara Mahapatra, Santosh Kumar	2022/10006	26-10-2022	South Africa	(Granted)
2	A digital wellbeing application-based system to reduce smartphone usage	Achala Shakya, Ashish Kumar, Gaurav Tripathi, Vikas Chaudhary, Santosh Kumar	202022105337	10-10-2022	Germany	(Granted)
3	A multi-purpose traffic safety device for long-distance drivers	Ashish Kumar, Sugandha, Amit Kumar, Monika, Achala Shakya, Garima Singh, Murari Kumar, Garima Singh, Gaurav Tripathi	20 2022 100 349	09/03/2022	Germany	(Granted)
4	A smart cutlery for preventing scalding during consumption of food	Ashish Kumar, Sugandha, Pankaj Agarwal, Shiraj Khurana, Shweta Sharad, Himanshu Dwivedi, Gaurav Tripathi	022/01061	13/03/2022	South Africa	(Granted)

14. Books/Reports/Chapters/General articles etc:

Sl. No.	Title	Author's Name	Publisher	Year
1	Monitoring Land Use and Land Cover Change Over Bhiwani District Using Google Earth Engine	Singh SK, Kanga S, Sajan B, Diwate SM, Tripathi G	Springer	2023
2	Landslide Susceptibility Mapping of Tehri Reservoir Region Using Geospatial Approach	Tripathi, G., Shakya, A., Upadhyay, R.K., Singh, S.K., Kanga, S., Pandey, S.K.	Springer	2023
3	GIS-Based Novel Ensemble MCDM-AHP Modeling for Flash Flood Susceptibility Mapping of Luni River Basin, Rajasthan	Kotecha MJ, Tripathi G, Singh SK, Kanga S, Meraj G, Sajan B, Rai PK	Springer	2023
4	Geospatial Modelling for Identification of Ground Water Potential Zones in Luni River Basin, Rajasthan	Kotecha MJ, Tripathi G, Singh SK, Kanga S, Sajan B, Meraj G, Mishra RK	Springer	2023
5	Flood Inundation and Floodwater Depth Mapping Using Synthetic Aperture Radar Data in the Gandak River Basin	Tripathi G, Phulwari BS, Parida BR, Pandey AC, Behera MD	CRC Press	2022

6	Comparative flood area analysis based on change detection and binarization methods using Sentinel-1 synthetic aperture radar data	Parida, B. R., Pandey, A. C., Kumar, S., & Tripathi, G Data Over North Bihar during the August 2017 Flood Event	Elsevier	2022
7	Role of Geo-Informatics in Natural Resource Management During Disasters: A Case Study of Gujarat Floods, 2017	Upadhyay, R. K., Pandey, S., & Tripathi, G	Wiley	2020
8	Development of a Smart Village Through Micro-Level Planning Using Geospatial Techniques—A Case Study of Jangal Aurahi Village of Gorakhpur District	Pandey, S., & Tripathi, G	Wiley	2020
9	Comparative Flood Inundation Mapping Utilizing Multi-Temporal Optical and SAR Satellite Data Over North Bihar Region: A Case Study of 2019 Flooding Event Over North Bihar	Tripathi Gaurav, Pandey Arvind Chandra, Parida Bikash Ranjan, and Shakya Achala	IGI	2020

15. Any other Information (maximum 500 words):

- Salient feature of PhD work:**

This study was intended to examine and analyse flooding events based on the primary and secondary data collected with objectives such as (i) to characterize flood inundation through remote sensing for flood risk mapping, (ii) to investigate temporal flood inundation through comparative study of optical and microwave remote sensing data, (iii) to characterize floodwater depth and sediment load using microwave remote sensing data, (iv) to analyse flood frequency based on rainfall variability with different return periods, and (v) to delineate the flood zoning over parts of North Bihar, and to delineate flood Hazard, Vulnerability and Risk using geospatial data.

- Serving as:**

Centre's 'Exam' Co-ordinator.

Centre's 'Training and Placement' Co-ordinator.

Serving as a 'Link Officer-1' for the Centre.

Centre's 'Implications of NEP in Course Curriculum' Co-ordinator.

Centre's 'Time-Table' Co-ordinator.

- Research Project (On-going/ Completed):**

Completed: SEED money project entitled "Ground Water Vulnerability Assessment using SINTAC and DRASTIC models in humid zone of

Rajasthan". Cost involved: 5.00 Lakhs. Duration: 6 months (January-June 2023).

On-going: Project proposal submitted for Extramural funding on project entitled "Non-stationary flood frequency analysis: a case study of Brahmaputra river basin, India". Cost involved: 5.00 Lakhs. Duration: 6 months (July-Dec 2023).

- **Dissertation under my guidance (Completed/ On-going):**

Mrs. Pranali Kathe (M. Tech Geoinformatics) worked on title "Groundwater Potential Zone mapping using AHP (Analytical Hierarchy Process) and MIF (multi influencing factor) techniques in Amravati district, Maharashtra". (Completed (Jan-June 2022), Co-Supervised)

Mr. Nadha Gowrish Narisetty (M.Sc. Geoinformatics) worked on title "Ground Water Vulnerability Assessment using different hydrological models in Udaipur, Rajasthan". (Completed (Jan-June 2022), Co-Supervised)

- **Edited Book (Published/ Accepted/ Submitted):**

Accepted an Edited book proposal in Springer Nature on topic 'Sustainability and Health Informatics: A Systems Approach to Address the Climate Action Induced Global Challenge'. Called for Chapters.

Editors: Gaurav Tripathi, Dr. Achala Shakya, Dr. Shruti Kanga, Dr LTS Guite, Dr. Suraj Kumar Singh

Accepted an Edited book proposal in Springer Nature on topic 'The Applicability of Big Data, AI, and Data Analytics in Climate Change Research to achieve Sustainable Development Goals'. Called for Chapters.

Editors: Gaurav Tripathi, Dr. Achala Shakya, Dr. Shruti Kanga, Dr P. K. Rai, Dr. Suraj Kumar Singh

- **Published Conference Proceedings:**

G. Tripathi, A. Chandra Pandey and B. Ranjan Parida, Spatio- Temporal Analysis of Turbidity in Ganga River in Patna, Bihar Using Sentinel-2 Satellite Data Linked with Covid-19 Pandemic, 2020 IEEE India Geoscience and Remote Sensing Symposium (InGARSS), 2020, pp. 29-32, doi: 10.1109/InGARSS48198.2020.9358965.

G. Tripathi, A. C. Pandey and B. Ranjan Parida, Flood Frequency Analysis Using ERA5-Land Based Precipitation for Kosi-Mahasetu Station in North Bihar, India, 2021 IEEE International India Geoscience and Remote Sensing Symposium (InGARSS), 2021, pp. 53-56, doi: 10.1109/InGARSS51564.2021.9792046.

Undertaking by the Fellow

I, Gaurav Tripathi, Son of Shri. Dileep Kumar Tripathi, resident of Village- Bahuara, Po.-Piparia, Dis.- Chandauli, Uttar Pradesh, Pin code: 232103 agree to undertake the following, If I am offered the SERBN-PDF

1. I shall abide by the rules and regulations of SERB during the entire tenure of the fellowship.
2. I shall also abide by the rules, discipline of the institution where I will be implementing my fellowship
3. I shall devote full time to research work during the tenure of the fellowship
4. I shall prepare the progress report at the end of each year and communicate the same to SERB through the mentor
5. I shall send two copies of the consolidated progress report at the end of the fellowship period.
6. I further state that I shall have no claim whatsoever for regular/permanent absorption on expiry of the fellowship.

Date: 09/08/2023

Signature





Article

Flood Hazard and Risk Zonation in North Bihar Using Satellite-Derived Historical Flood Events and Socio-Economic Data

Gaurav Tripathi , Arvind Chandra Pandey and Bikash Ranjan Parida *

Department of Geoinformatics, School of Natural Resource and Management, Central University of Jharkhand, Ranchi 835222, India; gaurav.tripathi@cuj.ac.in (G.T.); arvind.pandey@cuj.ac.in (A.C.P.)

* Correspondence: bikash.parida@cuj.ac.in

Abstract: North Bihar is one of the most flood-affected regions of India. Frequent flooding caused significant loss of life and severe economic damages. In this study, hydroclimatic conditions and historical flood events during the period of 2001 to 2020 were coupled over different basins in North Bihar. The main objective of this study is to assess the severity of floods by estimating flood hazards, vulnerability and risk in North Bihar. The uniqueness of this study is to assess flood risk at the village level as no such study was performed earlier. Other thematic data, namely, land-use and drainage networks, were also utilised with flood maps to validate the severity of the event. MOD09A1 satellite data (during 2001–2020) derived indices were used to derive inundation extents and flood frequency. Socio-economic vulnerability (SEV) was derived based on seven census parameters (i.e., population density, house-hold density, literacy rate, agricultural labour, and cultivator, total male, and female) and coupled with flood hazard to derive flood risk over the study region. The study exhibited that a total ~34% of the geographical area of North Bihar was inundated in the last 20 years and the maximum flood extent was seen in 2020. Flood risk map exhibited that ~7%, ~8%, ~13%, ~4%, and ~2% of the geographical area was mapped under Very High, High, Moderate, Low, and Very Low categories, respectively. The 2770 and 3535 number of villages was categorized under Very High and High flood risk zone which are located in north-central and central-western regions. These findings can be applied to distinguish and classify areas of various risk zones to assist in flood mitigation and management activities.



Citation: Tripathi, G.; Pandey, A.C.; Parida, B.R. Flood Hazard and Risk Zonation in North Bihar Using Satellite-Derived Historical Flood Events and Socio-Economic Data. *Sustainability* **2022**, *14*, 1472. <https://doi.org/10.3390/su14031472>

Academic Editors: Basu Bidroha, Laurence Gill, Francesco Pilla and Srikanta Sannigrahi

Received: 23 December 2021

Accepted: 25 January 2022

Published: 27 January 2022

Publisher's Note: MDPI stays neutral with regard to jurisdictional claims in published maps and institutional affiliations.



Copyright: © 2022 by the authors. Licensee MDPI, Basel, Switzerland. This article is an open access article distributed under the terms and conditions of the Creative Commons Attribution (CC BY) license (<https://creativecommons.org/licenses/by/4.0/>).

Keywords: North Bihar; flood frequency; flood characterization; hazard; vulnerability; risk

1. Introduction

During the last few decades, hydro-meteorological hazards, namely floods, droughts, and extreme weather events are causing catastrophes around the world [1,2]. Hydrological extreme events and their occurrences and magnitude are increasing due to global climate change [3,4]. Its multitude of impacts are seen across the various sector and its subsectors such as agriculture (crops, livestock, fisheries and forestry), environment, ecosystems, health, economy and increasing vulnerability of these hazards can be attributed to rapid growth in population, unplanned urbanization, and other anthropogenic activities [3] which affected almost 1 billion people worldwide [5]. Floods are generally originated from fluvial, pluvial, coastal and storms sources and cause significant economic, environmental, and social effects. Flooding is the major threat posed by climate change, especially in Southeast Asia with 237 million people at risk by 2050s from China, India, Vietnam, Bangladesh, Indonesia and Thailand [6]. Flood risk and associated human mortality and infrastructure losses are also heavily concentrated in these countries because of the high vulnerability and coping capabilities of people [7]. In Indonesia, the Philippines and Singapore, rainfall-related impacts of climate change, such as floods or rainfall-induced landslides, are becoming concerned [8]. Moreover, river floods are projected to appear

frequently and intense in some regions of Southeast Asia [8]. The extremity of extreme rainfall-induced flooding in Chennai (India) in 2015 was attributed to the warming trend of sea surface temperatures (SST) in the Bay of Bengal (BoB) and the strong El-Nino conditions [8,9]. An extreme weather event in Chennai in 2021 had recorded 210 mm of rainfall on a single day (6th November) due to the northeast monsoon which has been impacted by La Nina, a complex weather pattern caused by variations in ocean SST in the equatorial band of the Pacific Ocean [10]. Hence, to reduce flood losses, one has to understand both current and future risks, develop effective strategies, and increase the resilience of communities to flooding. This needs innovative approaches and space-based tools to assess flood zones, risk and resilience.

Geospatial techniques have emerged as an essential tool for mapping and monitoring flood hazards [11]. Some of the open-source platforms are available viz. Alaska Satellite Facility (ASF), United States Geological Survey (USGS)-Earth Explorer, etc. which ensures the availability of near real-time optical remote sensing satellite data with high spatial and temporal resolutions worldwide. The space-borne data such as Moderate Resolution Imaging Spectroradiometer (MODIS), Landsat, Indian Remote Sensing (IRS), and Sentinel have been used for determining the flood extent [12]. The only limitation with optical satellite data is cloud cover, it cannot sense beyond this. Getting clear satellite images during the rainy season is merely possible from optical sensors, whereas the composites products are sometimes beneficial for flood monitoring at regional scales. For instance, the MODIS-based near real-time (NRT) product was widely used for inundation mapping and impact analysis over several river basins worldwide [2,13,14]. Additionally, satellite images captured by the optical sensors have been broadly used for waterlogged extent mapping, standing water depth mapping, flood hazards, vulnerability and risk assessment [15,16].

Satellite reflectance data have been also employed for deriving spectral indices, such as the Normalized Difference Water Index (NDWI) and modified NDWI (mNDWI) to assess flooded regions as well as soil moisture zoning [17–20]. Other multi-spectral based indices such as the Normalized Difference Vegetation Index (NDVI), Enhanced Vegetation Index (EVI), Water Ratio Index (WRI), Spectrum Photometric Water Index (SPWI), and Standardized Photometric Water Index (SPWI) are utilized for the delineation of flooded areas and characterizing floods (e.g., estimating turbidity, sediments, etc.) [21–23]. Most of these spectral indices (SIs) have utilized near-infrared (NIR) band as floodwater reflects the lowest amount of light energy which helps to identify flooded pixels [24]. The NDWI and mNDWI are based on green and near-infrared bands, which can easily discriminate between water and non-water pixels [17,25]. Other than optical sensors, microwave sensors (Synthetic Aperture Radar (SAR)) are also used for flood inundation mapping and floodwater depth mapping as they can distinguish land and water precisely [16,26]. In addition to satellite data, several studies have proposed that various empirical, hydrodynamic, and 1D, 2D, and 3D flood models could be used for flood inundation and depth mapping [16,27]. Data-driven models e.g., Machine Learning (ML) methods are becoming popular because they can numerically do flood forecasting purely based on historical flood data without requiring knowledge of any physical processes [28]. In comparison with statistical models, ML methods showed greater accuracy while dealing with complex hydrological systems such as floods [29,30]. Several other ML algorithms, e.g., neuro-fuzzy (NF), convolutional neural network (CNN), support vector machine (SVM), and support vector regression (SVR), were also proved very effective for current as well as historical flood mapping, forecasting, and prognosis [31–33]. Accurate flood inundation extent mapping is a crucial input for hydrological models for damage assessment, vulnerability and flood risk evaluation. It also assists rescuers during flood disasters.

In order to identify vulnerability in a multidimensional space, numerous dimensions of vulnerability elements and datasets are used. Typically, multi-criteria decision analysis (MCDA), cluster analysis, and Analytical Hierarchy Process (AHP) techniques are employed for vulnerability and flood risk analysis [34–36]. High-resolution datasets (NOAA-AVHRR) coupling with Geographical Information Sciences (GIS) were used to

prepare flood hazard maps for Bangladesh [37]. Based on several studies, it has been recognized that socio-economic/physical/environmental vulnerability data along with flood hazard index are crucial components in flood risk assessment [25,35,38]. Some of the vital elements for flood hazard zonation are land cover, slope, elevation profile, evacuation route, proximity to breach sites (e.g., school, hospital, road, etc.), proximity to confluence, proximity to rivers, soil moisture. Additionally, to examine socio-economic vulnerability, population data, shelter home, statistical data on education (i.e., literacy rate, dependency on education and related jobs etc.), age proportion, labour (agricultural and migrated), cultivator, family structure, and social dependence are mainly considered [39,40]. However, recognition of the socio-economic data from different sources in the local context is more useful in mapping and analyzing the spatiotemporal dynamics of flood risk [41,42]. MCDA methods are frequently employed to examine integrated datasets comprising multiple geomorphological, hydrological, and socio-economic factors for vulnerability and flood risk analysis [35]. Several studies have considered MCDA for the regionalization of flood risk areas [35,43]. Clustering techniques are employed to identify flood risk zones in central India accompanying biophysical and socioeconomic variables, such as K-means for regional flood frequency analysis [44]. Satellite datasets comprising multi-sensor optical (IRS) and SAR (RADARSAT) data are employed to identify villages falling under various flood hazard zones in the Kopili river basin of Brahmaputra river in Assam [7]. To investigate flood risk at the regional level in the upper Brahmaputra River valley, a methodology was adopted based on GIS-based MCDA by integrating stakeholders' knowledge, hazard indicators (e.g., elevation, slope, and proximity to breach sites, drainage confluences, rivers), and vulnerability indicators (e.g., agriculture, safe drinking water, evacuation route, and elevated household/flood shelter) [42]. Studies have evaluated the flood hazard and flood vulnerability as separate entities and combines them to assess flood risk in the North Bihar region by considering various geomorphological, hydrological, socio-physical/environmental and socio-economical/physical parameters at block, municipality, and district level [15,35,38]. Even though studies have advised regionalizing flood zones based on hydrographic boundaries, this is rarely practicable in countries such as South Asia due to a lack of datasets at administrative levels and restrictions on data sharing mechanisms in transboundary basins. Furthermore, using administrative units as the foundation for regionalizing flood-risk areas allows authorities to allocate resources such as insurance premium subsidies [45,46]. The implication of hydraulic models in flood risk assessment is becoming more frequent and worthwhile. Some of the studies applied a variety of hydrological as well as hydraulic models to assess flood hazards for different applications [15,36]. The 1-D hydraulic model along with Digital Elevation Model (DEM) has been used to assess flood hazard, vulnerability and risk [47]. A new dimension in flood vulnerability assessment is introduced, which has focused on community-level flood vulnerability assessment by analyzing satellite images, coupled with a structured questionnaire, criteria mapping, observation and the secondary data [48].

Studies on flood risk assessment are limited in the North Bihar region in India which is a major flood-prone area of India. Various researchers have addressed the flooding problem and prognosis in the region utilizing multi-temporal satellite datasets and geospatial tools from time to time [2,49–51]. However, there is a lack of information on long-term flooding patterns to identify flood risk zones and reduction mechanisms. The present study demonstrates the utility of satellite-based flood inundation mapping for flood hazard, vulnerability and risk assessment. Therefore, the specific aim of this case study was to (1) assess long-term flood hazards spanning from 2001 to 2020, (2) establish linkage of flood hazards with sinuosity, drainage density, Euclidean distance from road and river, and relief map, (3) assess impacts of floods on agriculture and built-up, and (4) map flood vulnerability and flood risk in the region based on several socio-economic parameters.

2. Study Area

North Bihar is located between latitude $25^{\circ}20'01''$ N to $27^{\circ}31'15''$ N and longitude $83^{\circ}19'50''$ E to $88^{\circ}17'04''$ E with a geographical area of $54,223.02$ km 2 (Figure 1). It comprises 57.6% of the total geographical area and consists of 21 districts out of 38 districts of the Bihar state. Bihar is surrounded by the humid West Bengal in the east and the sub humid Uttar Pradesh in the west, surrounded by Nepal in the north and Jharkhand in the south. Ganges and Kosi are the main rivers, supplying most of the water to this state which further divided Bihar into two parts (i.e., North Bihar and South Bihar) by the river Ganges that passes through the middle from west to east. The geographical setting of the river channels of northern Bihar plains is the most dynamic system globally [52,53]. There are more than 250 seasonal and permanent rivers/dhars are present in the region which contributes majorly to flooding. A significant part of the land is flat with some mountains in the southern part. Bihar has a tropical monsoon climate with the average maximum and minimum temperature ranges between $24\text{--}25$ °C and $8\text{--}10$ °C, respectively. The hottest months are from April to June, whilst the coldest is during December to January. Most of the rainfall (80–90%) is concentrated during the monsoon season (mid-June to mid-October) and these months are very important for agriculture in this region. The 21 years of climatological mean rainfall map based on PERSIANN Dynamic Infrared–Rain Rate (PDIR-Now) during July to September showed that rainfall varied from 200 to 375 mm and was distributed across all basins, albeit the Tibetan plateau showed relatively lower rainfall (Figure 1b).

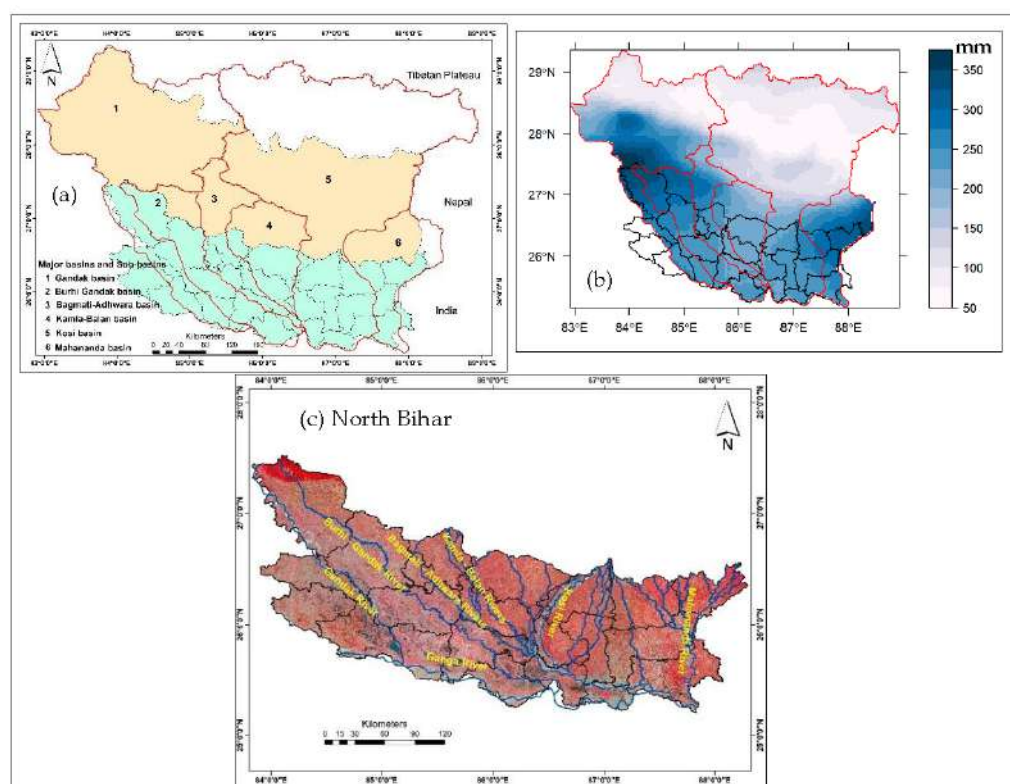


Figure 1. Study region with major river basins and sub-basins in North Bihar (a), 21 years of the climatological mean (2000–2020) rainfall in mm based on PDIR-Now (b). The False Color Composite (FCC) image in (c) is derived from Sentinel-2 images (i.e., median image over March to June 2020 to remove cloud pixels).

Based on the genesis, floods in India are due to riverine, glacial outburst, dam break, and storm surge [50,51]. North Bihar recurrent floods are mostly due to extreme rainfall-induced riverine floods, and some of the major flood events in the study region are 1987,

1998, 2000, 2001, 2003, 2004, 2008, 2010, 2013, 2017, 2018 and 2020. It was reported that ~16.5% geographical land of Bihar was prone to flooding with nearly 76% of the population living under the threat of flood in the study region [16]. Typically, floods are a recurring event observed annually that destroys thousands of human lives including live stocks and other assets [54]. In comparison to South Bihar, North Bihar is more vulnerable to flood due to its geographical-setting which receives a huge amount of water from the upstream river catchments flows through Nepal and Tibetan Plateau [2]. Due to the succession of high flows and unexpected changes in slope from steep rocky terrain to nearly flat terrain, this area comes under a high flood risk zone [16,54]. During the last 30 years, northern Bihar plains have experienced the highest and disastrous flood occurrences which also results in waterlogging at a major scale in low-lying areas throughout the year [35]. Kosi, Gandak, and Burhi Gandak are the major tributaries present in the region along with some of the minor viz. Kamla Balan, Adhwara group of rivers, etc., carries a huge amount of water and results in a massive inundation for the low lying area which also creates the biggest threat to loss of life, livelihood, and infrastructure [52].

Although there are industries present in the region, agriculture is the pivot of economic growth, majorly affected due to repetitive flooding events, needs to be prevented so that the crop yield can be increased regularly and living can be good [2]. Therefore, there is a need for better planning of land resource utilization that can reduce flood effects over hazard-prone areas. Recently, Bihar has made a tremendous and positive change in the monitoring and assessment of the flood hazards with the help of the Flood Management Information System Centre (FMISC) and State Disaster Management Authority, Patna (BSDMA). The open-source remote sensing satellite images in near real-time are also serving as vital information for emergency response support. Conventional methods like field survey and aerial observations for flood extent mapping require extensive work, large manpower, more time, and combinedly make it costly in comparison to Remote Sensing and GIS approaches. The capability of remote sensing made it more reliable and applicable in monitoring and assessing the impact of floods over land and urban areas during and immediately after the occurrence of flood events [16].

The Advanced Land Observing Satellite (ALOS) Phased Array type L-band Synthetic Aperture Radar (PALSAR) derived Global DEM V2 (GDEM V2) and Google Earth Pro derived elevation points are used to map the topographic undulations in the study region (Figure 2). The terrain is gentle slopy to nearly flat throughout the study region, exhibits majorly very low relief. Therefore, a contour map was generated by applying the interpolation technique at an interval of 5 and 10 m, and a relief map was also prepared based on derived contours. The relief map exhibits relief ranges from 20 m to more than 100 m over the study region. The terrain relief is also appeared as one of the major contributing factors to influence flooding patterns. Low relief region has always the potential of submergence due to high soil moisture. Such regions also have elevated groundwater levels and surface flows are higher as well.

The central and eastern part of the study region has relief between 20 to 50 m. whereas, the western, some of the central, and northern regions were having relief variation between 60 to 90 m. The Paschim Champaran is the highest elevated district with the relief variation of ~70 m to more than 100 m. Several studies stated that waterlogging is quite prominent in lower relief zones and decrease with the increase of relief zone.

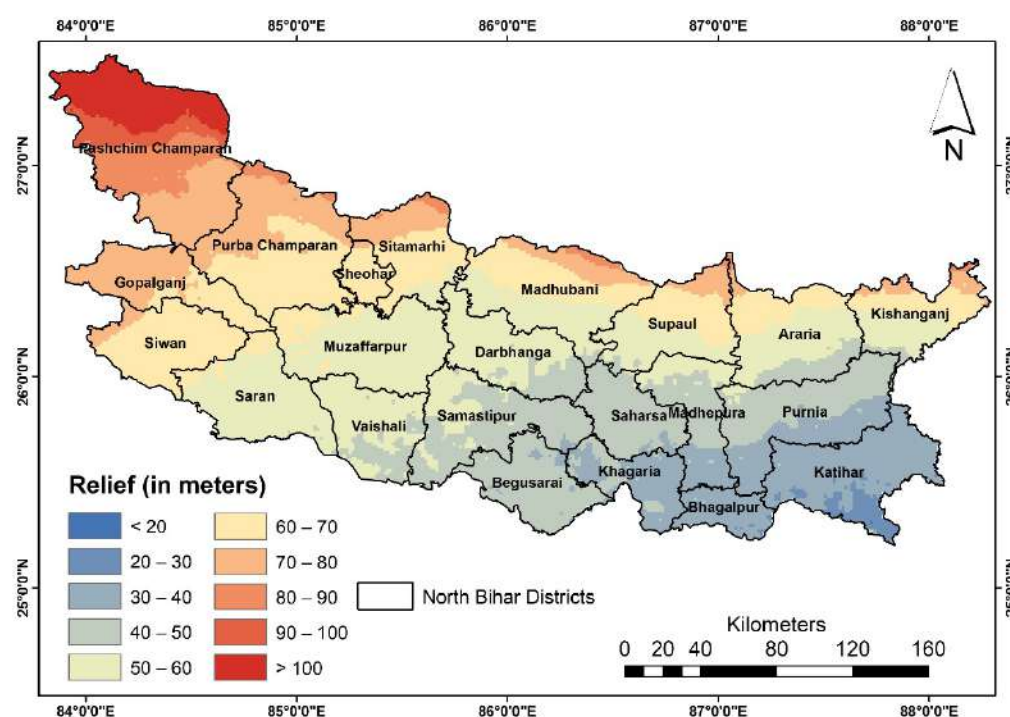


Figure 2. Relief variation in study region as derived from ALOS-based DEM. ESRI Shapefile of North Bihar districts is also overlaid.

3. Materials and Methods

The dataset used in this study were MODIS surface reflectance product (MOD09A1), Sentinel-2A/B optical satellite data, rainfall (PDIR-Now), Copernicus land use/land cover (LULC), ALOS based DEM, and socio-economic datasets (Census data). The detailed information is presented in Table 1. To link rainfall with flood inundation patterns, we used three-month mean satellite-derived rainfall data of PDIR-Now (CHRS Data Portal). MODIS surface reflectance products were used to map flood hazard zones. Census data such as population density, total male, female and population of cultivators, agricultural labourers, house-hold density, and literates were utilized to get village level socio-economic vulnerability. Furthermore, this information was coupled with flood hazards to generate a final risk map. Copernicus-based LULC data is used to assess the impact of flooding over various LULC.

3.1. Data Descriptions

3.1.1. MOD09A1 Based Reflectance Product

The MOD09A1 (V6) product provides surface reflectance at 500 m resolution and 8-day composite. These reflectance data were corrected for atmospheric conditions such as gasses, aerosols, and Rayleigh scattering. In this study, MODIS reflectance products were considered for July to September for each year during 2001–2020 to compute NDWI, mNDWI, SPWI, and EVI (Table 2). All these indices were utilized for extracting flood pixels. However, at some places where biases on flood pixels occurred, we rectified using FMISC, Patna based published annual flood reports and maps.

Table 1. Dataset used in this study and their characteristics.

Name of Dataset	Temporal Resolution	Spatial Resolution	Acquisition Date	Purpose	Source
MOD09A1	8 days	500 × 500 m	July–October (2000–2020)	Flood delineation	LP DAAC
Sentinel-2A/B	12 days	10 × 10 m	March–June (2020)	PWB and major/minor River channel, lineaments, and road	ASF
PDIR-Now	3-hourly	4 × 4 km	July–Sept (2000–2020)	Rainfall and anomaly maps	CHRS Data Portal
Copernicus LULC	Composite	100 × 100 m	–	LULC map	Copernicus
ALOS PALSAR DEM	Composite	12.5 × 12.5 m	–	Relief map	ASF
Census data	10 years	–	–	Socio-economic vulnerability mapping	Census of India
FMISC Flood Reports	–	–	July–October (2000–2020)	To validate flooding for the respective years	FMISC, Patna

Table 2. The indices utilized to derived flood pixels based on MODIS reflectance bands.

Sl. No.	Equations	Reference/Source
1.	$NDWI = (\text{Green} - \text{NIR}) / (\text{Green} + \text{NIR})$	[17]
2.	$mNDWI = (\text{Green} - \text{SWIR}) / (\text{Green} + \text{SWIR})$	[55]
3.	$SPWI = (B1 + B4) - (B2 - B6)$ Where, B1, B2, B4, B6 are the reflectance of band Red, NIR, Green, and MIR respectively	[22]
4.	$EVI = 2.5 * ((\text{NIR} - \text{R}) / (\text{NIR} + (6 * \text{RED}) - (7.5 * \text{BLUE}) + 1))$	[56]

3.1.2. Sentinel-2 Optical Satellite Data

Sentinel-2 optical satellite data is the most widely accessible satellite mission which provides moderate-to-high spatial resolution multispectral satellite measurements. It is a land monitoring mission with the constellation of two satellites that provide global coverage at every five days interval. L1C data have been available since June 2015 and L2A data have been available globally since January 2017. In this study, the satellite images during March–June, 2020 were being used to extract permanent/seasonal river streams, lineaments, major/minor roads in the North Bihar region. River centerlines were also drawn using Sentinel-2 satellite image which was further used to calculate sinuosity for each river.

3.1.3. PDIR-Now Based Precipitation

Precipitation Estimation from Remotely Sensed Information using Artificial Neural Networks–Cloud Classification System–Climate Data Record (PERSIANN) provides nearly global high spatio-temporal precipitation datasets. PDIR-Now provides precipitation estimates at 0.04° spatial and 3-hourly temporal resolutions from March 2000 to the present over the global domain of 60°S to 60°N . Development of PDIR-Now was motivated by the needs of the scientific community interested in a long-term, very high spatiotemporal resolution ($0.04^\circ \times 0.04^\circ$ spatial and 3-hourly temporal) precipitation data record relevant for hydro climatological applications, such as the study of diurnal precipitation patterns and extreme events with heavy rain rates. The mean rainfall dataset of July–September months from 2000 to 2020 is used in this study to show and analyze rainfall anomalies for the major flooding events over the study region during the last two decades.

3.1.4. Copernicus Land Use Land Cover

Copernicus Land Use Land Cover data is prepared on an annual basis at a very high spatio-temporal scale with an overall accuracy of 80% (in 2019) which were also validated

based on 28k ground-truthing points. The statistical validation meets the CEOS land product validation stage 4 requirements. Flood impacts at various LULC in the study region were assessed using Copernicus Land use data.

3.1.5. ALOS PALSAR Based DEM

The ALOS (PALSAR) based DEM data are available at 12.5 m spatial resolution and are obtained from the Japan Aerospace Agency (JAXA) portal. The DEM has been used to draw major/minor drainage. We used ALOS-based DEM because it possesses comparatively a more detailed spatial resolution than the ASTER-GDEM V2 (30 m) and Shuttle Radar Topography Mission (SRTM) DEM (90 m). Contour map was generated based on ALOS DEM at an interval of 5 to 10 m. Further, a relief map was also prepared with the help of DEM. It is also used as a key input to calculate sinuosity.

3.1.6. Census Data

Census data parameters viz. population density, house-hold density, total male, female population, agricultural labour, cultivator, and literacy rate were considered for mapping socio-economic vulnerable zones in the study region. All the parameters were taken from the Census of India 2011 survey database.

3.2. Methods

3.2.1. Flood Extent Mapping during 2001–2020 and Flood Hazard Estimation

In this study, MODIS-derived indices such as NDWI, mNDWI, SPWI, and EVI (Table 2) were applied to extract flood extents during 2001–2020 (July–September) by adopting threshold values. For instance, threshold values of more than 0, 0.1, and 0 were applied for NDWI, mNDWI, and SPWI, respectively for flood pixels extraction. The long-term flood extent maps were then utilized for producing flood frequency maps. Furthermore, the socio-economic dataset was coupled to generate vulnerability and finally flood risk. The comprehensive flowchart of the methodology has been given in Figure 3.

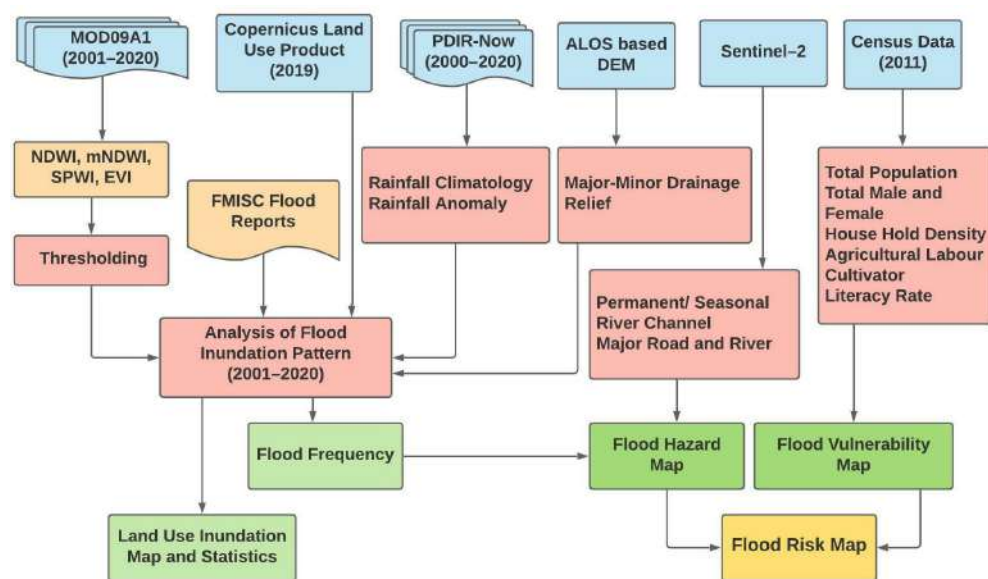


Figure 3. Methodology flow chart adopted in this study.

The NDWI highlights open waters from satellite images [17], whereas the mNDWI extracted shallow water bodies and separated built-up structures from water features [55]. SPWI is also capable of extracting water pixels accurately [22]. The EVI is represented as an optimized vegetation index to improve the vegetation signal with better sensitivity in high biomass areas. It is better than to as it reduced noises from atmospheric changes as well as soil background signals mainly in dense canopy zones [56,57]. The parameters adopted in

the MODIS-EVI algorithm are $L = 1$, $C1 = 6$, $C2 = 7.5$, and G (gain factor) = 2.5 and stated as follows:

- Non-flood pixel ($EVI > 0.3$)
- Permanent water bodies ($EVI < 0.05$)
- Water-related pixel ($EVI < 0.1$)

FMISC, Patna based flood inundation maps were also utilized to validate flood extent maps of this study during 2001–2020. The resultant 20 years flood maps at an annual basis were aggregated yearly in MATLAB R2020a to derive the frequency map. The aggregation process consists of three steps: (a) to read images using `imread` function, (b) to add images using `imadd` function, and (c) to display images using `imshow` function. At a time, two flood layers were added to create a flood frequency map.

Flood inundation extent of three months (during July, August, and September) were further aggregated and made annual flood inundation layer for each year during 2001–2020 based on (Equations (1)–(4)) and validated using the FMISC base flood maps. The yearly flood aggregated flood pixels were further used to derive flood frequency for each pixel. The composite flood extent maps for every 5 years (2001–2005, 2006–2010, 2011–2015, and 2015–2020) were prepared and the corresponding area statistics were generated. Furthermore, 20 years' composite flood extent map was also prepared to understand the long-term pattern as well as the impact of floods. However, flood frequency/occurrence for each flood pixel was estimated by considering all flood inundation layers from 2001 to 2020 on an annual basis. Furthermore, flood frequency is categorized into five different classes as shown in Table 3. Different flood hazard zones were considered based on the frequency of flood pixels e.g., Very High category is assigned to those pixels which have inundated ≥ 17 times, High for 13–16 times, Moderate for 9–12 times, Low for 5–8 times, and Very Low to those pixels which inundated ≤ 4 times.

Table 3. Flood hazard category and Flood frequency used in flood hazard map.

Flood Hazard Category	Flood Frequency
Very High	≥ 17 times
High	13–16 times
Moderate	9–12 times
Low	5–8 times
Very Low	≤ 4 times

The intensity of flood hazard (FH) is calculated as follows:

$$FH = (YF_1 + YF_2 + YF_3 + YF_4 + \dots \dots \dots YF_n) \quad (5)$$

where Y indicates yearly flooding events and F_n indicates flood frequency.

3.2.2. Village Wise Socio-Economic Vulnerability (SEV) Mapping

Flood vulnerability has been analyzed by many authors in the North Bihar region [36,52]. The most common concept of vulnerability is that it describes how a socio-economic system is susceptible to natural hazards. It is determined by including several factors the condition of human settlements, infrastructure, public policy and administration, organizational abilities, social inequalities, gender relations, economic patterns, etc. Census survey-based data were used in this study to get village-wise socio-economic vulnerability in terms of various several economic indicators, such as population density, sex ratio (male and female population), the population of cultivators, agricultural labourers, literacy rate, and house-hold density.

The present study has adopted the Socio-Economic Vulnerability (SEV) method developed by [58] to experiment with the spatial pattern to evaluate flood risk at village level to

describe and understand the physical and social burdens of risk. Four consecutive steps were followed to calculate SEV are: (i) geo-spatial and non-geospatial data collection, processing, and analysis, (ii) integration of spatial and non-spatial data, (iii) weighted indexing of the socio-economic parameter, and (iv) integration of all parameters. The composite village-level SEV map was generated by integrating all seven socio-economic indicators. Then the SEV map was categorized into five classes, namely, very low, low, medium, high, and very high based on their attribute's class values from lowest to the highest (Table 4). Furthermore, five classes are assigned as 1 to 5 scale, where very low represents 1 and very high represents 5, and vice versa for literacy rate. The SEV is calculated as follows:

$$SEV = PD + FM + M + AL + CL + CH + LR / \text{Number of Indicators} \quad (6)$$

where,

PD = population density;

HH = number house-hold;

FM = female ratio;

M = percentage wise male ratio;

AL = percentage wise population of agricultural labourers;

CL = percentage wise population of cultivators;

LR = percentage population of literates.

Table 4. Several economic indicators divided in five different vulnerability categories based on their class values.

Indicators	Very High	High	Moderate	Low	Very Low
Population density per km^2 (p/km^2)	≥ 4000	3000–4000	2000–3000	1000–2000	≤ 1000
House hold density (house/km^2)	≥ 2000	1500–2000	1000–1500	500–1000	≤ 500
Male Population (%)	36.1–45	27.1–36	18.1–27	9.1–18	≤ 9
Female Population (%)	44.1–55	33.1–44	22.1–33	11.1–22	≤ 11
Agriculture Labour (%)	≥ 56.1	42.1–56	28.1–42	14.1–28	≤ 14
Cultivator (%)	≥ 44.1	33.1–44	22.1–33	11.1–22	≤ 11
Literacy Rate (%)	≥ 24.1	18.1–24	12.1–18	6.1–12	≤ 6

3.2.3. Flood Risk Mapping

Flood Risk (R) was assessed by combining hazard (H) with vulnerability (SEV) as follows:

$$\text{Risk (R)} = H \times SEV \quad (7)$$

where H indicates hazard categories and SEV indicates vulnerability at village level. Various spatial analysis and geo-statistical tools are used for mapping and analyzing hazard and vulnerability. The village-level flood risk has been categorized in five classes viz; very low, low, medium, high, and very high.

4. Results

4.1. Spatio-Temporal Precipitation Maps during 2000–2020

The rainfall anomaly maps based on CHRS PDIR-Now data from July to September (i.e., mean) were shown in Figure 4. To assess the spatiotemporal rainfall variability across the Gandak (1), Burhi Gandak (2), Bagmati-Adhwara Group (3), Kama-Balan (4), Kosi (5), and Mahananda river basin's catchment (6), we showed only for extreme rainfall years like 2004, 2007, 2008, 2011, 2017, and 2020. The rainfall anomaly maps were presented to identify the districts as well as the basins (1–6), which received intense rainfall. Rainfall anomaly maps for the years 2004 (Figure 4a), 2007 (Figure 4b), 2008 (Figure 4c), 2011 (Figure 4d), 2017 (Figure 4e) and 2020 (Figure 4f) are showing heavy downpours during particular

years with respect to the rest of the years during 2000–2020. These results showed that during the year 2004, the majority of areas of the study region has received rainfall up to 200 mm. However, it is concentrated in the central part of the study region (i.e., Burhi Gandak, Bagmati-Adhwara Group, and Kamla-Balan basins) which further resulted in severe inundation in low catchment areas of North Bihar plain (Appendix A). The major district severely affected during the 2004 flooding event was Darbhanga, Madhepura, Katihar, and Khagaria (Figure A1). During the year 2007, it is shown that 6.4% of the geographical land of North Bihar districts got inundated (Figure A1g) due to severe rainfall occurred which were concentrated over the south-western part of the region (i.e., Gandak, Burhi Gandak, Bagmati-Adhwara Group and Kamla-Balan basins) with the rainfall of 100–200 mm, severely inundated Darbhanga, Katihar, Madhepura, and Purnea districts. During the year 2008, except upper catchment region especially in the western Nepal region, middle and lower catchment region has received rainfall up to 100 mm. This unprecedented rainfall has resulted in breaching of Kosi river near Kushaha bridge at 12 km upstream from Kosi barrage which has been shown in Figure A1h. Rainfall anomaly map during the year 2011 has shown that except Tibetan plateau, the whole study region has received less than 50 mm of rainfall and therefore, flood extent areas are limited to a few districts, such as Muzzafarpur, Bhagalpur, Katihar, and Khagaria. As per the rainfall anomaly map of the year 2017, it can be stated that the Northern Bihar region has received the distributed rainfall between 50–150 mm and concentrated over the western and southern region (i.e., Gandak, Burhi Gandak, Bagmati-Adhwara Group, Kamla-Balan and Kosi basins). The affected districts were Darbhanga, Madhepura, Khagaria, Saharsa, Katihar, and Bhagalpur. During the year 2020, the study area has received excessive rainfall between 50–200 mm that concentrated over the south-western part of the basin (i.e., Gandak, Burhi Gandak, Bagmati-Adhwara Group, Kamla-Balan, Kosi and Mahananda basins). Consequently, it was found that 17.7% geographical land of the study region was inundated and severely affected districts are Muzzafarpur, Darbhanga, Saharsa, Khagaria, Madhepura, Bhagalpur, Katihar, and Purnea. Notably, we found that during the year 2020, the maximum rainfall was occurred followed by the years 2004 and 2007 over North Bihar, Nepal, and Tibetan Plateau which subsequently led to flood-like conditions over downstream areas. The precipitated water traveled through a gentle slope from the upper (Tibetan Plateau and Nepal) to the lower catchment of North Bihar. The rainfall was concentrated mostly over the northern and south-west part of the basin as displayed in Figure 4a–f.

Concisely, it can be stated that the higher rainfall events were observed during 2004, 2007, and 2020 and were majorly concentrated over low catchment areas of Gandak, Burhi Gandak, Bagmati-Adhwara Group, Kamla-Balan, Kosi, and Mahananda river basin's catchment. Moreover, the composite rainfall data also showed that rainfall was concentrated in central and lower catchment areas. The districts which were adversely affected due to torrential rainfall are Paschim and Purbi Champaran, Madhubani, Darbhanga, Supaul, Araria, Saharsa and Katihar. Apart from these, some of the districts, such as Madhepura, Samastipur, Muzzafarpur, Purnea, Sitamarhi, Sheohar, Begusarai, Bhagalpur, Kishanganj, and Vaishali also witnessed high-intensity rainfall and followed by flood inundation.

4.2. Spatio-Temporal Annual Flood Extent Map during 2001–2020

During the last two decades (2001–2020), North Bihar districts witnessed major flooding events during 2001, 2002, 2004, 2007, 2008, 2013, 2014, 2017, 2019 and 2020. The present study has shown the year-wise spatiotemporal flooding events during 2001–2020 in Figure A1 and their flood inundation area statistics in Figure A2. Five-year composite flood inundation maps (Figure 5) exhibited a common region of North Bihar which were recurrently affected in the last twenty years (2001–2020). During 2001–2005 and 2006–2011, flooding took place over the central part of the region along the Kosi and Adhwara group of rivers and severely affected, Muzaffarpur, Darbhanga, Samastipur, Saharsa, Khagaria, Katihar, and Purnea districts (Figure 5a,b). A total of 10490.5 km² and 12594.8 km² area was inundated along with Kosi and Bagmati-Adhwara group of rivers during 2001–2005 and

2006–2010, respectively (Figure 5a,b). Notably, due to a breach near Kusaha in 2008, parts of Saharsa, Madhepura and Purnea districts were witnessed severe flood inundation, which can be seen in composite flood map during 2006–2010 (Figure 5b). During 2011–2015 and 2016–2020, an area of 8910.1 km^2 (Figure 5c) and 24145.5 km^2 (Figure 5d) were inundated, respectively and the latter one affected all most 19 districts in the North Bihar region.

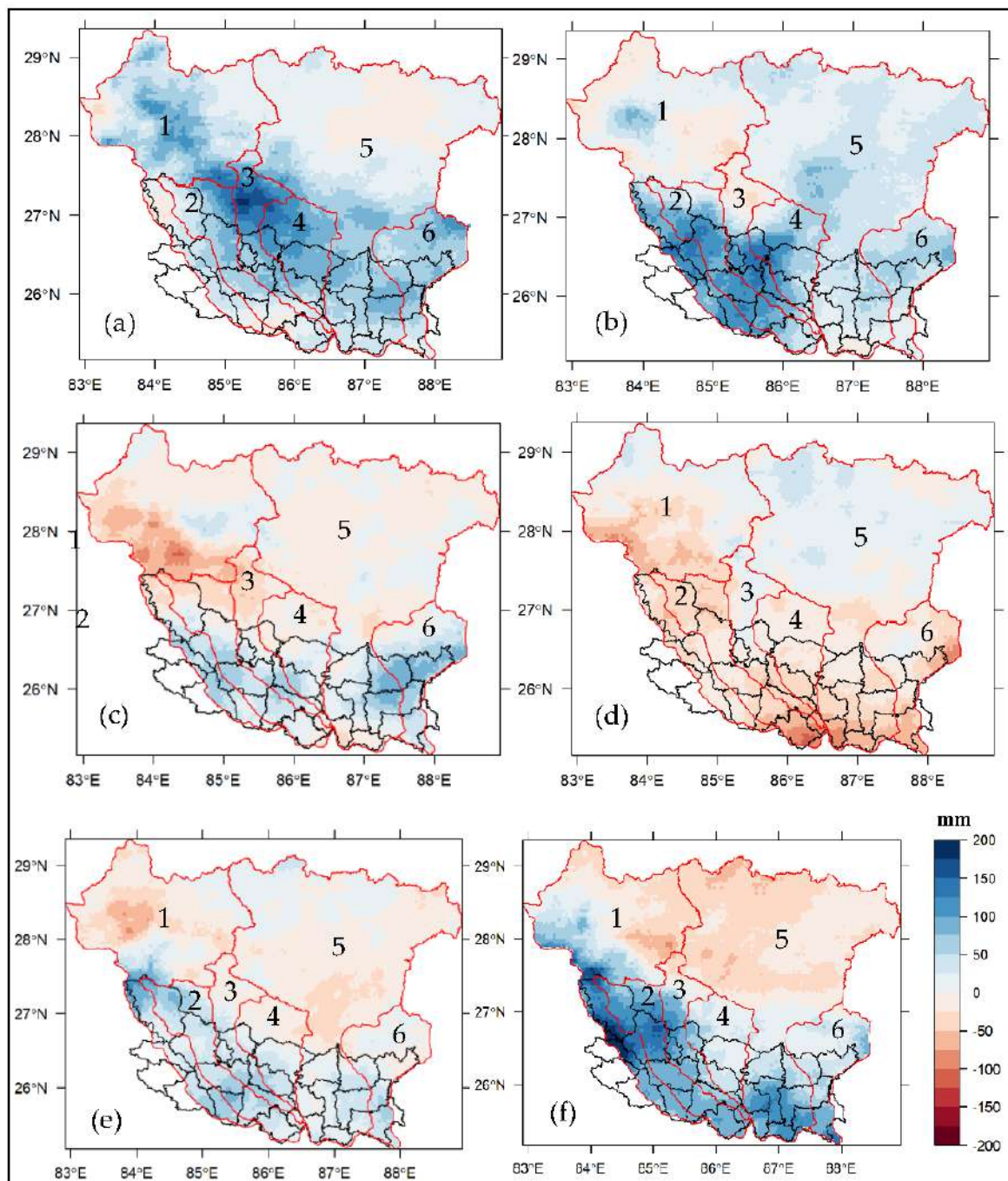


Figure 4. Rainfall anomaly (mm) maps (July to September) based on CHRS PDIR-Now during (a) 2004; (b) 2007; (c) 2008; (d) 2011; (e) 2017; and (f) 2020.

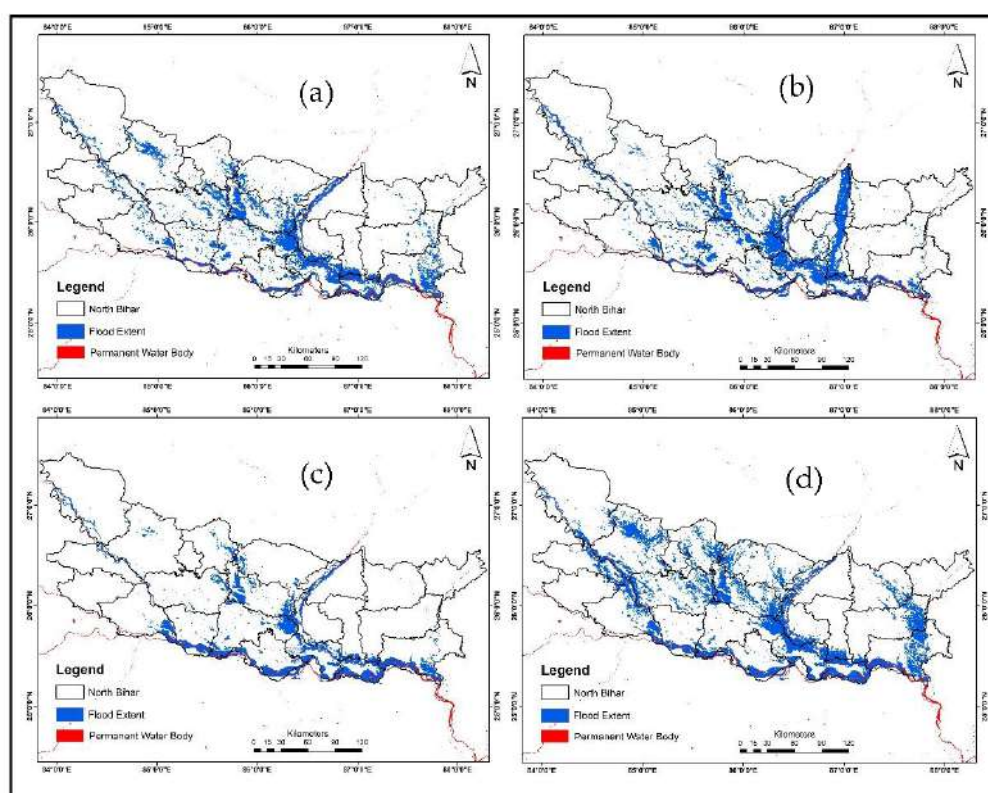


Figure 5. Five-year composite MOD09A1 based flood extent maps during (a) 2001–2005; (b) 2006–2010; (c) 2011–2015; (d) 2016–2020.

Flood inundated areas (i.e., hotspots) were majorly concentrated in the central part of North Bihar around Kosi and Bagmati-Adhwara group of rivers. Recurrent flood inundation due to the Ganges can be clearly seen over the last two decades, whereas, more prominent flooding was seen in the years 2013, 2016, 2019, and 2020 (Figure A1). The composite flood map over 2001–2020 has indicated that during the past two decades, one-third of Bihar's landmass was subjected to flooding accounting for 18640.24 km² inundated areas (~34%). The study also exhibited that during extreme rainfall-induced flooding events in 2007, 2019, and 2020, a total of 19%, 40%, and 52% of land are got inundated with respect to the total flooded area (i.e., 18,640.24 km²) (Figures 5 and A1). Flood maps exhibit that among all the districts of North Bihar, Sheohar, Supaul, Darbhanga, Saharsa, Khagaria, Bhagalpur, and Katihar experienced very severe floods disaster and getting inundated recurrently due to its geographical settings located in the lower catchment areas. The cumulative map shows Kosi, Gandak, Mahananda, and Bagmati-Adhwara rivers are the major source of flood disaster in North Bihar while seasonal water channels also play a major role.

4.3. Flood Hazard Assessment Based on Annual Flood Extent Map during 2001–2020

The flood frequency map was also presented in Figure 6 which showed that the areas located along the river have the highest number of frequencies. The flood hazard category was done on the basis of flood occurrences during 2001–2020 (Table 5), a method which is similar to [7]. For instance, flood frequency of 17 to 20 times was classified under Very High (hazard zone, whereas 13 to 16 times were kept under high hazard zone. Similarly, the yellow color represents a moderate hazard zone with a frequency of 9 to 12 times, whereas the cyan color represented flood frequency of 5 to 8 times (i.e., Low hazard zone). The lowest frequency was <4 times and it was seen very far away from rivers and mostly seen due to a break in embankment (Figure 6). It is also evident from Figure A1 that the spatial distribution and extent of flooding varies from year to year. The areas that are

common across the years were classified as the most vulnerable areas, such as the eastern, central and northern regions of North Bihar. Thus, produced flood maps are expected to be useful in identifying temporal changes in the simultaneous recession and expansion of flood cycles. It is evident based on the flood hazard map that North Bihar is mostly affected due to riverine floods where the Kosi river basin is a prime source for disaster occurrence followed by Bagmati-Adhwara, Kamla-Balan, Burhi Gandak, and Mahananda in the past 20 years.

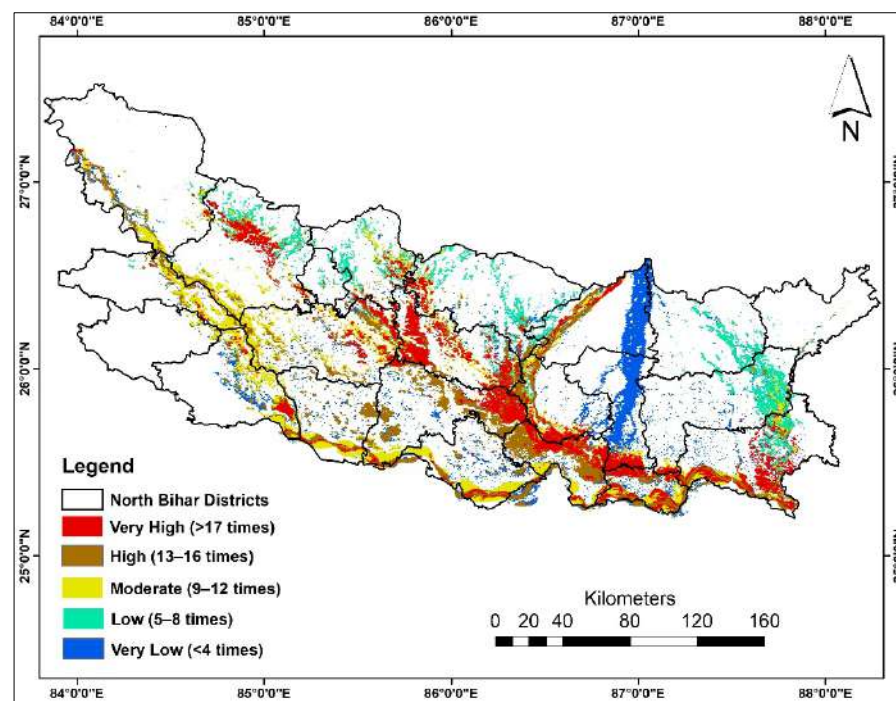


Figure 6. Annual flood occurrence map during 2001–2020 as derived from yearly flood maps.

Table 5. Flood hazard category and area statistics based on occurrences of floods during 2001–2020. The total geographical area is 54,223.02 km².

Sl. No.	Hazard Category	Flood Hazard Area (in km ²)	% Inundation (with Respect to the Geographical Area)	% Inundation (with Respect to the Total Inundation)
1.	Very High (>17)	3687.13	6.8	19.8
2.	High (13–16)	4328.67	8	23.2
3.	Moderate (9–12)	3188.36	5.9	17.1
4.	Low (5–8)	4169.11	7.7	22.4
5.	Very Low (<4)	3266.97	6.03	17.5

Based on the spatiotemporal flood inundation events during 2001–2020, the magnitude of flood hazard was assessed and the impact across the North Bihar administrative boundary was mapped. Composite flood inundation extent during 2001–2020 shows ~34% (18,640.24 km²) of the land area got submerged, where the majority of the area is shared by high flood hazard zone (4328.67 km²) followed by Low (4169.11 km²), Very High (3687.13 km²), Very Low (3266.97 km²), and Moderate (3188.36 km²) (Table 5).

4.4. Flood Impact Assessment on LULC

The predominant LULC classes are agriculture and vegetation (i.e., forest, shrublands) which account for 27,648 km² (51%) and 10,773 km² (19.9%), respectively (Figure 7). The area under the settlement, others, and water body classes were 5590 km² (10.3%) and 6569 km² (12.11%), and 3643 km² (6.71%), respectively. The flood inundation impact on different LULC classes was evaluated using flood frequency map as derived from 2001–2020 and the corresponding statistics were shown in Table 6. The results exhibited that floods were prominent in agricultural (8.6%) and settlement (2.2%) areas as both accounted for ~10.8% areas were affected by floods, under very high category (Table 6). Similarly, agricultural land followed by vegetation and other land use classes showed 9.9%, 5.5%, and 7.4% of inundation under the high flood hazard category. Under the moderate hazard category, prominently agricultural land showed about 7.7% inundation of total agricultural area. Similarly, in the low hazard category agricultural land was heavily affected followed by others and vegetation land-use class with 10.3%, 7%, and 5% of inundation, respectively. Agricultural Land was inundated prominently in the very low hazard category with 8.4% of total agricultural area.

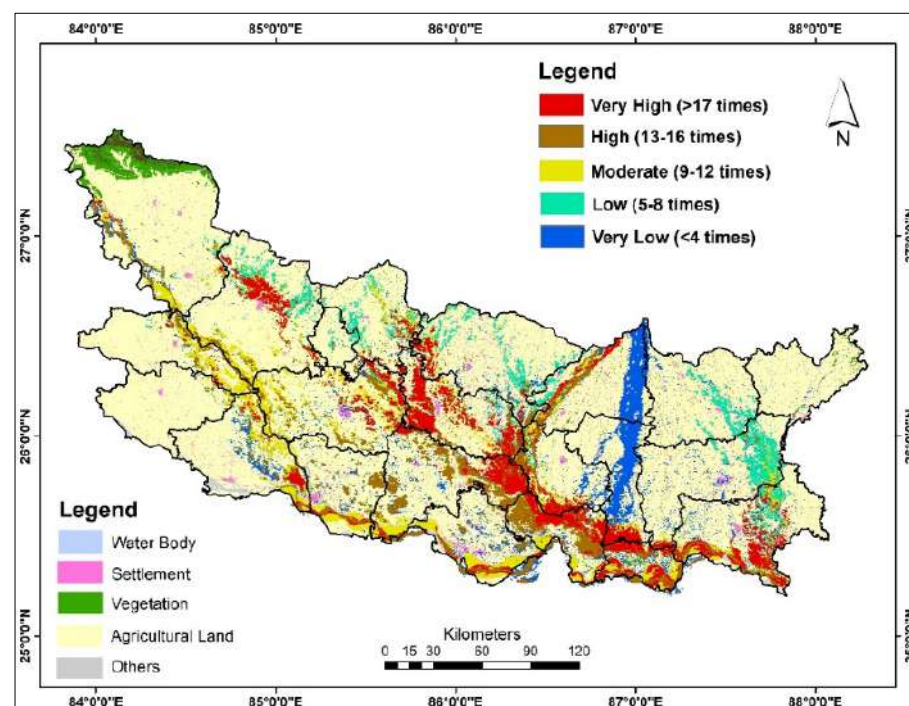


Figure 7. Flood frequency map as derived from 2001–2020 overlaid on Copernicus based land use land cover (LULC) map.

Table 6. Area statistics (in km²) of category wised flood-affected LULC classes. The % area affected (shown in bracket) is with respect to a total area of corresponding LULC.

Hazard Category	Water Body	Settlement	Vegetation	Agriculture	Others
Vey High	322.8 (8.9%)	122.4 (2.2%)	402.1 (3.7%)	2366.9 (8.6%)	473.1 (7.2%)
High	371.6 (10.2%)	137 (2.5%)	587.3 (5.5%)	2746.4 (9.9%)	486.4 (7.4%)
Moderate	298.6 (8.2%)	98.1 (1.8%)	428.7 (4%)	2126.4 (7.7%)	236.6 (3.6%)
Low	227.3 (6.2%)	108.5 (1.9%)	536.3 (5%)	2837.5 (10.3%)	459.5 (7%)
Very Low	267.3 (7.3%)	95.4 (1.7%)	356.1 (3.3%)	2331.4 (8.4%)	216.9 (3.3%)

4.5. Socio-Economic Vulnerability (SEV) and Flood Risk Map

Village level Socio-economic vulnerability (SEV) was assessed based on socio-economic factors taken from Census data collected during 2011. It was observed that districts present in central, eastern, and northern regions (i.e., East-Champaran, Sheohar, Sitamarhi, Darbhanga, Muzaffarpur, Katihar, Khagaria, Madhepura, Purnea, and Supaul) were under very-high vulnerability zone, whilst the north and central region (i.e., Sheohar, Madhubani, Darbhanga, Samastipur, Supaul Begusarai, and Saharsa) falls under high vulnerability zone (Figure 8a). The central part of the northern plains area alone accounted for 19.11% (12,376.17 km²) of the inundated area under high to very high–vulnerability zone. Apart from this, the eastern part (i.e., Araria, Madhepura, Purnea, Katihar, Bhagalpur, and Khagaria) showed under the moderate vulnerable zone. Some districts such as West Champaran and Kishanganj are under the low and very low vulnerable zone, respectively. The analysis exhibited that a total of 10,976.36 km² and 8139.76 km² (20.24% and 15.01% of total geographical area) were estimated under very high and high SEV, respectively. The moderate SEV category accounts for 14,671.2 km² of area (27.06%). Similarly, the low and very low categories have accounted for 9466.6 km² (17.46%) and 10,969.1 km² of land area (20.23%), respectively. The study also exhibited that among 23,632 villages in the North Bihar region, 4719 and 3571 villages are seen under very high and high vulnerability zones (Table 7).

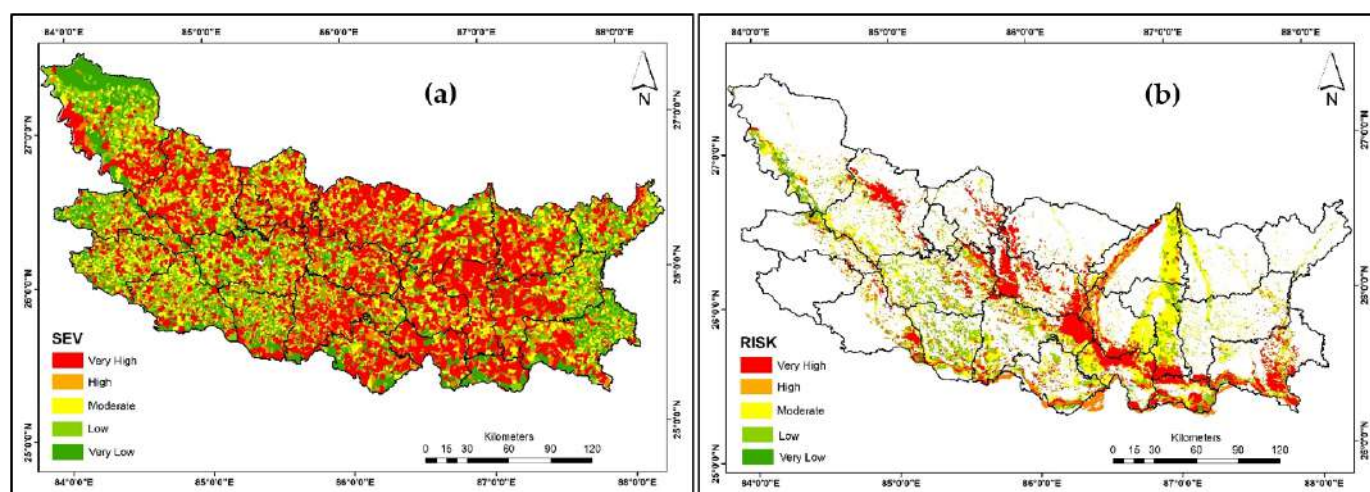


Figure 8. Village (a) level Socio-Economic Vulnerability (SEV) and (b) Flood Risk map.

Table 7. The number of villages affected as per the SEV and flood risk. The total number of villages in the North Bihar region is 23,632.

Category	SEV	Flood Risk
Vey High	4719	2770
High	3571	3535
Moderate	6391	5094
Low	4218	1297
Very Low	4733	896

Village level Flood risk areas were estimated based on varied flood hazard and vulnerability categories (Figure 8). It was found that villages situated along the river i.e., Kosi, Gandak, Burhi-Gandak, Kamla-Balan, were seen under high to very high flood risk zone. Villages located in the Mahananda basin are prominently under moderate risk zone. However, villages under low and very low-risk categories can be seen in the central-western region in Figure 8b. Darbhanga is the most flood-affected district during the last twenty

years with 587.7 km^2 (~26% of total Darbhanga geographical area) of inundation. Around 116 and 135 villages are under very high and high flood risk zone, whereas 87 villages came under moderate flood risk zone. Around 56 and 61 villages are considered in low-risk and very low-risk categories, respectively.

The study also exhibited that a total of 3973.64 km^2 (7.33% of total geographical area) and 4582.14 km^2 (8.45%) areas have been classified under very high and high flood risk zone, respectively. Whereas, 6833.86 km^2 area (12.6%) was shown under moderate flood risk zone. About 2187.67 km^2 (4.03%) and 1063.25 km^2 (1.96%) areas were classified under low and very low flood risk categories. The number of affected villages in each category of flood risk has been shown in Table 7. The total number of flood-affected villages under different risk categories was 13,592.

5. Discussion

India's 40% of the land area is vulnerable to flood, whilst North Bihar itself shares 17% of the area [50]. The major rivers such as Kosi, Gandak, Burhi-Gandak, Bagmati-Adhwara group, Mahananda always brings riverine flood during the monsoon season almost every year. Hence, understanding flood inundation character based on long-term flooding pattern data becomes essential information which further could be used to develop long-term flood management strategies in the North Bihar regions. The present study has utilized MOD09A1 satellite data to generate composite rainfall at every 5 years during 2001–2020. The study also reveals that during 2016–2020, on average half of the total North Bihar (~45% area) was inundated with a total area of $24,145.5 \text{ km}^2$ (Figure 5d) which affected all most all 23 districts of the North Bihar region followed by extreme rainfall events (Figure 4e,f). Flood impact assessment on varied land use classes was shown that ~45% of the agricultural land area was inundated followed by vegetation and settlement with ~22% and ~10% inundation, respectively. As per the long-term aggregated flood extent map, it was found that $18,640 \text{ km}^2$ (~34%) area was inundated. However, it fluctuates year to year with a minimum flood area $\sim 969 \text{ km}^2$ (~2%) in the year 2013 and the maximum flooded area of 9607.45 km^2 (~18%) in the year 2020. The fluctuation of area inundation is mainly attributed to rainfall received in upstream areas which can be seen in 2020 flood events. There was as such no study that was done for a longer period (2001–2020) for flood area mapping. However, some studies have been conducted by taking a single year that has been employed with MODIS NRT or SAR-based satellite data. The MODIS-based NRT based results indicated that $\sim 9230 \text{ km}^2$ (~17%) area was inundated due to the 2019 flood event over North Bihar [49]. Moreover, the spatial pattern of flood in this study was quite consistent with previous studies [49]. Flood extent map reveals that villages along Kosi, Gandak, and Burhi-Gandak rivers are more prone to flooding due to the availability of several major and minor river channels which activate during monsoons and contribute heavily to major streams to inundate low lying areas. Flood risk depends on a combination of the physical nature of flood severity and its interaction with a population or vulnerability. To study the risk of flood hazards, it is essential to study the severity, and spatial extent of these hazards as well as the socioeconomic ability of the region to anticipate and cope with the hazards.

In the present study, a geohazard map has been derived by integrating long-term flood information, SEV map to deduce the flood risk pattern at the village level. There is no such study carried out to assess flood risk at village level in the North Bihar region. However, some studies evaluated flood risk at district and block levels based on various indicators namely, major/minor river channels, road networks, hydro-geomorphology, sinuosity, demographics, flood report, and economic index [15,38,59]. A significant rainfall contribution from the upstream Himalayan region makes this region highly vulnerable to flood. The present study revealed that villages of the districts such as Bhagalpur, Darbhanga, Khagaria, and Samastipur are considered to be at very high risk owing to their geographical setting as it is located in lower catchment areas with a gentle slope and several seasonal/permanent river channels. It was also studied that pre and post-

monsoon waterlogging zones are prominently present in these districts owing to lower relief zones [60]. Flood not only causes population at risk but also agricultural loss and severe economic damages [15]. The study also suggested that braided and meandering river channels play a key role in flooding patterns [53,61]. Similarly, the flood risk map presented in Figure 8b, exhibited that very high flood risk areas can be seen prominently in the central and northern part of North Bihar region whereas some of the areas from central, eastern and western parts of the region can be seen under moderate to high flood risk zone. These areas of higher risk to flood are mainly attributed to regional hydro-geomorphology such as the presence of lower relief zones, waterlogging zones, flood plains, paleochannels, oxbow lakes, etc. The study also exhibited that a higher degree of sinuosity is also a key reason behind the occurrence of severe flooding phenomena. Moreover, siltation deposition and lack of maintenance of sediments from dams and barrages are also reported to be major factors for increasing flood events and associated damages [30]. Studies also projected that climate change-induced extreme rainfall intensity would be higher for the future and therefore, higher risk can be anticipated [3,4,31]. However, Kosi fan areas, part of Mahananda basin, and western region are showing under in moderate flood risk which can be attributed to inactive flood plains as well as shallow to deep alluvial plains [60]. Similarly, villages showing in Gandak and Burhi Gandak river basin are under low and very low flood risk category and primarily due to embankment structures, lower drainage density and lower sinuosity as well. However, low-quality structures or break-in embankments usually show higher flood damages across North Bihar. Additionally, deforestation at river banks and increasing urban compactness are some factors that could increase flood risks at river banks.

Flood risk evaluation becomes even more important when climate change induced extreme weather events are intensifying the flood events. According to the data provided by IPCC 2021 [8], there have been more than 999 natural disasters in the last 20 twenty years, of which 951 were related to weather resulting havoc situations in lower catchment regions. This has caused a lot of damage to the economy. Considering all these factors, it can be stated that flood hazard, vulnerability and risk estimation are very important to reduce the loss of life and property by incorporating high resolution satellite data and 1-D, 2-D, and 3-D hydrological and hydro-dynamic models [4,7,62]. Several studies have coupled high resolution satellite data with numerical models to evaluate flood risk [5,40]. Studies have indicated that without including the socio-economic data with the meteorological, geomorphological, geological, and historical flood data, the flood risk assessment will be considered as unfinished work [43,58,61]. The present study has employed MCDM approaches for flood risk mapping, which has used very limited input parameters. The socio-economic data were utilized from the Census 2011 survey report which is a decade-old dataset. As the latest Census dataset are not available, the derived SEI from Census 2011 dataset may be underestimated the vulnerability. Accordingly, the risk map of the present study may be underestimated flood-related vulnerability and risk. The availability of updated socio-economic data could lead to evaluate flood risk zone more efficiently. Nevertheless, the derived flood risk maps would be helpful to develop a flood preparedness plan during the mitigation process and risk assessment. Additional limitations of this study are unavailability of historical flood data and several hydro-climatic data. This study involved coarse spatial but high temporal resolution optical remote sensing satellite data (MOD09A1) to evaluate flood hazard over North Bihar. To overcome the shortcoming of optical remote sensing data owing to cloud cover, SAR-based satellite data can be used to map flood extent by integrating with several hydrodynamic and deep learning-based models.

It is worth mentioning that there is a scope to use high-resolution DEM data along with additional and updated socio-economic parameters and flood conditioning factors (i.e., geomorphology, Topographic wetness index, soil texture, curvature, and geology, among others) for flood risk zone mapping. More in-situ data can also be used to strengthen the models as well as the analysis. The AHP method coupled with GIS has been widely used for Flood susceptibility mapping (FSM), but other approaches, namely frequency ratio, fuzzy

logic, machine learning (e.g., support vector machines), artificial neural network (ANN), and hydrological models (e.g., SWAT, HEC-RAS, MIKE) can be applied for identifying the flood risk zones accurately.

6. Conclusions

The present study has demonstrated the utility of multi-temporal satellite images of MOD09A1 in understanding flood inundation dynamics (i.e., flood progression and regression) during 2001–2020. Furthermore, the potential of satellite-derived flood frequency map and socio-economic data in assessing flood hazard, vulnerability, and risk. The key findings suggested that flood events of 2007, 2017, 2019, and 2020 were the major disasters due to heavy downpours which inundated 6.4%, 5.8%, 13.8%, and 17.7% of total North Bihar's geographical area, respectively. Flood frequency exhibited that nearly 7% and 8% of the area of North Bihar is categorized under very high and high hazard category. As per the composite flood inundation over 2001–2020, ~34% of the total geographical area was affected and among the LULC category, agricultural land and settlement were adversely affected. Census of India (2011) based composite socio-economic vulnerability map showed that the central part of North Bihar region and preferably region along the rivers are having greater vulnerability which is further proved based on flood risk map. The flood risk map also showed that the central North Bihar region along the river was categorized in high to very high flood risk zone, affecting 6305 villages.

Based on the capability of space-based data and its cost-effectiveness in flood disaster management, satellite data are useful for monitoring flood patterns as well as flood occurrences. The MCDM approaches can help disaster managers in the state to take mitigation measures for prioritizing susceptible zones and flood mitigation measures. The digital spatial database on the spatial distribution of flood hazards prepared for the North Bihar state will serve as important baseline information for taking up flood mitigation activities and also assist in taking flood insurance measures in flood-affected regions. The inundation map and associated impact and risk information will help decision-makers to provide an operational service for flood management.

Author Contributions: G.T., A.C.P. and B.R.P.: Conceptualization, Investigation, Methodology, Software, Analysis, Visualization, writing—original draft, review and editing. All authors have read and agreed to the published version of the manuscript.

Funding: This research received no external funding.

Institutional Review Board Statement: Not applicable.

Informed Consent Statement: Not applicable.

Data Availability Statement: Publicly available datasets were analyzed in this study. This data can be found from the Source mentioned in Table 1.

Acknowledgments: Our sincere thanks to LP DAAC, Alaska Satellite Facility (ASF), Copernicus ESA, CHRS Data Portal, and Census of India for providing MOD09A1, Land Use Land Cover product, Rainfall data, and Socio-economic data, respectively used in this study. We also thank FMISC, Patna for providing flood maps during 2001–2020.

Conflicts of Interest: The authors declare no conflict of interest.

Appendix A

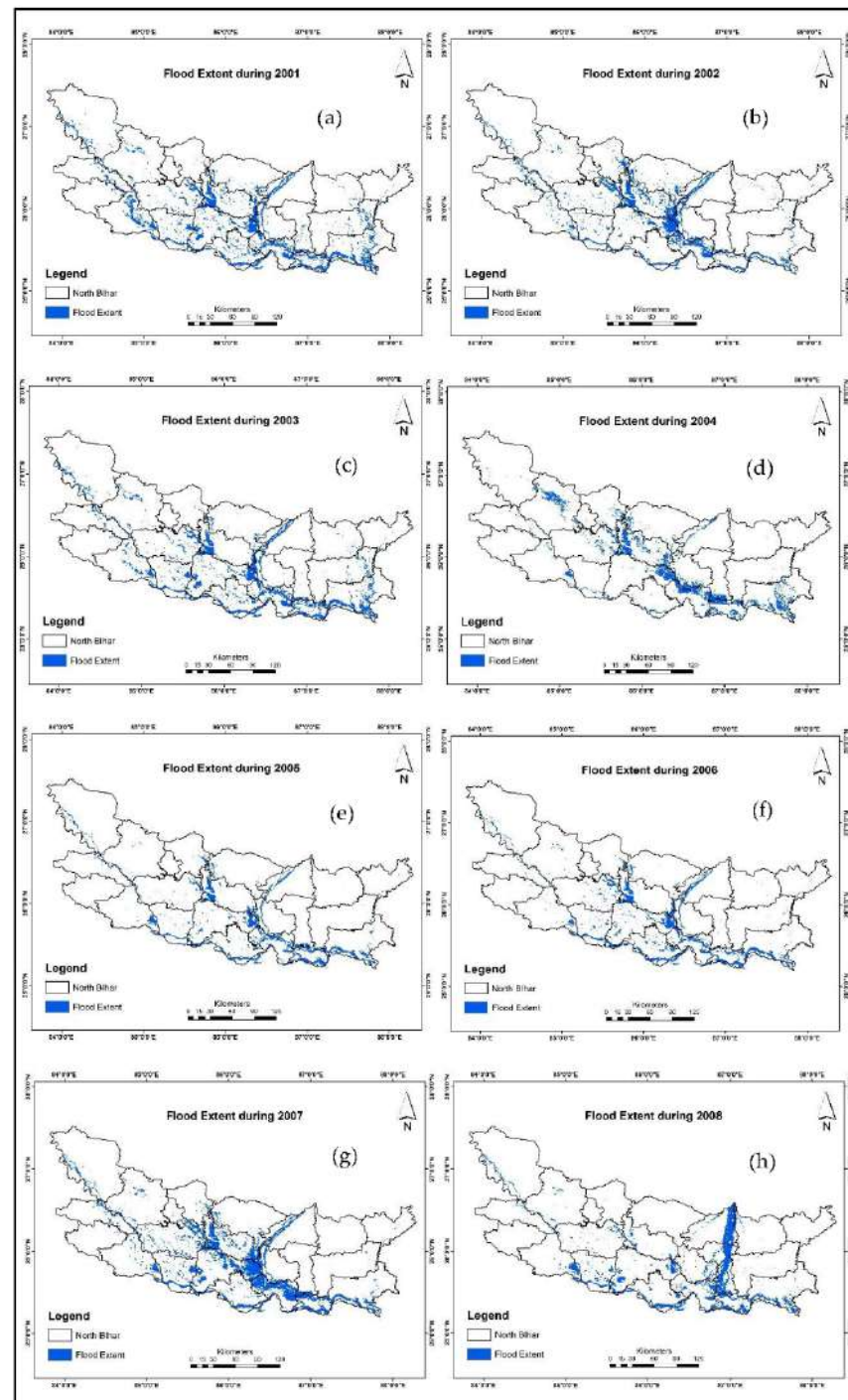


Figure A1. Cont.

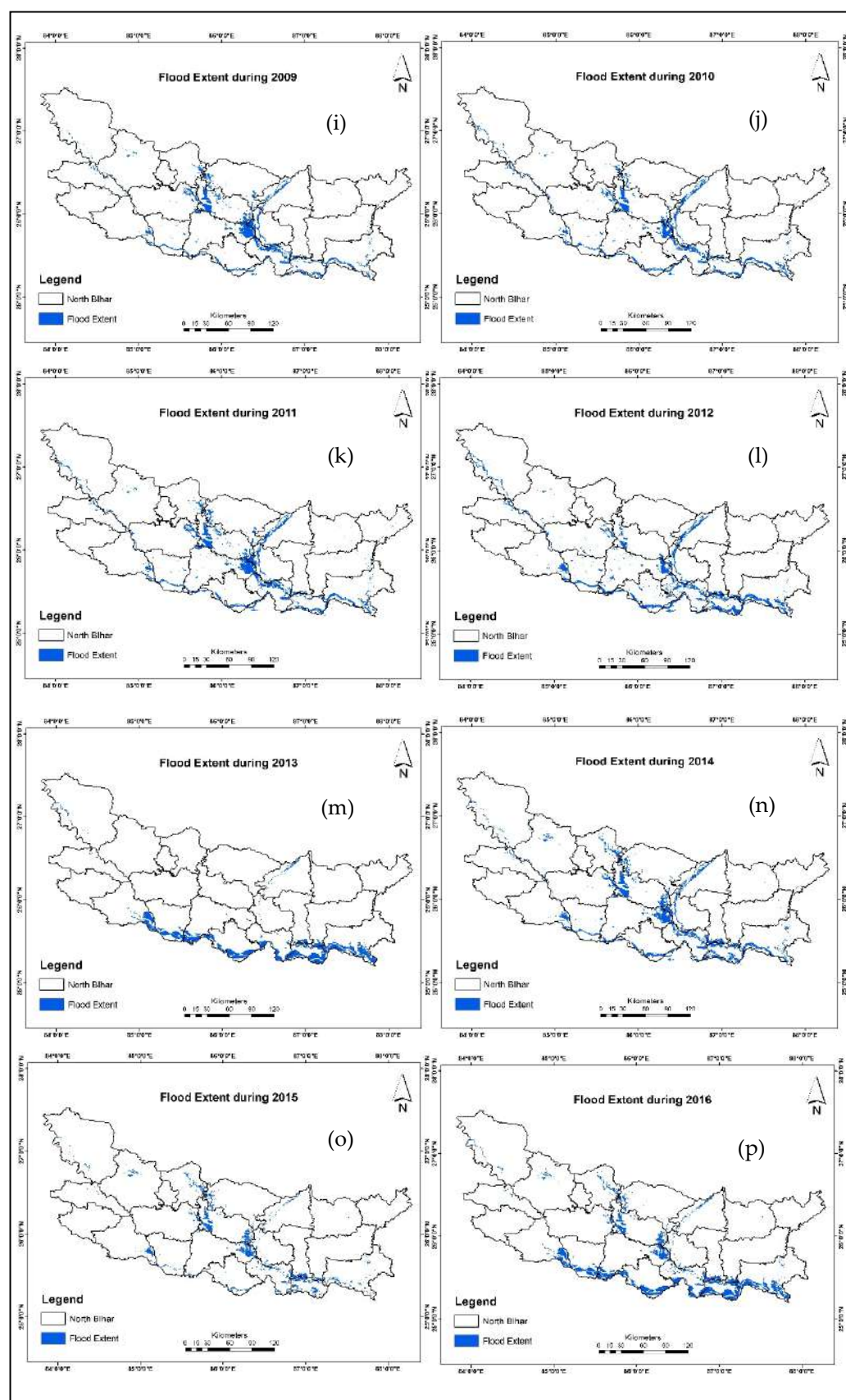


Figure A1. Cont.

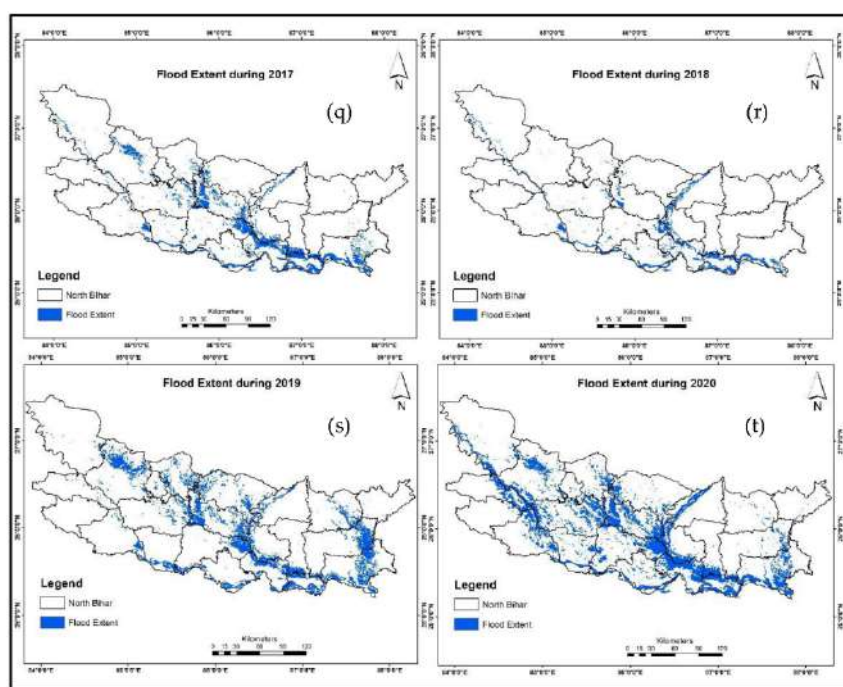


Figure A1. Annual flood extent map during 2001–2020 based on multiple indices from MOD09A1 reflectance data. (a) Flood Extent during 2001, (b) Flood Extent during 2002, (c) Flood Extent during 2003, (d) Flood Extent during 2004, (e) Flood Extent during 2005, (f) Flood Extent during 2006, (g) Flood Extent during 2007, (h) Flood Extent during 2008, (i) Flood Extent during 2009, (j) Flood Extent during 2010, (k) Flood Extent during 2011, (l) Flood Extent during 2012, (m) Flood Extent during 2013, (n) Flood Extent during 2014, (o) Flood Extent during 2015, (p) Flood Extent during 2016, (q) Flood Extent during 2017, (r) Flood Extent during 2018, (s) Flood Extent during 2019, (t) Flood Extent during 2020.

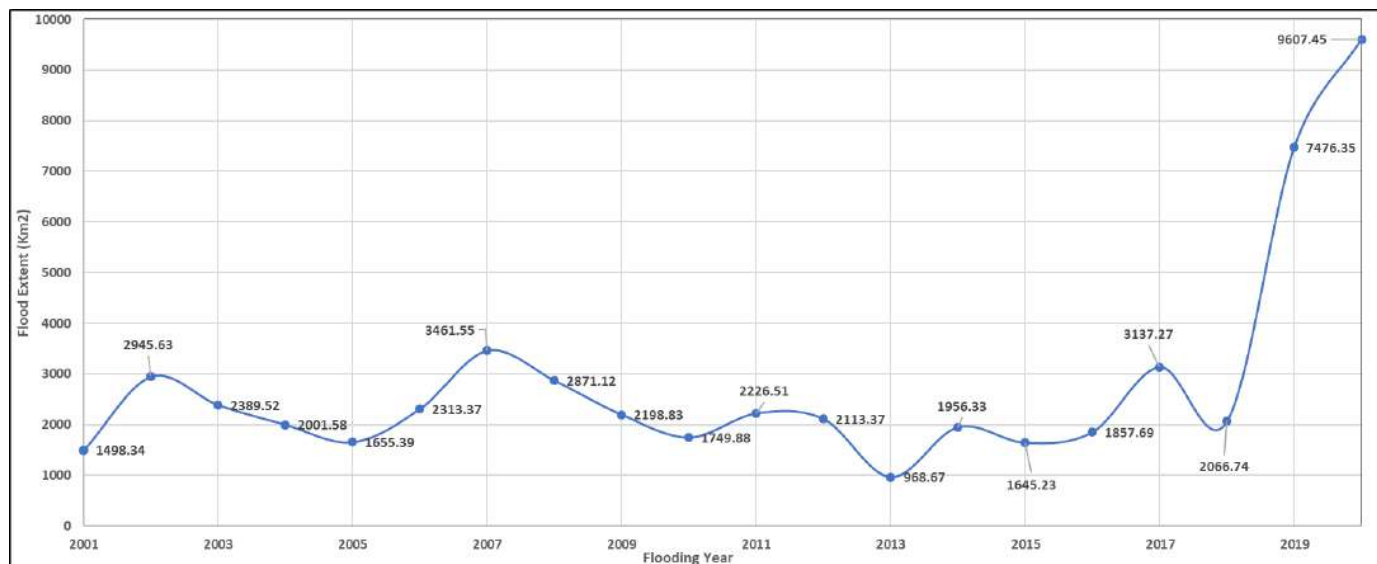


Figure A2. Flooding year with respect to the flood extent (in km^2) during 2001–2020.

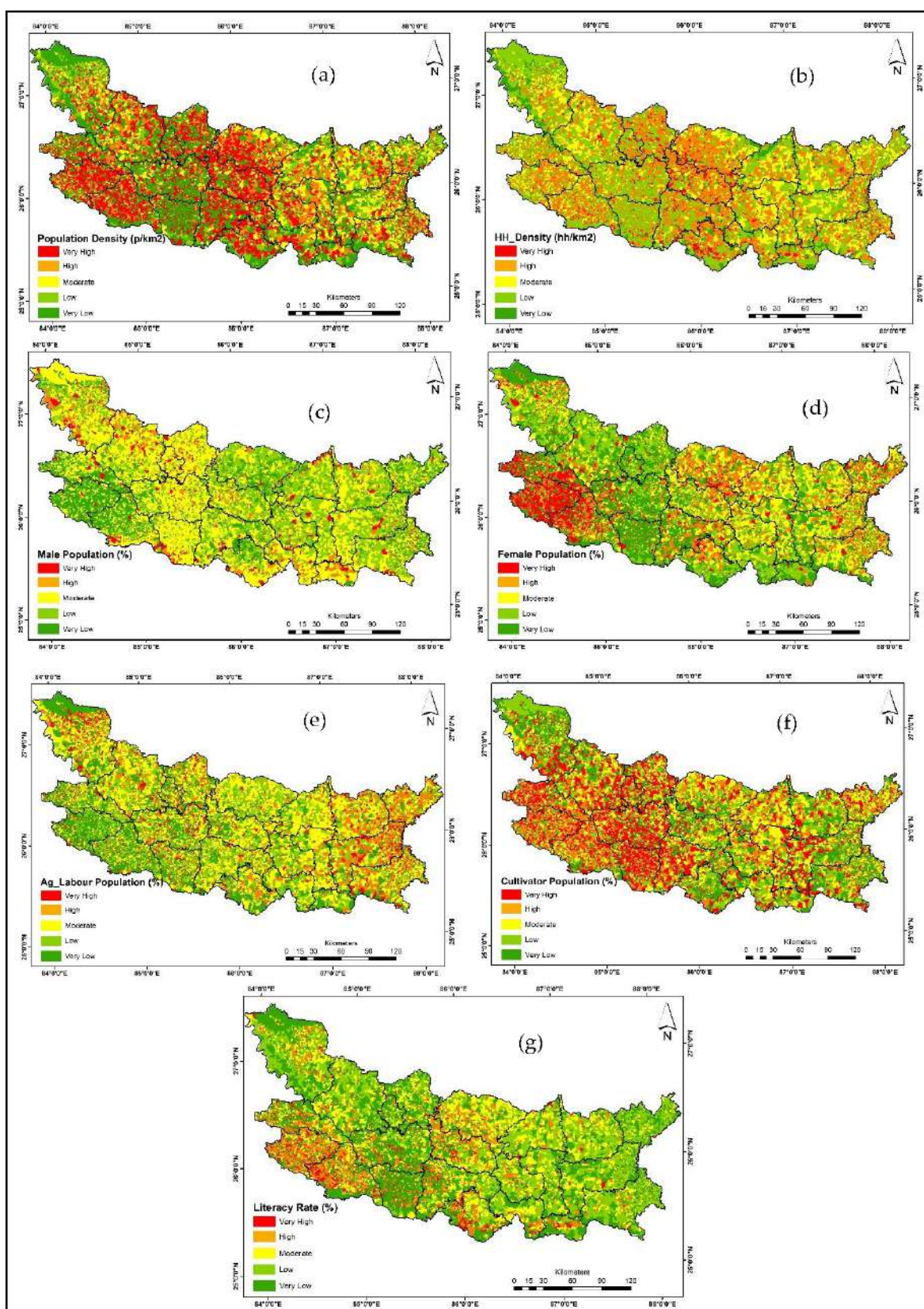


Figure A3. Socio-economic indicators map showing (a) population density (p/km^2), (b) house-hold density (hh/km^2), (c) male population (%), (d) female population (%), (e) agricultural labour (%), (f) cultivator population (%), and (g) literacy rate (%).

References

- Samela, C.; Manfreda, S.; Troy, T.J. Dataset of 100-Year Flood Susceptibility Maps for the Continental U.S. Derived with a Geomorphic Method. *Data Brief* **2017**, *12*, 203–207. [\[CrossRef\]](#)
- Tripathi, G.; Parida, B.R.; Pandey, A.C. Spatio-Temporal Rainfall Variability and Flood Prognosis Analysis Using Satellite Data over North Bihar during the August 2017 Flood Event. *Hydrology* **2019**, *6*, 38. [\[CrossRef\]](#)
- Blöschl, G.; Hall, J.; Viglione, A.; Perdigão, R.A.P.; Parajka, J.; Merz, B.; Lun, D.; Arheimer, B.; Aronica, G.T.; Bilibashi, A.; et al. Changing Climate Both Increases and Decreases European River Floods. *Nature* **2019**, *573*, 108–111. [\[CrossRef\]](#)
- Loukas, A.; Garrote, L.; Vasilades, L. Hydrological and Hydro-Meteorological Extremes and Related Risk and Uncertainty. *Water* **2021**, *13*, 377. [\[CrossRef\]](#)
- Haltas, I.; Demir, I.; Yildirim, E.; Oztas, F. A Comprehensive Flood Event Specification and Inventory: 1930–2020 Turkey Case Study. *Int. J. Disaster Risk Reduct.* **2021**, *56*, 102086. [\[CrossRef\]](#)
- Kulp, S.A.; Strauss, B.H. New Elevation Data Triple Estimates of Global Vulnerability to Sea-Level Rise and Coastal Flooding. *Nat. Commun.* **2019**, *10*, 4844. [\[CrossRef\]](#)
- Shivaprasad Sharma, S.V.; Sharma, S.; Roy, P.S. Extraction of Detailed Level Flood Hazard Zones Using Multi-Temporal Historical Satellite Data-Sets—A Case Study of Kopili River Basin, Assam, India. *Geomat. Nat. Hazards Risk* **2017**, *8*, 792–802. [\[CrossRef\]](#)
- IPCC, 2021: *Climate Change 2021: The Physical Science Basis. Contribution of Working Group I to the Sixth Assessment Report of the Intergovernmental Panel on Climate Change*; Cambridge University Press: Cambridge, UK, 2021.
- Boyaj, A.; Ashok, K.; Ghosh, S.; Devanand, A.; Dandu, G. The Chennai Extreme Rainfall Event in 2015: The Bay of Bengal Connection. *Clim. Dyn.* **2018**, *50*, 2867–2879. [\[CrossRef\]](#)
- Chandrababu, D. Record Rainfall Wreaks Havoc in Chennai. *Hindustan Times New Delhi*, 8 November 2021. Available online: <https://www.hindustantimes.com/india-news/record-rainfall-wreaks-havoc-in-chennai-101636310510384.html> (accessed on 25 November 2021).
- Bisht, D.S.; Chatterjee, C.; Kalakoti, S.; Upadhyay, P.; Sahoo, M.; Panda, A. Modeling Urban Floods and Drainage Using SWMM and MIKE URBAN: A Case Study. *Nat. Hazards* **2016**, *84*, 749–776. [\[CrossRef\]](#)
- Alahcoon, N.; Matheswaran, K.; Pani, P.; Amarnath, G. A Decadal Historical Satellite Data and Rainfall Trend Analysis (2001–2016) for Flood Hazard Mapping in Sri Lanka. *Remote Sens.* **2018**, *10*, 448. [\[CrossRef\]](#)
- Belabid, N.; Zhao, F.; Brocca, L.; Huang, Y.; Tan, Y. Near-Real-Time Flood Forecasting Based on Satellite Precipitation Products. *Remote Sens.* **2019**, *11*, 252. [\[CrossRef\]](#)
- Rai, P.K.; Singh, P.; Mishra, V.N.; Kumar, J.; Sahoo, S. Monitoring North Bihar Flood of 2020 Using Geospatial Technologies. In *It Is Correct Recent Technologies for Disaster Management and Risk Reduction*; Earth and Environmental Sciences Library; Springer International Publishing: New York, NY, USA, 2021; pp. 135–155. ISBN 978-3-030-76115-8.
- Matheswaran, K.; Alahcoon, N.; Pandey, R.; Amarnath, G. Flood Risk Assessment in South Asia to Prioritize Flood Index Insurance Applications in Bihar, India. *Geomat. Nat. Hazards Risk* **2019**, *10*, 26–48. [\[CrossRef\]](#)
- Parida, B.R.; Tripathi, G.; Pandey, A.C.; Kumar, A. Estimating Floodwater Depth Using SAR-Derived Flood Inundation Maps and Geomorphic Model in Kosi River Basin (India). *Geocarto Int.* **2021**, *1*–26. [\[CrossRef\]](#)
- McFeeters, S.K. The Use of the Normalized Difference Water Index (NDWI) in the Delineation of Open Water Features. *Int. J. Remote Sens.* **1996**, *17*, 1425–1432. [\[CrossRef\]](#)
- Guerschman, J.P.; Warren, G.; Byrne, G.; Lymburner, L.; Mueller, N.; Van Dijk, A.I.J.M. MODIS-Based Standing Water Detection for Flood and Large Reservoir Mapping: Algorithm Development and Applications for the Australian Continent. *CSIRO* **2011**. [\[CrossRef\]](#)
- Singh, K.V.; Setia, R.; Sahoo, S.; Prasad, A.; Pateriya, B. Evaluation of NDWI and MNDWI for Assessment of Waterlogging by Integrating Digital Elevation Model and Groundwater Level. *Geocarto Int.* **2015**, *30*, 650–661. [\[CrossRef\]](#)
- Patel, N.R.; Mukund, A.; Parida, B.R. Satellite-Derived Vegetation Temperature Condition Index to Infer Root Zone Soil Moisture in Semi-Arid Province of Rajasthan, India. *Geocarto Int.* **2022**, *37*, 179–195. [\[CrossRef\]](#)
- Sakamoto, T.; Van Nguyen, N.; Kotera, A.; Ohno, H.; Ishitsuka, N.; Yokozawa, M. Detecting Temporal Changes in the Extent of Annual Flooding within the Cambodia and the Vietnamese Mekong Delta from MODIS Time-Series Imagery. *Remote Sens. Environ.* **2007**, *109*, 295–313. [\[CrossRef\]](#)
- Zhou, S.L.; Zhang, W.C. Flood Monitoring and Damage Assessment in Thailand Using Multi-Temporal HJ-1A/1B and MODIS Images. *IOP Conf. Ser. Earth Environ. Sci.* **2017**, *57*, 012016. [\[CrossRef\]](#)
- Sajjad, A.; Lu, J.; Chen, X.; Saleem, N. Rapid Riverine Flood Mapping with Different Water Indexes Using Flood Instances Landsat-8 Images. In Proceedings of the 5th International Electronic Conference on Water Sciences, Online, 16–30 November 2020; MDPI: Basel, Switzerland, 2020; p. 8049. Available online: <http://sciforum.net/conference/ECWS-5/paper/8049> (accessed on 13 November 2020).
- Jain, S.K.; Singh, R.D.; Jain, M.K.; Lohani, A.K. Delineation of Flood-Prone Areas Using Remote Sensing Techniques. *Water Resour. Manag.* **2005**, *19*, 333–347. [\[CrossRef\]](#)
- Kumar, R.; Singh, R.; Gautam, H.; Pandey, M.K. Flood Hazard Assessment of August 20, 2016 Floods in Satna District, Madhya Pradesh, India. *Remote Sens. Appl. Soc. Environ.* **2018**, *11*, 104–118. [\[CrossRef\]](#)
- Shakya, A.; Biswas, M.; Pal, M. CNN-Based Fusion and Classification of SAR and Optical Data. *Int. J. Remote Sens.* **2020**, *41*, 8839–8861. [\[CrossRef\]](#)

27. Haque, M.M.; Seidou, O.; Mohammadian, A.; Gado Djibo, A. Development of a Time-Varying MODIS/2D Hydrodynamic Model Relationship between Water Levels and Flooded Areas in the Inner Niger Delta, Mali, West Africa. *J. Hydrol. Reg. Stud.* **2020**, *30*, 100703. [\[CrossRef\]](#)
28. Mekanik, F.; Imteaz, M.A.; Gato-Trinidad, S.; Elmahdi, A. Multiple Regression and Artificial Neural Network for Long-Term Rainfall Forecasting Using Large Scale Climate Modes. *J. Hydrol.* **2013**, *503*, 11–21. [\[CrossRef\]](#)
29. Xu, Z.X.; Li, J.Y. Short-Term Inflow Forecasting Using an Artificial Neural Network Model. *Hydrol. Process.* **2002**, *16*, 2423–2439. [\[CrossRef\]](#)
30. Abbot, J.; Marohasy, J. Input Selection and Optimisation for Monthly Rainfall Forecasting in Queensland, Australia, Using Artificial Neural Networks. *Atmos. Res.* **2014**, *138*, 166–178. [\[CrossRef\]](#)
31. Gizaw, M.S.; Gan, T.Y. Regional Flood Frequency Analysis Using Support Vector Regression under Historical and Future Climate. *J. Hydrol.* **2016**, *538*, 387–398. [\[CrossRef\]](#)
32. Mosavi, A.; Ozturk, P.; Chau, K. Flood Prediction Using Machine Learning Models: Literature Review. *Water* **2018**, *10*, 1536. [\[CrossRef\]](#)
33. Shakya, A.; Biswas, M.; Pal, M. Parametric Study of Convolutional Neural Network Based Remote Sensing Image Classification. *Int. J. Remote Sens.* **2021**, *42*, 2663–2685. [\[CrossRef\]](#)
34. Sinha, R.; Bapalu, G.V.; Singh, L.K.; Rath, B. Flood Risk Analysis in the Kosi River Basin, North Bihar Using Multi-Parametric Approach of Analytical Hierarchy Process (AHP). *J. Indian Soc. Remote Sens.* **2008**, *36*, 335–349. [\[CrossRef\]](#)
35. Mishra, K.; Sinha, R. Flood Risk Assessment in the Kosi Megafan Using Multi-Criteria Decision Analysis: A Hydro-Geomorphic Approach. *Geomorphology* **2020**, *350*, 106861. [\[CrossRef\]](#)
36. Baky, M.A.A.; Islam, M.; Paul, S. Flood Hazard, Vulnerability and Risk Assessment for Different Land Use Classes Using a Flow Model. *Earth Syst. Environ.* **2020**, *4*, 225–244. [\[CrossRef\]](#)
37. Islam, M.M.; Sado, K. Development of Flood Hazard Maps of Bangladesh Using NOAA-AVHRR Images with GIS. *Hydrol. Sci. J.* **2000**, *45*, 337–355. [\[CrossRef\]](#)
38. Jha, R.K.; Gundimeda, H. An Integrated Assessment of Vulnerability to Floods Using Composite Index—A District Level Analysis for Bihar, India. *Int. J. Disaster Risk Reduct.* **2019**, *35*, 101074. [\[CrossRef\]](#)
39. Basheer Ahammed, K.K.; Pandey, A.C. Coastal Social Vulnerability and Risk Analysis for Cyclone Hazard Along the Andhra Pradesh, East Coast of India. *KN J. Cartogr. Geogr. Inf.* **2019**, *69*, 285–303. [\[CrossRef\]](#)
40. Phongsapan, K.; Chishtie, F.; Poortinga, A.; Bhandari, B.; Meechaiya, C.; Kunlamai, T.; Aung, K.S.; Saah, D.; Anderson, E.; Markert, K.; et al. Operational Flood Risk Index Mapping for Disaster Risk Reduction Using Earth Observations and Cloud Computing Technologies: A Case Study on Myanmar. *Front. Environ. Sci.* **2019**, *7*, 191. [\[CrossRef\]](#)
41. Deepak, S.; Rajan, G.; Jairaj, P.G. Geospatial Approach for Assessment of Vulnerability to Flood in Local Self Governments. *GeoenvIRON. Disasters* **2020**, *7*, 35. [\[CrossRef\]](#)
42. Hazarika, N.; Barman, D.; Das, A.K.; Sarma, A.K.; Borah, S.B. Assessing and Mapping Flood Hazard, Vulnerability and Risk in the Upper Brahmaputra River Valley Using Stakeholders' Knowledge and Multicriteria Evaluation (MCE): Assessing and Mapping Flood Hazard. *J. Flood Risk Manag.* **2018**, *11*, S700–S716. [\[CrossRef\]](#)
43. Shadmehri Toosi, A.; Calbimonte, G.H.; Nouri, H.; Alaghmand, S. River Basin-Scale Flood Hazard Assessment Using a Modified Multi-Criteria Decision Analysis Approach: A Case Study. *J. Hydrol.* **2019**, *574*, 660–671. [\[CrossRef\]](#)
44. Burn, D.H.; Goel, N.K. The Formation of Groups for Regional Flood Frequency Analysis. *Hydrol. Sci. J.* **2000**, *45*, 97–112. [\[CrossRef\]](#)
45. Roder, G.; Hudson, P.; Tarolli, P. Flood Risk Perceptions and the Willingness to Pay for Flood Insurance in the Veneto Region of Italy. *Int. J. Disaster Risk Reduct.* **2019**, *37*, 101172. [\[CrossRef\]](#)
46. Hudson, P.; Botzen, W.J.W.; Aerts, J.C.J.H. Flood Insurance Arrangements in the European Union for Future Flood Risk under Climate and Socioeconomic Change. *Glob. Environ. Chang.* **2019**, *58*, 101966. [\[CrossRef\]](#)
47. Masood, M.; Takeuchi, K. Assessment of Flood Hazard, Vulnerability and Risk of Mid-Eastern Dhaka Using DEM and 1D Hydrodynamic Model. *Nat. Hazards* **2012**, *61*, 757–770. [\[CrossRef\]](#)
48. Hoque, M.A.-A.; Ahmed, N.; Pradhan, B.; Roy, S. Assessment of Coastal Vulnerability to Multi-Hazardous Events Using Geospatial Techniques along the Eastern Coast of Bangladesh. *Ocean. Coast. Manag.* **2019**, *181*, 104898. [\[CrossRef\]](#)
49. Bhatt, C.M.; Gupta, A.; Roy, A.; Dalal, P.; Chauhan, P. Geospatial Analysis of September, 2019 Floods in the Lower Gangetic Plains of Bihar Using Multi-Temporal Satellites and River Gauge Data. *Geomat. Nat. Hazards Risk* **2021**, *12*, 84–102. [\[CrossRef\]](#)
50. Manjusree, P.; Bhatt, C.M.; Begum, A.; Rao, G.S.; Bhanumurthy, V. A Decadal Historical Satellite Data Analysis for Flood Hazard Evaluation: A Case Study of Bihar (North India). *Singap. J. Trop. Geogr.* **2015**, *36*, 308–323. [\[CrossRef\]](#)
51. Tripathi, G.; Pandey, A.C.; Parida, B.R.; Shakya, A. Comparative Flood Inundation Mapping Utilizing Multi-Temporal Optical and SAR Satellite Data Over North Bihar Region: A Case Study of 2019 Flooding Event Over North Bihar. In *Spatial Information Science for Natural Resource Management; Advances in Environmental Engineering and Green Technologies*; IGI Publisher: Hershey, PA, USA, 2020; p. 20, ISBN 978-1-79985-027-4.
52. Pandey, A.C.; Singh, S.K.; Nathawat, M.S. Waterlogging and Flood Hazards Vulnerability and Risk Assessment in Indo Gangetic Plain. *Nat. Hazards* **2010**, *55*, 273–289. [\[CrossRef\]](#)
53. Gaurav, K.; Métivier, F.; Devauchelle, O.; Sinha, R.; Chauvet, H.; Houssais, M.; Bouquerel, H. Morphology of the Kosi Megafan Channels. *Earth Surf. Dyn.* **2015**, *3*, 321–331. [\[CrossRef\]](#)

54. Tripathi, G.; Pandey, A.C.; Parida, B.R.; Kumar, A. Flood Inundation Mapping and Impact Assessment Using Multi-Temporal Optical and SAR Satellite Data: A Case Study of 2017 Flood in Darbhanga District, Bihar, India. *Water Resour. Manag.* **2020**, *34*, 1871–1892. [[CrossRef](#)]
55. Xu, H. Modification of Normalised Difference Water Index (NDWI) to Enhance Open Water Features in Remotely Sensed Imagery. *Int. J. Remote Sens.* **2006**, *27*, 3025–3033. [[CrossRef](#)]
56. Jiang, Z.; Huete, A.; Didan, K.; Miura, T. Development of a Two-Band Enhanced Vegetation Index without a Blue Band. *Remote Sens. Environ.* **2008**, *112*, 3833–3845. [[CrossRef](#)]
57. Parida, B.R.; Kumari, A. Mapping and Modeling Mangrove Biophysical and Biochemical Parameters Using Sentinel-2A Satellite Data in Bhitarkanika National Park, Odisha. *Model. Earth Syst. Environ.* **2021**, *7*, 2463–2474. [[CrossRef](#)]
58. Cutter, S.L. The Vulnerability of Science and the Science of Vulnerability. *Ann. Assoc. Am. Geogr.* **2003**, *93*, 1–12. [[CrossRef](#)]
59. Sarkar, D.; Saha, S.; Mondal, P. GIS-Based Frequency Ratio and Shannon’s Entropy Techniques for Flood Vulnerability Assessment in Patna District, Central Bihar, India. *Int. J. Environ. Sci. Technol.* **2021**, *1*–22. [[CrossRef](#)]
60. Singh, S.K.; Pandey, A.C. Geomorphology and the Controls of Geohydrology on Waterlogging in Gangetic Plains, North Bihar, India. *Environ. Earth Sci.* **2014**, *71*, 1561–1579. [[CrossRef](#)]
61. Gaurav, K.; Tandon, S.K.; Devauchelle, O.; Sinha, R.; Métivier, F. A Single Width–Discharge Regime Relationship for Individual Threads of Braided and Meandering Rivers from the Himalayan Foreland. *Geomorphology* **2017**, *295*, 126–133. [[CrossRef](#)]
62. Amarnath, G.; Matheswaran, K.; Pandey, P.; Alahcoon, N.; Yoshimoto, S. Flood mapping tools for disaster preparedness and emergency response using satellite data and hydrodynamic models: A case study of Bagmati Basin, India. *Proc. Natl. Acad. Sci. India Sect. A Phys. Sci.* **2017**, *4*, 941–950. [[CrossRef](#)]

क्रमांक (Sr. No.)

1898644

86107592

शिक्षा परिषद्. उत्तर प्रदेश

Board of High School and Intermediate Education, U.P.



हाईस्कूल परीक्षा-२००७ High School Examination - 2007

प्रमाणपत्र-सह-अकापत्र (CERTIFICATE-CUM-MARKS SHEET)

अनुक्रमांक Roll No.	जनपद/केन्द्र/विद्यालय कोड Distt./Centre/School Code	संस्थागत/व्यवितरण Regular / Private	परीक्षा प्रवर्ग Exam. Type	प्रमाणपत्र क्रमांक Certificate No.
2760726	86/21254 /1041	REGULAR	FULL EXAM	86121219

प्रमाणित किया जाता है कि (This is to certify that)

परिषद् के अभिलेखानुसार (according to the Board's record)-

GAURAV TRIPATHI

आत्मज / आत्मजा श्रीमती (son/daughter of Mrs.)-

KUSUM LATA TRIPATHI

एवं श्री (and Mr.)-

DILEEP KUMAR TRIPATHI

जिनकी जन्मतिथि (whose date of birth is)-

15TH JULY NINETEEN HUNDRED NINETY TWO (15-07-92)

ने मार्च/अप्रैल 2007 की हाईस्कूल परीक्षा विद्यालय/केन्द्र (has passed High School Examination held in March/April-2007 from

School/Centre)- A N GOVT INTER COLLEGE CHAKIA CHANDAULI

से श्रेणी (with division)- FIRST

में उत्तीर्ण की है।

परीक्षार्थी द्वारा उत्तीर्ण विषयों के प्राप्तांक निम्नवत् हैं (Marks obtained by the candidate in passed subjects are as under):-

विषय Subjects	अधिकतम अंक Max. Marks	विषयवार प्राप्तांक एवं प्रयोगात्मक विषयों के ग्रेड Paper-wise Obtained Marks with Grades in Prct. Subj.				योग Total	सम्पूर्ण योग एवं परीक्षाफल Grand Total & Result
HINDI	100	1/28	2/35			063	360
ENGLISH	100	1/34	2/28			062	PASSED
SANSKRIT	100	1/58				058	
MATHEMATICS	100	1/22	2/30			052	
SCIENCE	100	1/27	2/10	3/27	GR-A	064	
SOCIAL SCIENCE	100	1/29	2/32			061	

Category of Moral, Sports and Physical Education-

A

'D' indicates Distinction in that particular subject.

'HONOURS' indicates candidate "passed with honour".

Note : For Important Instructions see overleaf.

तिथि (Date)- 5TH JUNE 2007

स्थान (Place)-Allahabad, Uttar Pradesh(India).


 (बासुदेव यादव)
 (Basudeo Yadav)
 सचिव / Secretary

Manabendra Saharia

Address and Contact Information

Assistant Professor, Department of Civil Engineering

Associate Faculty, Yardi School of Artificial Intelligence

V-224, Department of Civil Engineering, Indian Institute of Technology Delhi, Hauz Khas, Delhi 110016, India

 [Google Scholar](#) |  [ResearchGate](#) |  [Github](#) |  [LinkedIn](#) |  [Twitter](#) | CV Updated: June 2023

 [Work Email](mailto:msaharia@iitd.ac.in): msaharia@iitd.ac.in |  [Personal Email](mailto:msaharia@live.com): msaharia@live.com |  [Office](tel:+91-011-26591260): +91-011-26591260

 [IIT Delhi Lab](https://hydrosense.iitd.ac.in/): <https://hydrosense.iitd.ac.in/> |  [Personal Website](https://www.msaharia.com/): <https://www.msaharia.com/>

Research Bio

My passion lies in developing solutions for reducing the impact of natural hazards and advancing sustainable water resources management. My current focus is on developing cutting-edge techniques for forecasting and mitigating the effects of floods, droughts, and landslides at local to global scales. My research seeks to unravel the complex interplay between climate, precipitation, land surface, and water flow, utilizing physics-based and machine learning models.

Research Interests

Land surface modeling, AI/ML applications, Hydrometeorology, flood forecasting, radar/satellite precipitation, citizen science, landslides.

Experience

2020-now **Assistant Professor, Indian Institute of Technology Delhi.**

○ Dept. of Civil Engineering & Yardi School of Artificial Intelligence (Associate Faculty)

2019 **Postdoctoral Research Associate, NASA Goddard Space Flight Center, USA.**

○ A West Africa Land Data Assimilation System for Forecasting Extreme Hydrological Events

2017-18 **Postdoctoral Fellow, National Center for Atmospheric Research (NCAR), Colorado, USA.**

○ (1) Developing a real-time and distributed HUC-based modeling system for ensemble streamflow forecasting over large domains. (2) Uncertainty quantification and sensitivity analysis of flood frequency estimates.

2013-17 **Advanced Radar Research Center, National Weather Center/The University of Oklahoma.**

2011-13 **Hydrology and Water Resources Laboratory, University of Texas at Arlington.**

Education

2013-17 **Ph.D. in Water Resources Engineering, The University of Oklahoma, USA.**

○ Dissertation: Characterization and Prediction of Flash Flood Severity.

○ Advisors: Dr. Yang Hong and Dr. Jonathan Gourley

2011-13 **M.S. in Water Resources Engineering, The University of Texas at Arlington, USA.**

○ Thesis: Ensemble Streamflow Forecasting For The Upper Trinity River Basin In Texas

2007-11 **B.Tech. in Civil Engineering, National Institute of Technology, Silchar, Assam, India.**

○ Major Project: Flood Forecasting in Multiple River Sections using Artificial Neural Networks

Awards and Mentions

○ **CDRI (Coalition for Disaster Resilient Infrastructure) Fellowship** for 2023-24

○ **Son of the Soil Award Assam 2022**, Emerging Professional category, March 25, 2023

○ **Visiting Scientist**, Research and Applications Laboratory, National Center for Atmospheric Research, 2023

○ **Guest Professor (Global)**, Keio University, Japan, 2023

○ **Geospatial World 50 Rising Stars 2023**, Geospatial World Forum, Rotterdam, Netherlands.

- **NASI Platinum Jubilee Young Scientist Award**, The National Academy of Sciences, India, 2023
- **Sir CV Raman Young Scientist Award**, The International Society for Energy, Environment and Sustainability (ISEES), 2022
- **French Embassy's Faculty Mobility Initiative Award**, Sponsored Visit to University of Eiffel, 2021
- **Young Faculty Incentive Fellowship**, 2019-2022, IIT Delhi
- **Early Career Scientist Assembly Award**, National Center for Atmospheric Research (NCAR), USA, 2018
- Citation and cash award in the oral presentation category of the Student Water Conference, Oklahoma Water Resources Center, Mar 23, 2017.
- Advanced Radar Research Center Student Paper Cash Award *in recognition of research accomplishments and scholarly publication*
- First prize and cash award in the oral presentation category of the Student Research and Creativity Day, University of Oklahoma, Feb 24, 2017.
- Advanced Radar Research Center Student Paper Cash Award *in recognition of research accomplishments and scholarly publication*
- First prize and cash award in the oral presentation category of the Student Research and Creativity Day, University of Oklahoma, March 4, 2016.
- Student Recognition, President's Monthly Research and Development Highlights, Volume 10, Issue 7, University of Oklahoma, Oct 2015.
- Best Poster Award in the Graduate Student Poster Contest, Annual Meeting of the Society of Environmental Journalists (SEJ), Norman, October 7-11, 2015

Grants and Fellowships

Here, PI - Principal Investigator

Ongoing ## Completed

Funding Agency	Project Title	Role	Amount (INR)	Duration
Ministry of Earth Sciences (MoES)	DeepINDRA: An experimental system for forecasting street-scale flood inundation by coupling physical and deep learning models	PI	62 Lakhs	2023-25 #
Monsoon Mission-III, Ministry of Earth Sciences (MoES)	BrahmaSATARK: A real-time impact-based 2D flood forecasting system for the Brahmaputra River basin using hydrologic-hydrodynamic and statistical-dynamical approaches	PI	73 Lakhs	2023-26 #
DST Indo-Canada IC-IMPACTS	GBM-CLIMPACT: Development of an end- to-end modeling and analysis toolset to assess climate impact and readiness of water sector in the Ganga, Brahmaputra, and Meghna basins	PI	60 Lakhs	2023-25 #
CDRI (Coalition for Disaster Resilient Infrastructure)	Detecting Flood Inundation Using Deep Learning and Citizen ScienceFellowship	Fellow	\$15,000	2023-24 #
IIT Delhi Institute of Excellence (IoE) Grant	Geohazard assessment and mitigation via multiscale digital twinning	Co-PI	74.5 Lakhs	2022-24 #
IIT Delhi Seed Grant	Development of an Interpretable Machine Learning Framework for Detection and Attribution of Hydroclimatic Extremes	PI	20 Lakhs	2021-23 ##
Principal Scientific Adviser to the Government of India	# Portable and High Precision Compact Gravimeter for Field Applications	Co-PI	10 Crores	2021-26 #
Indian Space Research Organization (ISRO)	# Establishing a coupled Indian Land Data Assimilation System (ILDAS) for identifying hydrologic extremes	PI	35 Lakhs	2021-24 #

UCL-IITD Strategic Partner Fund	Making local knowledge matter for landslides and flood-preparedness	PI	5 Lakhs	2020-21 ##
IRD, IIT Delhi	New Faculty Grant	PI	1 Lakh	2019
IIT Delhi	Young Faculty Incentive Fellowship	Fellow	25,000 pm	2019-22

Textbooks

- 2023 "Introduction to Civil Engineering", Textbook for undergraduate students of Civil Engineering, Authors: **Dr. Manabendra Saharia** and Dr. Nagendra R. Velaga, Published by the All India Council for Technical Education (AICTE), 2023. Available in E-Kumbh platform

Journal Publications

- 2023 Ravi Raj, **Saharia, Manabendra**, and Sumedha Chakma. Mapping soil erodibility over India. *CATENA*, volume 230, page 107271, September 2023. [doi:10.1016/j.catena.2023.107271](https://doi.org/10.1016/j.catena.2023.107271).
- 2022 Shruti Dharma Sarma, Akashit Kumar Verma, Saket Sanjay Phadkule, and **Saharia, Manabendra**. Towards an interpretable machine learning model for electrospun polyvinylidene fluoride (PVDF) fiber properties. *Computational Materials Science*, volume 213, page 111661, 2022. [doi:10.1016/j.commatsci.2022.111661](https://doi.org/10.1016/j.commatsci.2022.111661).
- 2022 Ravi Raj, **Saharia, Manabendra**, Sumedha Chakma, and Arezoo Rafieinasab. Mapping rainfall erosivity over India using multiple precipitation datasets. *CATENA*, volume 214, page 106256, 2022. [doi:10.1016/j.catena.2022.106256](https://doi.org/10.1016/j.catena.2022.106256).
- 2022 Sai Kiran Kuntla, **Saharia, Manabendra**, and Pierre Kirstetter. Global-scale characterization of streamflow extremes. *Journal of Hydrology*, volume 615, page 128668, December 2022. [doi:10.1016/j.jhydrol.2022.128668](https://doi.org/10.1016/j.jhydrol.2022.128668).
- 2022 Sushma Kumari, Avinash Chand Yadav, **Saharia, Manabendra**, and Soumyabrata Dev. Spatio-temporal analysis of air quality and its relationship with COVID-19 lockdown over Dublin. *Remote Sensing Applications: Society and Environment*, volume 28, page 100835, 2022. [doi:10.1016/j.rsase.2022.100835](https://doi.org/10.1016/j.rsase.2022.100835).
- 2021 **Saharia, Manabendra**, Pierre-Emmanuel Kirstetter, Humberto Vergara, Jonathan J. Gourley, Isabelle Emmanuel, and Hervé Andrieu. On the Impact of Rainfall Spatial Variability, Geomorphology, and Climatology on Flash Floods. *Water Resources Research*, volume n/a, page e2020WR029124, 2021. [doi:10.1029/2020WR029124](https://doi.org/10.1029/2020WR029124).
- 2021 **Saharia, Manabendra**, Avish Jain, Ronit Raj Baishya, Saagar Haobam, O. P. Sreejith, D. S. Pai, and Arezoo Rafieinasab. India flood inventory: creation of a multi-source national geospatial database to facilitate comprehensive flood research. *Natural Hazards*, March 2021. [doi:10.1007/s11069-021-04698-6](https://doi.org/10.1007/s11069-021-04698-6).
- 2021 Akhil Sanjay Potdar, Pierre-Emmanuel Kirstetter, Devon Woods, and **Saharia, Manabendra**. Towards Predicting Flood Event Peak Discharge in Ungauged Basins by Learning Universal Hydrological Behaviors with Machine Learning. *Journal of Hydrometeorology*, volume -1, August 2021. [doi:10.1175/JHM-D-20-0302.1](https://doi.org/10.1175/JHM-D-20-0302.1). Publisher: American Meteorological Society Section: Journal of Hydrometeorology.
- 2021 A. J. Newman, A. G. Stone, **Saharia, M.**, K. D. Holman, N. Addor, and M. P. Clark. Identifying sensitivities in flood frequency analyses using a stochastic hydrologic modeling system. *Hydrology and Earth System Sciences*, volume 25, pages 5603–5621, 2021. [doi:10.5194/hess-25-5603-2021](https://doi.org/10.5194/hess-25-5603-2021).

- 2018 Sunghee Kim, Hossein Sadeghi, Reza Ahmad Limon, **Saharia, Manabendra**, Dong-Jun Seo, Andrew Philpott, Frank Bell, James Brown, and Minxue He. Assessing the skill of medium-range ensemble precipitation and streamflow forecasts from the Hydrologic Ensemble Forecast Service (HEFS) for the Upper Trinity River Basin in North Texas. *Journal of Hydrometeorology*, August 2018. doi:10.1175/JHM-D-18-0027.1.
- 2017 **Saharia, Manabendra**, Pierre-Emmanuel Kirstetter, Humberto Vergara, Jonathan J. Gourley, Yang Hong, and Marine Giroud. Mapping Flash Flood Severity in the United States. *Journal of Hydrometeorology*, volume 18, pages 397–411, February 2017. doi:10.1175/JHM-D-16-0082.1. Publisher: American Meteorological Society Section: Journal of Hydrometeorology.
- 2017 **Saharia, Manabendra**, Pierre-Emmanuel Kirstetter, Humberto Vergara, Jonathan J. Gourley, and Yang Hong. Characterization of floods in the United States. *Journal of Hydrology*, volume 548, pages 524–535, May 2017. doi:10.1016/j.jhydrol.2017.03.010.
- 2016 Weiyue Li, Chun Liu, Yang Hong, **Saharia, Manabendra**, Weiwei Sun, Dongjing Yao, and Wen Chen. Rainstorm-induced shallow landslides process and evaluation – a case study from three hot spots, China. *Geomatics, Natural Hazards and Risk*, volume 7, pages 1908–1918, November 2016. doi:10.1080/19475705.2016.1179685.
- 2016 Wei-yue Li, Chun Liu, Yang Hong, Xin-hua Zhang, Zhan-ming Wan, **Saharia, Manabendra**, Wei-wei Sun, Dong-jing Yao, Wen Chen, Sheng Chen, Xiu-qin Yang, and Yue Yue. A public Cloud-based China's Landslide Inventory Database (CsLID): development, zone, and spatiotemporal analysis for significant historical events, 1949–2011. *Journal of Mountain Science*, volume 13, pages 1275–1285, July 2016. doi:10.1007/s11629-015-3659-7.
- 2014 Yu Zhang, Yang Hong, Xuguang Wang, Jonathan J. Gourley, Xianwu Xue, **Saharia, Manabendra**, Guangheng Ni, Gaili Wang, Yong Huang, Sheng Chen, and Guoqiang Tang. Hydrometeorological Analysis and Remote Sensing of Extremes: Was the July 2012 Beijing Flood Event Detectable and Predictable by Global Satellite Observing and Global Weather Modeling Systems? *Journal of Hydrometeorology*, volume 16, pages 381–395, October 2014. doi:10.1175/JHM-D-14-0048.1.
- 2014 Yan Shen, Anyuan Xiong, Yang Hong, Jingjing Yu, Yang Pan, Zhuoqi Chen, and **Saharia, Manabendra**. Uncertainty analysis of five satellite-based precipitation products and evaluation of three optimally merged multi-algorithm products over the Tibetan Plateau. *International Journal of Remote Sensing*, volume 35, pages 6843–6858, 2014.
- 2014 Parthajit Roy, **Saharia, Manabendra**, and P. Choudhury. River Reaches Flood Flow Prediction using PRNN Models. *International Journal of Civil, Structural, Environmental and Infrastructure Engineering Research and Development (IJCSEIERD)*, volume 1, pages 119–126, 2014.
- 2013 S. K. Jain, Vijay Kumar, and **Saharia, M.** Analysis of rainfall and temperature trends in northeast India. *International Journal of Climatology*, volume 33, pages 968–978, 2013. doi:https://doi.org/10.1002/joc.3483. eprint: https://rmets.onlinelibrary.wiley.com/doi/pdf/10.1002/joc.3483.
- 2012 **Saharia, Manabendra** and Rajib Kumar Bhattacharjya. Geomorphology-based Time-Lagged Recurrent Neural Networks for runoff forecasting. *KSCE Journal of Civil Engineering*, volume 16, pages 862–869, July 2012. doi:10.1007/s12205-012-1463-2.

Book Chapters

- 2016 **Saharia, Manabendra**, Li Li, Yang Hong, Jiahua Wang, Robert Adler, Fritz Policelli, Shahid Habib, D. Irwin, Tesfaye Korme, and Lawrence Okello. Real-Time Hydrologic Prediction System in East Africa through SERVIR: Capacity Building for Sustainability and Resilience. pages 247–258. October 2016.

2016 Yan Shen, Anyuan Xiong, Yang Hong, Jingjing Yu, Yang Pan, Zhuoqi Chen, and **Saharia, Man-abendra**. Uncertainty Analysis of Five Satellite-Based Precipitation Products and Evaluation of Three Optimally Merged Multialgorithm Products over the Tibetan Plateau: Capacity Building for Sustainability and Resilience. pages 215–232. October 2016.

Teaching Experience

- Instructor, CVP735 Finite Element Methods, IIT Delhi, 2022
- Instructor, CVL834 Urban Water Infrastructure, IIT Delhi, 2021
- Instructor, CVL282 Engineering Hydrology, IIT Delhi, 2020, 21
- Instructor, CVL381 Design of Hydraulic Structures, IIT Delhi, 2019, 2020, 2022, 2023
- Instructor, CVP731 Simulation Lab II, IIT Delhi, 2019, 2020, 2021, 2022, 2023
- Instructor, CVP731 Simulation Lab I, IIT Delhi, 2021, 2022
- Instructor, CVP731 NEN 100 Professional Ethics and Social Responsibility, IIT Delhi, 2019
- Teaching Assistant and co-taught, CEES 5843 Hydrology, University of Oklahoma, Spring 2017
- Teaching Assistant, CEES 5903 Remote Sensing Hydrology, University of Oklahoma, Spring 2016

Thesis Supervision

Graduated from IIT Delhi - 3 Masters

(*)Synopsis Completed

Ph.D. Scholar	Title	Year
Ravi Raj*	Geospatial Modeling and Mapping of Soil Erosions	2020-
Sai Kiran Kuntla	Embracing Large-sample Hydrology for Characterization and Mapping of Flooding over India	2020-
Bhanu Magotra	Flood Forecasting using process-based Machine Learning	2020-
Nirdesh Sharma	India Landslide Model	2020-
Anagha P.	Deep Learning Applications in Hydrology	2020-
Prateek Sharma	Gravimetry	2022-
Ved Prakash	Indian Land Data Assimilation System	2022-
Avnish Varshney	Urban flood forecasts	2022-
Priyam Deka	An impact-based flood forecasting system for the Brahmaputras	2022-

MS(R) Scholar	Title	Year
Arijit Chakravarty	Erosion	2022-
Anuj	Drought and soil moisture	2022-

M.Tech. Scholar	Title	Year
Shashank	Streamflow Timings in India	2022-23
Suneet Bansal	Analysis of Long-term terrestrial water storage variations in the Brahmaputra river basin	2022-23
Gautam Kunwar	Detection and Attribution of Groundwater Changes in India	2021-22
Khusboo Alvi	Multi-Dimensional Characterization of Flooding Events over India	2020-21



.

07 August 2023

Undertaking by the Principal Investigator

To

The Secretary
SERB, New Delhi

Sir

I Gaurav Tripathi

herby certify that the research proposal titled Enhancement of Compound Extreme Event Forecasting by Integrating Machine Learning and Physical-based Approaches

submitted for possible funding by SERB, New Delhi is my original idea and has not been copied/taken verbatim from anyone or from any other sources. I further certify that this proposal has been checked for plagiarism through a plagiarism detection tool i.e. Turnitin approved by the Institute and the contents are original and not copied/taken from any one or many other sources. I am aware of the UGCs Regulations on prevention of Plagiarism i.e. University Grant Commission (Promotion of Academic Integrity and Prevention of Plagiarism in Higher Educational Institutions) Regulation, 2018. I also declare that there are no plagiarism charges established or pending against me in the last five years. If the funding agency notices any plagiarism or any other discrepancies in the above proposal of mine, I would abide by whatsoever action taken against me by SERB, as deemed necessary.



Signature of PI with date

09/08/2023

Name / designation

Gaurav Tripathi, PhD Scholar (Thesis Submitted)
Department of Geoinformatics,
Central University of Jharkhand, Ranchi
&
Assistant Professor, Centre for Climate Change and
Water Research, Suresh Gyan Vihar University, Jaipur



झारखण्ड केन्द्रीय विश्वविद्यालय

Central University of Jharkhand

(Established by an Act of Parliament of India, 2009)

Ref. No. : CUJ/COE/2018/285/3367

Date: 13/10/2022

Thesis Submission Certificate

Certified that **Mr. Gaurav Tripathi** of the Department of Geoinformatics has submitted thesis for the degree of Doctor of Philosophy (Ph.D.) of the University. The details are as under

Registration No: CUJ/P/2016/PHD/LRM/02

Title of the thesis submitted: *"Flood Inundation Characterization through Remote Sensing for Flood Risk Mapping and Monitoring in parts of North Bihar region, India"*

Name of Supervisor(s) : Prof.A.C Pandey, Professor, Department of Geoinformatics.

Name of Co-supervisor : Dr.B.R Parida, Assistant Professor, Department of Geoinformatics.

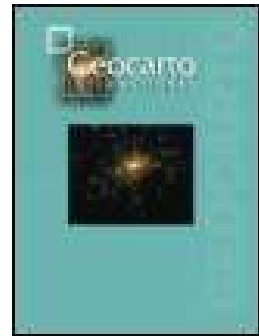
Date of Pre-Ph. D. Thesis submission seminar (open): 08th September 2022

Date of thesis submission: 14th September 2022

This certificate is issued with the approval dated 10.10.2022 by the competent authorities.

13/10/2022
Controller of Examinations
Central University of Jharkhand

Cheri- Manatu, Kanke, Ranchi - 835222 Jharkhand



Estimating floodwater depth using SAR-derived flood inundation maps and geomorphic model in kosi river basin (India)

Bikash Ranjan Parida, Gaurav Tripathi, Arvind Chandra Pandey & Amit Kumar

To cite this article: Bikash Ranjan Parida, Gaurav Tripathi, Arvind Chandra Pandey & Amit Kumar (2021): Estimating floodwater depth using SAR-derived flood inundation maps and geomorphic model in kosi river basin (India), *Geocarto International*, DOI: [10.1080/10106049.2021.1899298](https://doi.org/10.1080/10106049.2021.1899298)

To link to this article: <https://doi.org/10.1080/10106049.2021.1899298>

 View supplementary material 

 Published online: 22 Mar 2021.

 Submit your article to this journal 

 View related articles 

 View Crossmark data 
CrossMark



Estimating floodwater depth using SAR-derived flood inundation maps and geomorphic model in kosi river basin (India)

Bikash Ranjan Parida , Gaurav Tripathi , Arvind Chandra Pandey  and Amit Kumar 

Department of Geoinformatics, School of Natural Resource Management, Central University of Jharkhand, Ranchi, India

ABSTRACT

Flooding is the most widespread and frequent natural disaster in developing countries. Until recent years, determining flood extent and inundation depth were undertaken using hydrodynamic models but have pertinence constraints in data-scarce regions. This has given the new potential to characterize floods (e.g., inundation, depth, duration) at a large-scale using a geomorphic approach. The SAR data was employed to derive flood extent and the 12.5 m resolution DEM-based geomorphic method was applied to determine inundation depth in flooded domains of Kosi River Basin (KRB) in North Bihar (India) to characterize 2017 floods. The total inundated area in flooded domains over KRB was estimated at 4,108.2 km² (20.88%). Most of the area (2,750 km², 14%) of flooded domains over land had a water depth of 0.1 to 1 m. The geomorphic approach is appropriate for characterizing floods over large-scale and data-sparse basins like KRB and afforded a new horizon for flood risk assessment on flood vulnerable areas.

ARTICLE HISTORY

Received 31 May 2020

Accepted 11 February 2021

KEYWORDS

Floodwater depth; inundation; duration; C-band SAR; DEM; FwDET geomorphic model; Kosi River Basin (KRB)

1. Introduction

Flooding is one of the most common natural disasters that affect human societies worldwide than any other disaster (Parker 2017). Floods impose a high economic liability mostly in developing countries in Asia. In the Indian context, monsoon floods are a recurring meteorological and hydrological hazard led by natural and anthropogenic reasons. Floods are the most vulnerable natural calamity in densely populated nations like India that affect both humans and the economy. India's 12% (40 million hectares) of land area is prone to floods (NIDM 2018), which comprises states like Bihar, Gujarat, West Bengal, Odisha, Assam. These states are well known for recurring floods in response to monsoonal rainfall, river overflow, and the siltation of riverbeds (Kumar et al. 2014). Flood frequency, intensity, duration, and even hydrological extreme events have triggered

CONTACT Arvind Chandra Pandey  arvindchandrap@yahoo.com  Department of Geoinformatics, School of Natural Resource Management, Central University of Jharkhand, Ranchi-835222, India

 Supplemental data for this article can be accessed at <https://doi.org/10.1080/10106049.2021.1899298>.

© 2021 Informa UK Limited, trading as Taylor & Francis Group

flood events in response to climate change and have increased abruptly in the last few decades (Zhang et al. 2018). The increasing impact of anthropogenic activities on fluvial hydrological processes has also prompted flooding. So, the advancement of flood mapping using remotely sensed satellite data (Parida et al. 2017) and hydrological models (Teng et al. 2017) has become an essential application in monitoring and assessing the impact of floods over land and urban areas.

Optical and Synthetic Aperture Radar (SAR) remote sensing (RS) data have been widely used in monitoring surface water dynamics. The optical satellite data have a dependency on atmospheric conditions (Matgen et al. 2011), whereas SAR sensors (e.g., RADARSAT, RISAT, ENVISAT ASAR, TerraSAR & TanDem-X) are independent of weather conditions (Alsdorf et al. 2007; Schlaffer et al. 2015). SAR sensors can penetrate cloud cover, severe rain, insufficient sunlight, haze, etc. during and post-flood events, and thereby, SAR data are preferred over optical data. SAR data provides an essential input in real-time flood damage assessment (Matgen et al. 2011) as it can distinguish land and water precisely (Brivio et al. 2002). However, the only shortcoming of the SAR sensor is its revisit time (e.g., 12 to 24 days) (Bovenga et al. 2018), which results in less availability of SAR images during flood events. The SAR images with VV (Vertical Transmit and Vertical Receive) and VH (Vertical Transmit and Horizontal Receive) polarizations are typically deployed in floodwater monitoring and compared their suitability in flood inundation mapping (Clement et al. 2018; Agnihotri et al. 2019). Some studies deduced that VV polarization can provide a slightly better or even similar level of accuracy to VH (Twele et al. 2016; Clement et al. 2018). For instance, the overall accuracy was reported at 97 and 97.4% for VH and VV, respectively during the 2015 flood event in Yorkshire, UK (Clement et al. 2018). By contrast, some studies concluded that VH polarization accomplished the best results for flood mapping (Conde & Muñoz 2019; Ezzine et al. 2020). It was also suggested that the integration of both VH and VV polarizations combined with digital elevation model (DEM), slope, and aspect are more suitable to delineate flooding (Hassan et al. 2020). A small- and large-scale flood inundation mapping were performed by various studies using RS optical sensors data and hydrological models (Matgen et al. 2011; Tsyganskaya et al. 2018; Cohen et al. 2018; Tripathi et al. 2019; Cohen et al. 2019). Using optical sensors, various studies have employed spectral indices, such as the Normalized Difference Water Index (NDWI) and modified NDWI (mNDWI) to assess flooded regions (Vishnu et al. 2019) as well as soil moisture (Patel et al. 2019).

Especially, over the Kosi River Basin (KRB), several studies have been done to map flood inundation but none of them have addressed floodwater depth and their duration. . Various hydrological flood models such as Soil Water Assessment Tool (SWAT) and Hydraulic Engineering Centre-River Analysis System (HECRAS) were used to map and forecast flood inundation with the help of different hydrological parameters (Afshari et al. 2018; Macchione et al. 2019; Wan et al. 2019). Moreover, none of the studies have attempted to map floodwater depth and floodwater duration during flood events in KRB. Flood Susceptibility Modeling (FSM) is an important tool to display inundation regions and this information is useful to policymakers and disaster managers in mitigating and protecting risk-prone flooded regions and the natural resources. Accordingly, the flood's risk maps can be developed with the help of RS methods coupled with SAR and DEM data. Several methods are available for FSM and some of them are the analytical hierarchy process (Sinha et al. 2008), fuzzy logic (Sahana and Patel, 2019), ensemble machine learning algorithms (Towfiqul Islam et al. 2021), and (4) hydrological models, namely SWAT (Brunner 1995), HECRAS (Getahun & Gebre, 2015), MIKE (Zhou et al., 2012), among others.

Floodwater depth and duration information during flood events are very essential to map or predict vulnerability because it helps in flood risk assessment and flood forecasting (Townsend & Walsh 1998; García-Pintado et al. 2013; Wan et al. 2019). In this context, the floodwater level can be estimated through RS satellite images either directly or indirectly. LiDAR and wide swath Altimetry usually directly produced floodwater levels. Whereas, flood extent maps with the help of DEM can be used indirectly to determine floodwater depth over flooded domains. Radar altimeters calculate the two-way return time between the instrument and the target. The final product always represents the average water level over the altimeter footprint (Smith 1997). However, its poor temporal resolution (10–35 days) and footprint (8 km for AltiKa), made it the least useful or secondary source of information for monitoring flood events. Mostly, altimeters are utilized to derive surface water level over riverbeds but not over the inundated land surface. The topographical convergence or wetness index was considered as key factors and used to measure floodwater depth, but generally fails over nearly flat terrain (Beven et al. 1979; Moore et al. 1991; Wolock & McCabe 1995). Flooded domains are being identified using a topography-based flood inundation tool HAND (Height Above Nearest Drainage) that utilized DEM-based data (Nobre et al. 2016). The HAND is a zero-dimensional (0D) model and this simplified conceptual model has been applied in India for 2016 flood events and over Utah, the USA for 2017 flood events (Garousi-Nejad et al. 2019; Johnson et al. 2019). The RAPIDE (RAPid GIS tool for Inundation Depth Estimation) is also a recent 0D tool to determine flood depth within an inundated zone, which employs satellite-derived inundated extent and DEM (Scorzini et al. 2018). This simplified model has been applied as a case study in the North-West of Italy for the 2002 Adda flood event. (Schumann et al. 2007) calculated floodwater depth using steady-state regression analysis (REFIX—Regression and Elevation based Flood Information eXtraction) to interpolate between HEC-RAS cross-sections along the river centerline. Townsend and Walsh (1998) used a hydrodynamic model to simulate the floodwater depth, which assumes that for any potential site, inundation is linked with the topography and its surrounding geography. Floodwater depth can be estimated by deducting terrain elevation from the inundated water elevation (Bates et al. 2006; Matgen et al. 2007). The root mean square errors (RMSE) has been reported between water levels and *in situ* data to deduce floodwater depth (Oberstadler et al. 1997; Schumann et al. 2007; Schumann et al. 2009; Di Baldassarre & Claps 2011).

There are hydrodynamic, 1-D, 2-D and 3-D models, such as HECRAS, Delft-3D, MIKE, and LISFLOOD-FP are available, which could effectively simulate water level and floodwater depth. These models can forecast water level and depth, but it needs various hydrological inputs, such as rainfall, soil moisture, flood map, gauge discharge, cross-section, etc. (Refsgaard et al. 1988; Najibi et al. 2017; Teng et al. 2017; Afshari et al. 2018; Macchione et al. 2019). Numerical simulations are frequently used in near-real-time flood mapping applications and play a vital role in flood management. In fact, hydrodynamic models are complex as it demands bulky input dataset with the requirement of high computational time and calibration processes. These complexities may render hydrodynamic models unfeasible in large-scale flood depth mapping over data-limited areas. Consequently, a new viable substitute approach has emerged for these complex hydraulic models in recent years, wherein zero-dimensional (0D) geomorphic model (i.e., DEM-based method) can be engaged to determine flood depths within the flooded area (Teng et al. 2017; Manfreda & Samela 2019).

In this context, Cohen et al. (2019) developed a new approach in which a GIS-based tool was developed that can identify the floodwater elevation for each cell within the

flooding domain using its nearest flood-boundary grid-cell. The tool is known as Floodwater Depth Estimation Tool (FwDET), which can determine floodwater depth using two crucial inputs, namely, satellite-derived flood inundation map and DEM data. The FwDET can estimate floodwater depth over riverbeds as well as over the land and urban areas. In the FwDET, high spatial resolution DEM data play a vital role to determine accurate floodwater depth. Cohen et al. (2018, 2019) has used high resolution (1 m LiDAR) as well as medium resolution (10 m NED) DEM for large and small flood events, respectively, over the Brazos River, Texas, USA, and suggested that the FwDET model can provide accurate floodwater depth maps and operationally used by Global Flood Partnership (GFP) (Alfieri et al. 2018; Rogers et al. 2018). Their flood depth maps are well comparable with the FaSTMECH (Flow and Sediment Transport with Morphological Evolution of Channels) hydraulic model. By contrast, the high-resolution DEM including LiDAR DEM is limited for most of the countries and makes a limitation to derive floodwater depth. In addition to the floodwater depth, depth duration is associated with a risk factor in flooded areas. It enables to locate flooded areas that were submerged for days or longer duration (Kent & Johnson 2001; Warwick & Brock 2003; Chen et al. 2010). At lower elevations, flood duration is generally longer. The adverse effect of flood duration on agriculture and forest was reported by limiting crop production, plant growth, and biomass (Warwick & Brock 2003; Chen et al. 2010).

North Bihar is the most flood-affected region in the country. Identifying flood-damaged areas is therefore highly essential for effective flood response. To date, there were no studies available on floodwater depth estimation over any flood regions of India. In this context, this study will guide other researchers including various stakeholders of disaster management authorities to give importance to characterizing floodwater depth and duration and to assess its impacts on various land use and land cover classes at a regional scale. Moreover, there is no framework exist for large-scale mapping of floodwater depth and duration which generally needs high computational cost. So, in this study, we aimed to analyze the flood event of 2017 as a case study over Kosi River Basin (KRB) located inside the North Bihar boundary, which occurred during the August and September months. The overarching objectives of the study are, (i) flood inundation mapping using Sentinel-1A (C-band) SAR data, (ii) to estimate floodwater depth using a geomorphic DEM-based 0D model (FwDET), and (iii) to generate a floodwater duration map using the floodwater depth maps.

2. Study area

The study area North Bihar, India consists of 22 districts and geographical location is between $85^{\circ} 03' 30''$ E to $87^{\circ} 18' 00''$ E longitude and $25^{\circ} 20' 00''$ N to $26^{\circ} 52' 30''$ N latitude (Figure 1a). The Kosi River is the major river of North Bihar and has a basin area of 19,674 km². The elevation is ranged up to 40 m above mean sea level (MSL), whereas most of the downstream areas are within the range of 0 to 2 m (Figure 1b). The KRB has three major tributaries, namely, Tamur, Sun Kosi, and Arun. As it originated from a very high altitude (at 7000 m), apart from the rainy season, it also contributes water during the summer season. The Arun river meets the Kosi river in Tibet and from the Nepal Himalayas, seven rivers drain, namely, the Indrawati, Bhote Kosi, Tama Kosi, Dudh Kosi, SunKosi, Arun, and Tamor. All these rivers reach at Chatara gauge station by crossing Tribeni (known as Sapt Kosi) and ultimately flows towards Northern Bihar plains (Sinha et al. 2008). From the foothill of the Himalayas, there are several seasonal channels/tributaries/dhars, namely, Sugarwe, Balan, Kamla, and Thomani that activate during the

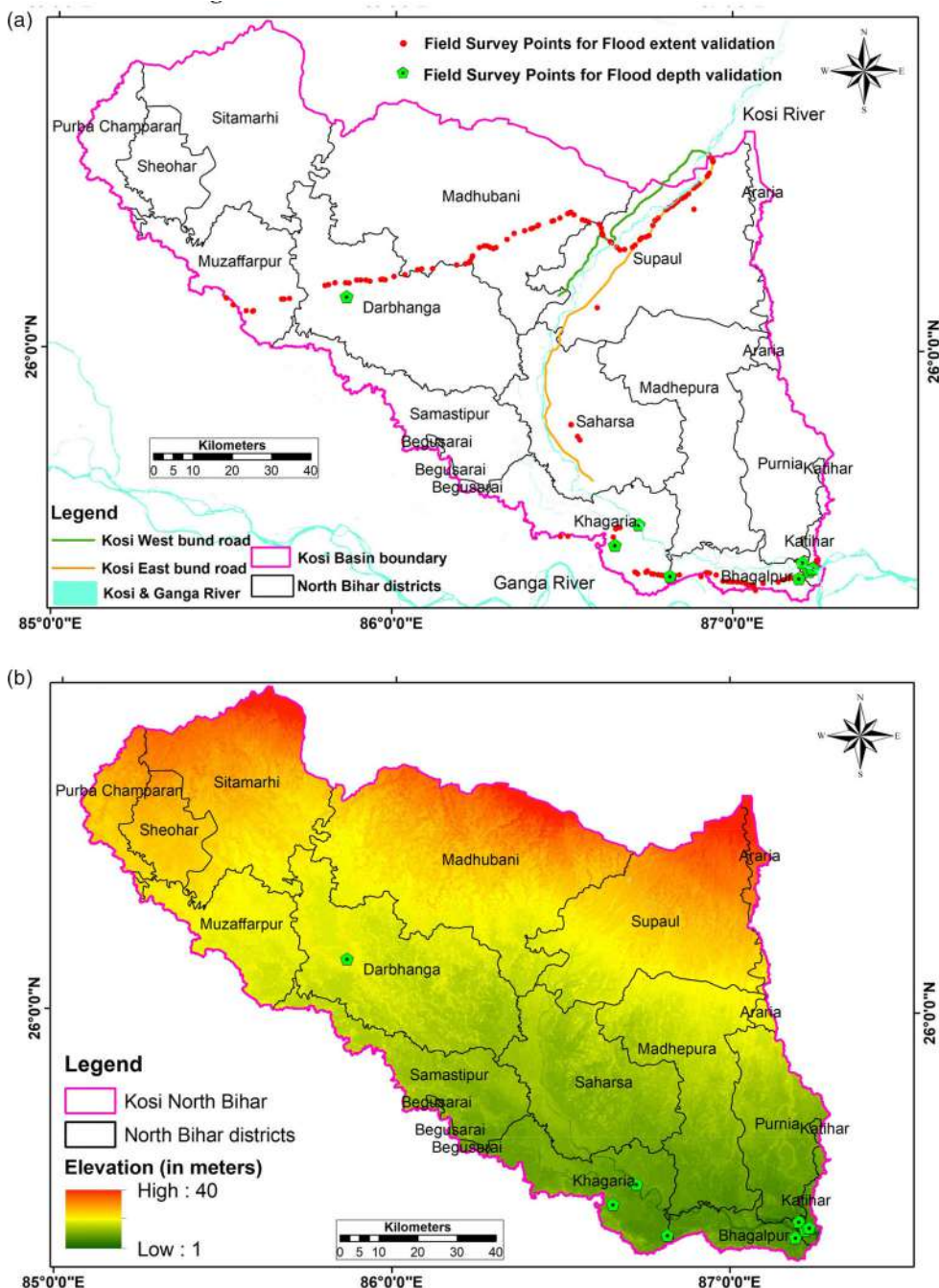


Figure 1. a. Location map of part of Kosi River Basin (pink color boundary) over North Bihar, India. The Eastward and westward bunds of the Kosi river were shown in orange and green colors. The field survey's GPS locations on flood-water inundation (red dots) and depth (green dots) were overlaid on the map. b. ALOS PALSAR based 12.5 m digital elevation model (DEM) over Kosi River Basin (KRB) in North Bihar, India.

monsoon period and cause severe inundation for downstream areas. Around 80% of the land area of KRB is shared by Nepal and Tibet, while 20% area falls under India's boundary (in North Bihar districts). About 22% of the total drainage area of KRB with high

elevation topography and flat plateau lies in Tibet, 40% of drainage area passes through Nepal Himalayas, whereas, 38% of the drainage area is inside North Bihar. The climate pattern based on Koppen's classification is subtropical monsoon, mild and dry winter, hot summer (Cwa). The average annual rainfall ranged from 1036–1625 mm (mean over 1980–2009) and the maximum rainfall (86%) occurred during the monsoon season (June–September) (Tesfaye et al. 2017). The annual average temperature ranged from 19.2–32.7 °C and is projected to increase by 1.6–2.2 °C in 2050 depending on the emission scenario (Tesfaye et al. 2017).

The alluvial plains of North Bihar comprising 38% of the total drainage area with low elevation and nearly flat terrain with very high population density. The Kosi river drains the northern slopes of the Himalaya in the Tibet region and the southern slopes of the Himalayas in Nepal before it finally enters the Northern Bihar flood plains in India. Afterward, it joins the Ganga river near Patna city. The Kosi river is also known as the "Sorrow of Bihar" due to recurring flood occurrences over KRB. The main reason for the Bihar floods is due to the breach of the bank alongside the river Kosi owing to excessive rainfall throughout the monsoon period. Plenty of curative measures such as dams, water channels, storage ponds, etc. have been executed by the Bihar (Indian) and Nepal government to limit regular flooding (Sinha et al. 2008). Despite all these flood preventive actions, the Kosi river's overflow happens around every year and creates critical harm to infrastructure and human lives. The North Bihar districts, such as Saharsa, Darbhanga, Khagaria, Bhagalpur, Muzaffarpur, Araria, Kishanganj are located along the Kosi river and recurrently being affected due to flooding (Tripathi et al. 2019; Tripathi et al. 2020). River in the monsoon season makes higher cumulative runoff due to a substantial amount of rainfall and subsequently, inundated lower catchment areas (Sinha et al. 2008), which makes the downstream areas prone to flooding as well as waterlogging (Pandey et al. 2010).

The plains of North Bihar have recorded various significant flood events in 1978, 1987, 1995, 1998, 1999, 2000, 2001, 2002, 2003, 2004, 2007, 2008, 2010, 2013, 2016, 2017, 2018, 2019, and 2020 (Sinha et al. 2008; Pandey et al. 2010; Tripathi et al. 2019). The flood event in 2017 was started in the middle of August and continued till mid of September month. During the August 2017 flood event, more torrential rainfall in the upper catchment has caused disastrous flooding conditions for lower areas, which inundated several North Bihar districts. The India Meteorological Department (IMD) based rainfall as represented by the mass curve for July to September period has been shown in Figure 1S (supplement). The mass curve indicated that the rainfall abruptly increased across three IMD stations namely, Hayaghat, Kamtaul in Darbangha district, and Khagaria station from July to September 2017 (1-4 weeks represented as July, 5-8 weeks represented as August, 9-12 weeks represented as September). Notably, during weeks 5 and 6 (or 1st to 15th August 2017), the IMD stations Hayaghat, Kamtaul, and Khagaria recorded rainfall of 243, 397.2, 204.2 mm, respectively (Figure 1S). In the Darbangha district, 432.4 mm (+ 46% departure from the long-term mean) and 443.4 mm (+ 56% departure) of rainfall recorded by IMD in July and August month, respectively. Additionally, the spatio-temporal distribution of weekly rainfall as derived from Tropical Rainfall Measuring Mission (TRMM) during floods can be seen in Figure 2S (supplement).

We are particularly focused on measuring the flooding characteristics that occurred during the monsoon season (June to October) mainly caused by heavy rain and hit nearby districts from the river channels/dhars. This disaster quickly spread to other districts as well causing serious damage to their infrastructure and livelihoods. Similar events can also be considered as the extreme ones where information on flood forecasting during the event is being the most valuable and essential input towards the rescue and management exercises.

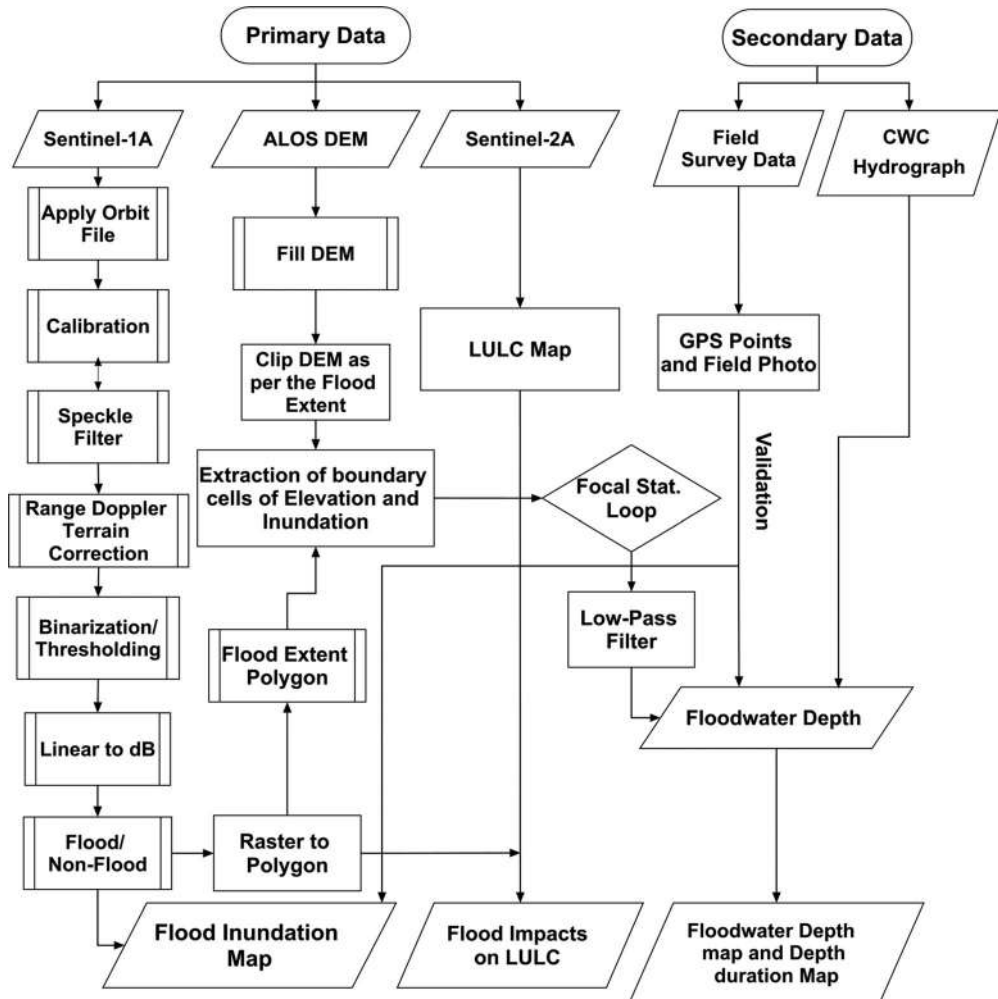


Figure 2. The detailed methodology for inundation mapping and flood depth calculation adopted in this study.

3. Materials and methods

This study utilized time-series Sentinel-1A (C-band) SAR satellite data to demarcate flooded regions over the KRB, Northern region of Bihar. The description of the SAR data used is presented in [Table 1](#). These SAR images are available at 12-day intervals and utilized to represent flood progression and recession during August and September 2017. Flood inundation maps were coupled with the ALOS PALSAR DEM V2 (12.5 m) to estimate floodwater depth during the flood period. Furthermore, extensive fieldwork has been carried out to validate the flood extent and floodwater depth.

3.1. Sentinel-1A and sentinel-2A satellite data

The Sentinel-1 SAR satellite mission was launched by the European Space Agency (ESA) that consisted of a pair of radar satellites. It provides C-band data in dual-polarization (VV, VH) mode with a repeat cycle of 12 days and resolution of 20×22 m (i.e., range \times azimuth) with a pixel spacing of 10×10 m (range \times azimuth). The Sentinel-1 SAR

Table 1. Characteristics of the satellite and secondary data used in this study.

Data Used	Temporal Resolution	Spatial Resolution	Acquisition Dates	Purpose	Source
Sentinel-1A (C-band SAR)	12 days	20 × 22 m (range × azimuth)	23 rd Aug, 04 th and 16 th Sept 2017 15 th May, 09 th June	Flood extent maps PWB	ESA
Sentinel-2A (Optical)	10 days	10 × 10 m	18 th Aug 2017	LULC map	ESA
ALOS PALSAR DEM	14 days	12.5 × 12.5 m	2009	Elevation map	JAXA
IMD rainfall	Daily	–	2017	Mass curve	IMD
TMPA rainfall (3B42RT)	3 h	0.25° × 0.25°	2017	Spatial pattern	GIOVANNI
Hydrographs	03 Hrs.	–	Daily (station-wise) in 2017 (monsoon)	Gauge level	CWC
Flood impact reports	07/15 days	–	–	Affected area	BSDMA, FMISC, etc.

Note: The satellite data were procured in August and September 2017. The abbreviations used are Permanent Water Body (PWB), European Space Agency (ESA), ASF (Alaska Satellite Facility), JAXA (Japan Aerospace Agency), CWC (Central Water Commission) and BSDMA (Bihar State Disaster Management Authority, FMISC (Flood Management Information and Support Centre).

(Level-1) Interferometric Wide Swath (IW) data of August and September 2017 was obtained free of charge from Alaska Satellite Facility (ASF) and acquisition dates were provided in [Table 1](#). The pre-flood data acquired on 15th May and 09th June 2017 were used to extract permanent water bodies (PWB) in the study area.

The Sentinel-2A series optical satellite data were obtained from the United States Geological Survey (USGS) Earth Explorer. Data were used to demarcate various land use land cover (LULC) classes. The sensor has 12 spectral bands covering the visible to short wave infrared range of the electromagnetic spectrum. The Sentinel-2A data were acquired on 18th August 2017, which corresponds to the during-flood conditions.

3.2. Dem data (ALOS PALSAR V2)

The ALOS (PALSAR) Digital Elevation Model (DEM) data are available at 12.5 m spatial resolution and are obtained from the Japan Aerospace Agency (JAXA) portal. The DEM has been used to calculate floodwater depth with the help of the FwDET model (Cohen et al., 2018). We used ALOS-based DEM because it possesses comparatively a more detailed spatial resolution than the ASTER-GDEM V2 (30 m) and Shuttle Radar Topography Mission (SRTM) DEM (90 m).

3.3. Station-wise IMD rainfall data and TMPA-based product

The station-wise rainfall data distributed in India are provided by Indian Meteorological Department (IMD). Around 200 rain gauge stations are distributed across Bihar state and provide daily rainfall data. In this study, daily rainfall data of few stations like Hayaghat, Kamtaul, and Khagaria stations are used to display mass curves for July to September 2017. Rainfall data was procured through the IMD data supply portal. The IMD provides

a standard time-series rainfall product and is used for various hydrometeorological applications in India (Parida et al. 2018).

Tropical Rainfall Measuring Mission (TRMM)-based Multi-satellite Precipitation Analysis (TMPA) products 3B42RT has been used for spatio-temporal mapping of rainfall over KRB. The accumulated rainfall over a week (mm/day) was derived from the originally available 3-hourly product at $0.25^\circ \times 0.25^\circ$ spatial resolution which is downloaded from GIOVANNI (Geospatial Interactive Online Visualization ANd aNalysis Infrastructure).

3.4. Hydrographical data of Central Water Commission (CWC)

The Central Water Commission (CWC) was established by the Ministry of Water Resources, Government of India in 1952. The CWC gauges are responsible to manage hydro-meteorological sites, which offer gauge data, discharge, sediment load, and water quality parameters (GDSQ) for the Indian region. We collected hydrographs that were used to interpret varying water levels during August and September 2017. It provides essential information on different water levels, such as; warning level (WL), danger level (DL), and the highest flood level (HFL). Floodwater level data obtained from different gauge stations, such as Muzaffarpur, Ahirwalia, and Samastipur, *etc.* and used to validate floodwater depths.

3.5. Flood impact report of BSDMA and FMISC

During flood time many of the government/non-government organizations provide flood situation reports and flood maps at daily or weekly intervals. We have used information shared by the Bihar State Disaster Management Authority (BSDMA) and Flood Management Information and Support Centre (FMISC) reports to validate the flooding extent in 2017 flood events.

3.6. Methods

The flow diagram of methods is presented in Figure 2. The multi-dates Sentinel-1 SAR (C-band) images are carried out in various pre-processing steps. The pre-processing steps were applied using ESA's Sentinel Application Platform (SNAP). The open-access SNAP toolbox is used for reading, pre-processing, and visualizing Sentinel-1A SAR images. GIS-based floodwater depth analysis has been implemented using ESRI Arc Map, QGIS, and PyCharm software. The Sentinel-2 data was used to produce a LULC map using supervised classification (maximum likelihood algorithm) with the major LULC classes, such as built-up, agriculture, fallow land, forest, water bodies, and others.

3.6.1. Sentinel-1A SAR data processing

The Sentinel-1A Level-1 ground range detected (GRD) data was pre-processed comprising data import, radiometric calibration, speckle filtering, and geometric terrain correction. The flood pixels are obtained using the binarization process also known as the thresholding approach as illustrated in several studies (Matgen et al. 2011; Small 2011; Manjusree et al. 2012; Ajadi et al. 2016). The Otsu image threshold method has been widely used for flood mapping and the approach is capable to provide precise flood maps at a larger-scale using Sentinel-1 (Cao et al. 2019; Tiwari et al. 2020) or Radarsat-2 SAR data (Li & Wang 2015). The threshold value of -22.8 , -23.7 , and -23.6 dB was applied

for 23rd August, 04th and 16th September 2017, respectively, wherein VH polarization of SAR images are used to extract flood pixels.

The backscatter intensity values both in VV and VH polarizations are deployed for flood mapping using the C-band Sentinel-1 data (Manjusree et al. 2012). Among these two polarizations, the VH-based backscatter intensity values of floodwater are normally -15 to -20 dB but VV-based backscatter intensity values are usually -6 to -15 dB (Manjusree et al. 2012; Conde & Muñoz 2019). Therefore, the VH manifests the highest darkness or black tones than the VV (Martinis & Rieke 2015) that make C-band VH polarization is more suitable for delimiting flooded areas (Conde & Muñoz 2019; Lal et al. 2020). Nevertheless, the VV can be applied to identify partially submerged features in flooded areas as it is sensitive to the roughness of the surface (Manjusree et al. 2012; Klemas 2015).

The threshold values are decided using the binarization procedure with the help of a manual histogram such that it detects flood pixels. Several studies used the thresholding approach using the sigma naught (dB) based-on either manual or automatic procedure for flood mapping (Manjusree et al. 2012; Zhang et al. 2020; Tiwari et al. 2020). Moreover, the dB threshold of VH polarization applied in this study remained within the limits that are seen in the literature (Manjusree et al. 2012). The total study area of the KRB basin is $19,674 \text{ km}^2$, whereas about 134 km^2 area is of permanent water body (i.e., rivers, lakes, etc.). The flood inundation area has been calculated by subtracting the permanent surface/water bodies from the respective SAR images.

While pre-processing Sentinel-1A, the Level-1 VH polarization SAR images were imported into SNAP. These SAR images were then corrected radiometrically, where Sentinel-1A images were calibrated to reach physically essential radar backscatter coefficient values (sigma naught or σ_o). The refined lee speckle filter (7×7 window size) was employed to diminish the effect of the granular noise in SAR data. The geometric terrain correction is applied to correct the geometric distortions present in SAR images by transforming the coordinates into a usual reference frame. A radiometric conversion from a linear scale to a dB scale can be expressed as:

$$\sigma_o = \beta_o \cdot \sin \alpha \quad (\text{Equation 1})$$

where α is the local incidence angle.

The Sentinel-1A radar backscattering coefficient ' σ_o ' in decibels is evaluated as follows (Laur et al. 2003):

$$\sigma_o(\text{dB}) = 10 \log 10(\sigma_o) \quad (\text{Equation 2})$$

The image binarization technique was used to separate image pixel values into two different groups as non-flood and flood pixels. The thresholding technique was used to derive flood inundated areas by fixing the range of dB values. The 1-D Otsu thresholding method was used to separate image ($I(x, y)$), which contains brighter objects from the darker background image as follows (Laur et al. 2003; Manjusree et al. 2012).

$$I(x, y) = \{1 \text{ } I(x, y) > T; 0 \text{ } I(x, y) < T\} \quad (\text{Equation 3})$$

where T is the Threshold value

The conventional digital classification algorithms used to obtain flooded pixels are machine learning algorithms and some of the algorithms applied are Random Forest Classifier (RFC) and Support Vector Machine (SVM) (Dumitru et al. 2015; Rana & Suryanarayana 2019). These classifiers were applied for the rapid mapping of floods in Assam in 2019 and Kerala in 2018 using Sentinel-1 data (Rana & Suryanarayana 2019),

floods in Germany in 2013 using TerraSAR-X data (Dumitru et al. 2015), and floods in the Neuse River in North Carolina, the USA in 2016 using Sentinel-1 data (Aristizabal et al. 2020). The SVM classifier was also applied on SAR images of Sentinel-1 to delineate the extent of flood inundation water due to Super Cyclone Amphan in 2020 across the southwest region of Bangladesh, comprising 16 coastal districts (Hassan et al. 2020). The change detection methods are also generally employed using pre and during flood time SAR data (Lal et al. 2020). However, a backscatter binarization study was meant to be the most fitted technique concerning flood pixels extraction (Li & Wang 2015; Kordelas et al. 2018; Cao et al. 2019; Tiwari et al. 2020). Distinctly over the Northern region of Bihar, the image binarization technique was adopted using Sentinel-1A data for flood pixels extraction. There are additional procedures to distinguish flooded regions, namely, rainfall-runoff modeling, hydrological models, and machine learning techniques.

The flooded area was calculated by multiplying the number of flood pixels with pixel spacing dimension of 10×10 m and converted to the km^2 by dividing it to 10^6 . The composite flood inundation map for the 2017 flood event has been prepared by combining the flood extent of multi dates, such as 23rd August, 04th September, and 16th September 2017.

3.6.2. Floodwater depth calculation

Floodwater depth was calculated using the FwDET model (Cohen et al., 2018, 2019), wherein flood inundation maps of SAR images and DEM of ALOS PALSAR data are used as inputs to the model. The methodology adopted has been shown in Figure 2. All flood inundation related raster datasets were resampled to 10×10 m. The FwDET recognizes the floodwater elevation for each cell inside the flooded area based upon its most proximal flood-boundary grid-cell (Figure 2). The FwDET water depth calculation follows five steps, namely,

1. the transformation of the flood polygon into a line layer,
 2. production of a raster layer from the line layer that possesses the identical grid-cell extent plus arrangement as the DEM,
 3. deriving the DEM values (elevation) concerning certain grid-cells (boundary grid-cells),
 4. allotment of the confined floodwater rise concerning each grid-cell inside the flooded area from its most proximal extent grid-cell, and
 5. computation of floodwater depth by analyzing restricted floodwater elevation from the topographic elevation at every grid-cell inside the flooded area.

In step 1, the polylines are being generated using a spatial tool called “Polygon to Polyline” in ArcGIS, and then in step 2, it has been converted to a raster layer using a tool “Polyline to Raster”. The raster layer must have the same resolution as that of DEM data (e.g., 12.5 m in case of ALOS PALSAR). In step 3, a new raster layer has been generated wherein cells are simply filled with the elevation by the DEM data. In step 4, the “Focal Statistics” tool has been used to create a new raster layer to assign DEM value in cells based on the nearest boundary cell. The number of iterations to assign DEM values in cells depends on flood extent raster layer and DEM resolution. In step 5, floodwater depth has been calculated by subtracting two raster layers obtained from steps 3 and 4. Finally, a low-pass filter (3×3 window size) has been applied to remove if any negative pixels are found in the floodwater depth map. FwDET (Version 1) standalone Python script was used to compute floodwater depth.

3.6.3. Floodwater duration map

The floodwater durations map was calculated by combining all three floodwater depth maps at 12 days intervals, such as 23rd August, 4th September, and 16th September. The duration (in days) of each flood period has been computed between its start and end date. For estimating floodwater duration maps, floodwater depth maps were re-classified into two binary classes like 0 (no flood pixels) and 1 (flood pixels) (Rättich et al. 2020), if the water depth is more than 10 cm. These three dates' binary images were summed in a raster calculator that provides output as 0, 1, 2, and 3. The pixel value 1 represents no duration (i.e., 23rd August), 2 indicates 12 days duration (i.e., from 23rd August to 4th September or from 4 to 16th September), and 3 indicates 24 days duration (i.e., from 23rd August to 16th September). A similar method was also deployed using the multi-temporal flood extent masks from multiple satellite data (Rättich et al. 2020).

3.6.4. Field data collection during September 2017 (post-disaster survey)

The post-disaster survey was conducted from 17th–21st September 2017, wherein GPS points were collected covering flood inundated areas, permanent, and temporary water-logged zones over the Kosi River Basin. The Mobile Mapper 50 (Trimble Spectra Precision) has been used to collect GPS locations that offer tri-constellations GNSS accurate positioning (i.e., GPS + Galileo + Glonass or GPS + Galileo + Beidou) with 1 to 2 m positioning accuracy. Most of the houses (Kaccha-Pakka) and a large number of agricultural fields were found submerged during the post-disaster survey and some selected field photographs are shown in Figure 3S (supplement). The visited eleven sample points related to floodwater depth measurement are also shown in Figure 1. The measured floodwater depth sample points are used to compare the FwDET model-based inundated depth. The eleven points showed post-flood measurements which were just after 24 days from the peak flood (23rd August) and one day after the receding phase (16th September) (Table 2). The GPS point number 10 and 11 represent the water level at the CWC gauge station above the mean sea level (MSL) whilst other GPS points represent the existing water level in meters during 17th–21st September 2017. The GPS locations of about 150 points on floodwater inundation (Figure 1a) have been collected over various districts of North Bihar and has been used to verify and validate the inundation maps.

4. Results

4.1. Flood inundation mapping during Aug-Sept, 2017 in KRB based on SAR data

The spatio-temporal flood inundation maps during August and September 2017 over KRB was shown in Figure 3. As per the analysis, the maximum flood inundation occurred on 23rd August and the inundated area was calculated as 3,348 km² (~17%) over the KRB. A widespread flood inundation was noticed in Darbhanga, Samastipur, Saharsa, Araria, Purnea, Katihar, and Bhagalpur districts. Besides these districts, downstream districts, namely Katihar, Purnea, Bhagalpur, and Khagaria have also been affected adversely due to floodwater inundation. The satellite-derived flood extent map was also compared with the field-based GPS points. Results showed 137 inundated GPS points out of 150 accorded with the flood inundation map. Some relevant field conditions flood photos over agricultural land and settlement have been shown in Figure d-g.

During this period, the inundation extent rapidly increased as the catchment received extreme rainfall over KRB (Figure S1) as well as rainfall that occurred in the upstream region in Nepal (Tripathi et al. 2019). The inundation extent subsequently decreased by

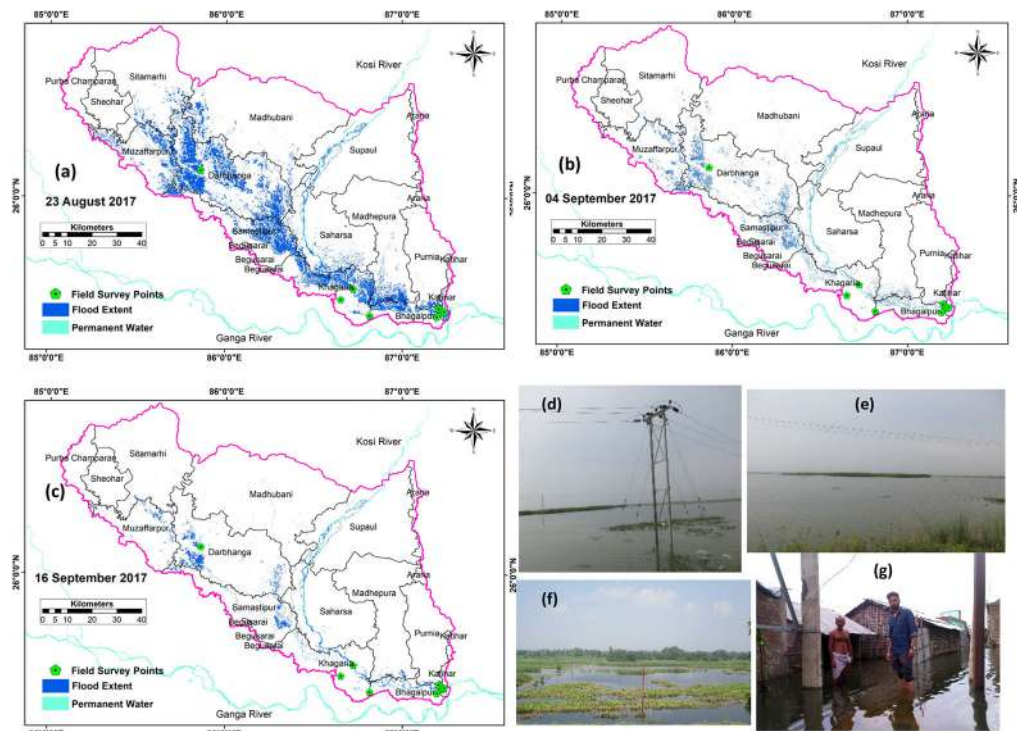


Figure 3. Flood inundation maps over the KRB on (a) 23rd August, (b) 04th September, and (c) 16th September 2017 as derived from the SAR data. Flood extent validation points were added over the flood extent map of 23rd August and the corresponding field photographs were shown to show inundated agricultural land in (d) Darbhanga, (e) Khagaria, and (f) Katihar, respectively. The inundated settlement area in Bhagalpur was shown in (g). The corresponding d-g geolocations were shown in Table 2 with field point serial no. 3, 5, 9, and 2, respectively.

Table 2. Field-based measured floodwater depth over eleven GPS locations during 17th–21st September 2017 that collected after 24 days from peak floods. Points 10 and 11 are taken at CWC gauge stations which are from above MSL.

Field Points	Longitude (E)	Latitude (N)	Location details	LULC details	Measured water depth (in m)
1.	86.74°	25.41°	Khagaria	Agriculture	1.21
2.	87.22°	25.41°	Bhagalpur	Settlements	1.85
3.	85.69°	26.13°	Pirochha Village, Muzaffarpur	Agriculture	1.52
4.	86.65°	25.48°	Khagaria	Agriculture	0.9
5.	86.72°	25.53°	Khagaria, Near Kosi River	Agriculture	1.1
6.	86.81°	25.40°	Khagaria	Agriculture	0.6
7.	87.19°	25.39°	Bhagalpur	Agriculture	0.5
8.	85.17°	25.39°	Bhagalpur	Agriculture	0.6
9.	87.24°	25.42°	Katihar	Agriculture	1.6
10.	87.23°	25.42°	Kosi CWC gauge	30.8 above MSL	
11.	85.87°	26.11°	Ekmighat CWC gauge	24.06 above MSL	

4th September 2017 and the inundation area was 566.3 km². Thereafter, the flood receded and by 16th September, the area under floodwater inundation was 452.3 km². The four adversely affected districts are Darbhanga, Khagaria, Saharsa, and Muzaffarpur and the respective inundation area statistics have been shown in Table 3. The corresponding floodwater extent for these four districts is shown in supplement Figure S4 (composite of 23rd August to 16th September). The inundation has caused floodwater stagnation over

Table 3. Floodwater inundation statistics (in km^2 and %) during 23rd August, 04th September, and 16th September 2017 (of 12 days interval) over the KRB as estimated from SAR data. The total geographical area of KRB is 19,674 km^2 under North Bihar, India.

Name of the districts	23 rd August		04 th September		16 th September	
	Inundated area (km^2)	Inundated area w.r.t KRB (%)	Inundated area (km^2)	Inundated area w.r.t KRB (%)	Inundated area (km^2)	Inundated area w.r.t KRB (%)
Bhagalpur*	159	0.8	28	0.2	36.9	0.18
Darbhanga	894.6	4.5	175.7	0.9	133.9	0.67
Katihar*	034.8	0.2	13.2	0.1	5.9	0.02
Khagaria	369.1	1.9	47	0.3	50.5	0.25
Madhubani	261.4	1.3	9.9	0.1	5.3	0.02
Muzaffarpur*	232.1	1.2	61.8	0.4	31	0.15
Purnea*	77.4	0.4	10.4	0.1	6.7	0.03
Saharsa	380.7	1.9	40.4	0.2	53.4	0.26
Samastipur*	351.3	1.8	107.9	0.6	66.6	0.33
Sitamarhi	184.5	0.9	14.4	0.1	6.3	0.03
Supaul	136.1	0.7	37.7	0.2	42.4	0.21
Madhepura	267	1.3	19.9	0.1	13.4	0.06
TOTAL	3348	17.1%	566.3	2.88%	452.3	2.3%

*indicates the part of the district that falls under KRB (refer to [Figure 1](#)) and bold districts are the adversely affected ones.

urban areas, agricultural areas, and other land use and land covers. The standing rainy seasonal crops are adversely affected due to floodwater.

The floodwater inundation area statistics and percentage of inundation with respect to KRB at 12 days intervals are presented in [Table 3](#). By 23rd August 2017, the area under inundation was about 17% ($3,348 \text{ km}^2$) of KRB. The district's wise statistics indicate that inundation varied between 0.2% (Katihar) and 4.5% (Darbhanga). The four adversely affected districts are Darbhanga, Khagaria, Saharsa, and Muzaffarpur and the respective inundation area is 894 km^2 (4.5%), 369.1 km^2 (1.9%), 380.7 km^2 (1.9%), and 1.8%, respectively. The least affected districts are Katihar and Purnea, wherein 0.2 to 0.4% area was affected by floodwater. By 4th September 2017, the area under inundation was reduced from 17% to 2.8% (566 km^2) of KRB. The inundation across the district varied from 0.2% to 0.9% on 4th September 2017. Furthermore, by 16th September the floodwater inundated area was reduced to 2.3% (452 km^2) and across the districts, it varied between 0.02% (Madhubani) and 0.67% (Darbhanga).

4.2. Floodwater depth maps during August and September 2017 in KRB

The floodwater depth maps were derived from the method represented in [Figure 4](#). The results depict that the depth typically varies from 0.10 to 2 m over KRB. On 23rd August 2017, the inundated area with less than 1 m depth was 2206.17 km^2 (11.21% of KRB), whereas more than 1 m depth was 1141.83 km^2 (5.8%). On 4th September 2017, the inundated area with less than 1 m depth was 464.46 km^2 (2.36%), whereas more than 1 m depth was 101.84 km^2 (0.52%) over the KRB. On 16th September 2017, the inundated area with less than 1 m depth was 379.66 km^2 (1.93%), whereas more than 1 m depth was 72.64 km^2 (0.37%) over the KRB. These area statistics indicated that the majority of the inundated area (i.e., 11.21%, 2.36%, and 1.93% of KRB) was under the floodwater depth of 1 m across all three dates over the KRB.

The floodwater depth maps for four adversely affected distress, such as Darbhanga, Khagaria, Saharsa, and Muzaffarpur have also been shown in supplement [Figure 5S](#) (on 23rd August) and [Figure 6S](#) (on 4th September). These maps revealed that in Darbhanga

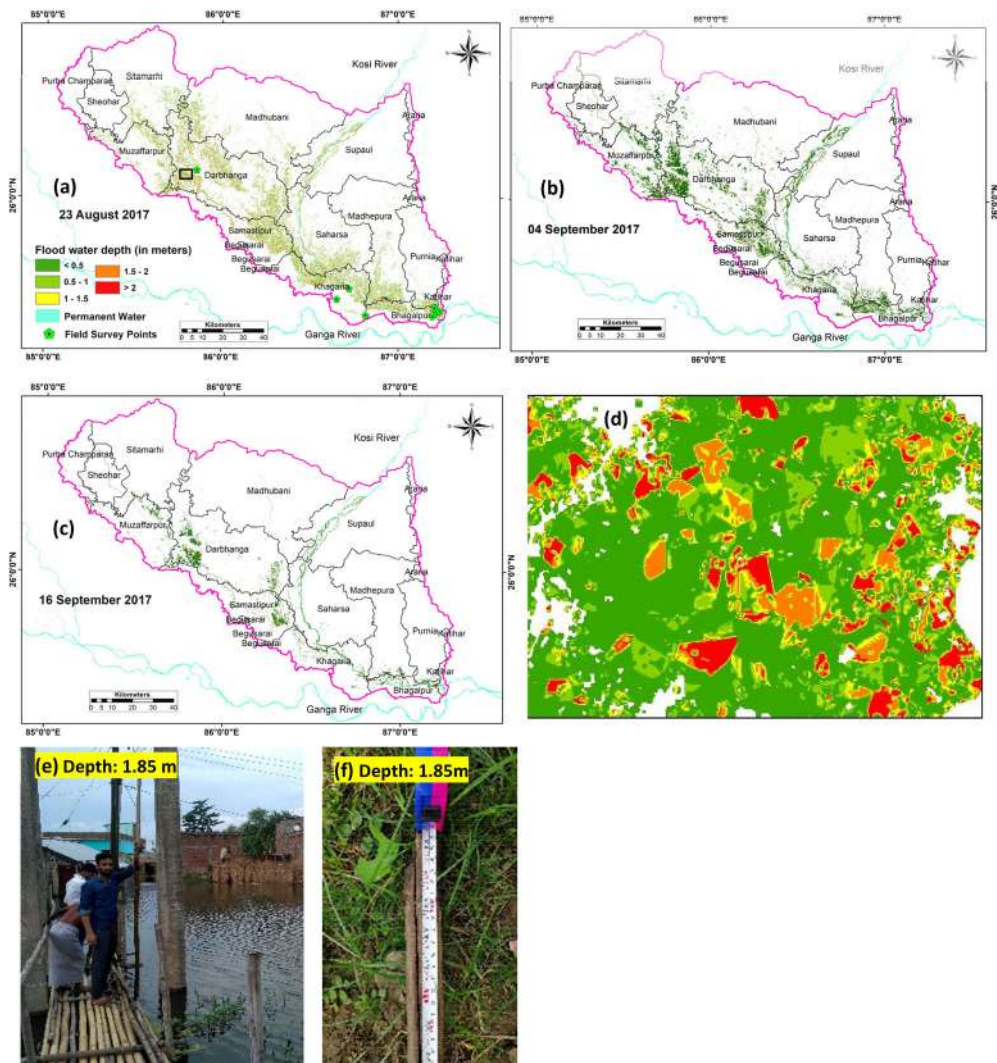


Figure 4. Floodwater depth maps (0.1 to 2 m) over the KRB during 23rd August, 04th September, and 16th September 2017. In (d), floodwater depth was highlighted in some parts of Darbhanga (rectangular box is shown in Figure 4a). Floodwater depth validation points were added and the corresponding field photographs were shown in parts of Khagaria (e-f).

district, about 189.8 km² out of 894 km² area was estimated as submerged with less than 0.5 m floodwater depth by 23rd August 2017. Subsequently, the submerged area under floodwater depth of < 0.5 m increased to 427.63 km² by 4th September and reduced to 169.45 km² by 16th September. In the Khagaria district, about 98 km² out of 369 km² area was estimated as submerged with less than 0.5 m floodwater depth by 23rd August 2017. Subsequently, the submerged area under floodwater depth of < 0.5 m increased to 108 km² by 4th September and reduced to about 53 km² by 16th September.

In the Saharsa district, about 94 km² out of 380 km² area was estimated as submerged with less than 0.5 m floodwater depth by 23rd August 2017. Subsequently, the submerged area under floodwater depth of < 0.5 m increased to 97 km² by 4th September and reduced to 55 km² by 16th September, respectively. In the Samastipur district, about 88 km² out of 351 km² area was estimated as submerged with less than 0.5 m floodwater

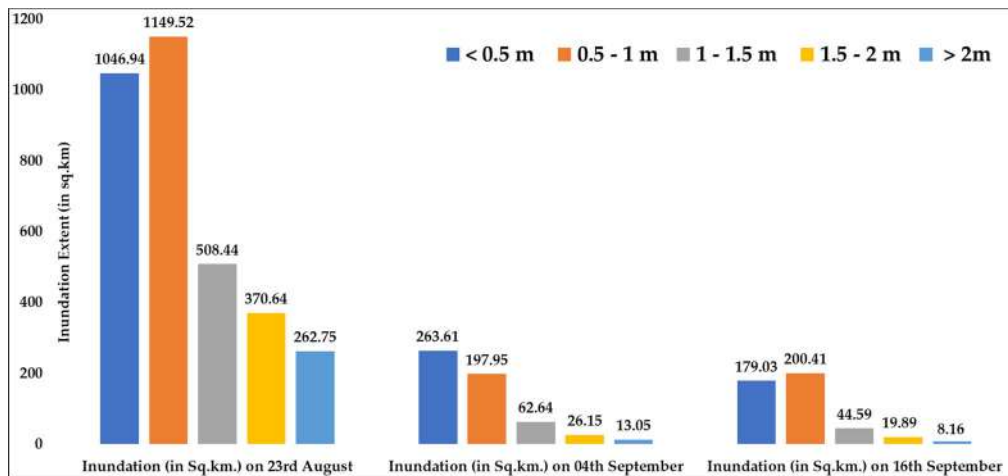


Figure 5. Date wise flood extent (in km^2) pattern with respect to the floodwater depth.

depth by 23rd August 2017. Subsequently, the area under floodwater depth of < 0.5 m increased to 178 km^2 by 4th September and reduced to 77 km^2 by 16th September, respectively. The floodwater depth on four districts (i.e., Darbhanga, Khagaria, Saharsa, and Muzaffarpur) showed that there is a rise in the area submerged with less the 0.5 m water depth from peak flood (23rd August) to recession flood (4th September) and this is because of flood recession wherein it was also observed that area submerged with more than 0.5 water depth becomes very smaller.

By 23rd August, about 5.4% submerged area of KRB showed floodwater depth less than 0.5 m. By 4th Sept and 16th September, about 1.35% and 1% submerged area of KRB's showed floodwater depth with less than 0.5 m, respectively. The floodwater depth near the Kosi river and or over the river channel was estimated in the range of 8 to 30 m, however, those pixels are excluded from the map.

The multi date-wise inundation extent (in km^2) for floodwater depth having five intervals has been shown in Figure 5. These results showed that across all three depth maps of the KRB region during August and September 2017, the floodwater depth of 0.1 to 1 m is prevalent. By 23rd August, about 1047 km^2 and 1150 km^2 inundated area was having water depth up to 0.5 and 1 m, respectively. The inundated area in the interval of floodwater depth up to 1.5 m, 2 m, and > 2 m, was 508, 370, and 263 km^2 , respectively. Accordingly, by 4th and 16th September, the area statistics in km^2 are shown in Figure 5.

4.3. Floodwater duration maps during August and September 2017 in KRB

The floodwater duration maps (Figure 6) are presented at 12-days intervals owing to the sensor's revisit period. These results showed that extensive floodwater existed by 23rd August 2017 and the $3,348 \text{ km}^2$ area was already inundated by floodwater. As the previous data was not available, the duration is simply called zero days. The duration maps for four adversely affected districts, such as Darbhanga, Khagaria, Saharsa, and Muzaffarpur have been shown in Figure 7S. The inundated area by 23rd August (i.e., 0 days duration) was estimated as $3,348 \text{ km}^2$ (or 17%) of KRB. These results indicated that in the 497.15 km^2 (2.52%) area, the floodwater stayed up to 12 days, whereas the 312.96 km^2 (1.59%) area had a floodwater duration of 24 days. As the duration calculated based on only three dates at 12 days interval and the duration varied from 12 to 24 days. However,

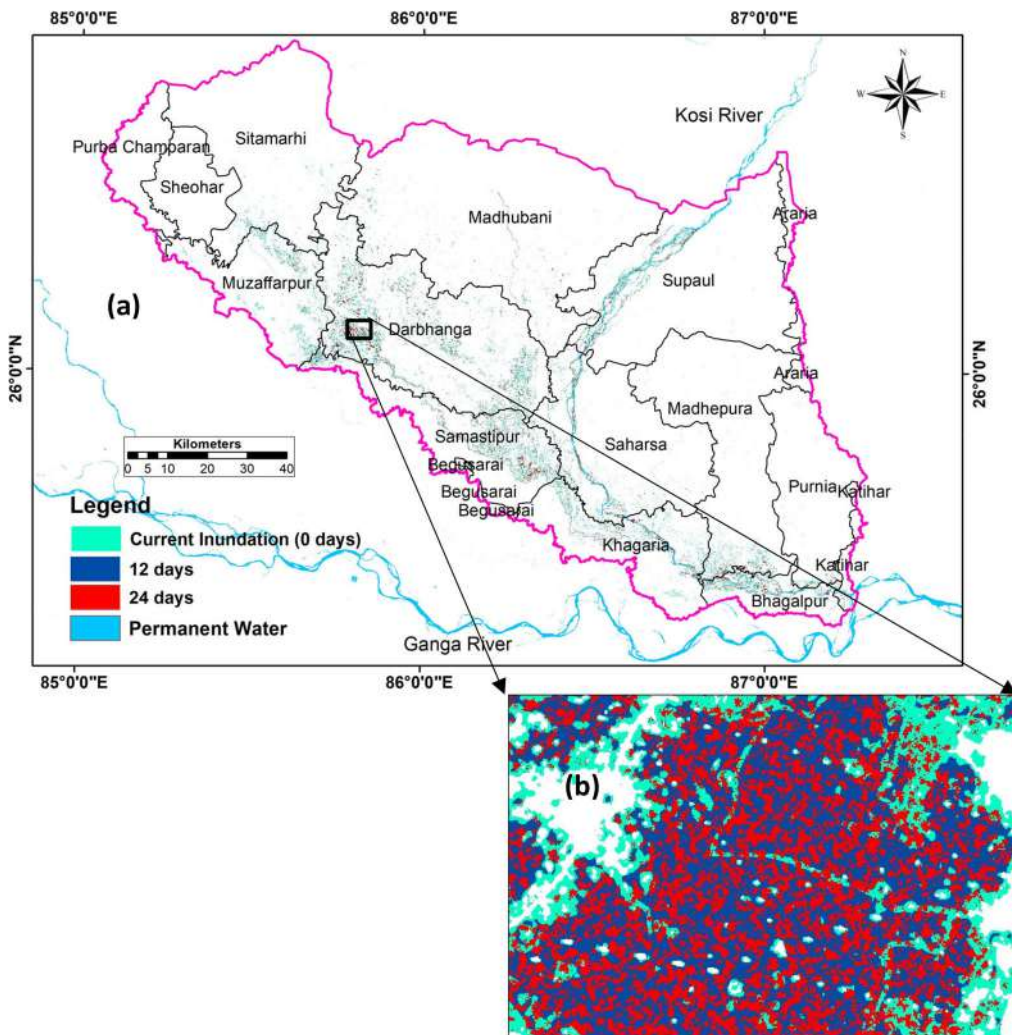


Figure 6. Floodwater duration map over KRB during August and September 2017. The zoomed image is shown in (b) in some parts of Darbhanga (rectangular box of Figure 6a).

these estimates will cause underestimation of floodwater duration and it can be presumed that the inclusion of the 11th August 2017 SAR image may lead to a floodwater duration of 24 to 36 days. As compared to our estimates on floodwater duration, a recent study demonstrated floodwater duration between 30 and 40 days over the KRB which has used a similar binary method but it deployed multi-sensors and multi-temporal satellite data (Rättic et al. 2020).

4.4. Validating model-based floodwater depth with field/survey data

According to field measurements, the minimum and maximum flood depth of the study area were 0.5 and 1.85 m, respectively. The model-based floodwater depth has been compared against field-based measured depth (Figure 7). The field data showed underestimation against modeled depth on 23 August because the field depth was collected after the receding flood over a month. However, the model-based floodwater depth estimated on

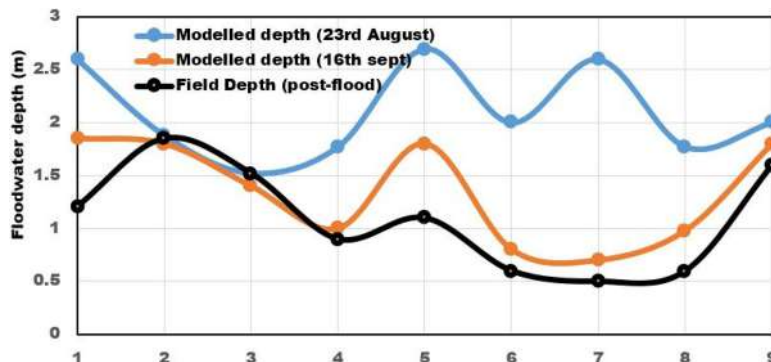


Figure 7. Comparison of floodwater depth as derived from the FwDET model (23 August and 16 September 2017) with field-based measured depth (data were taken on 17 – 21 September 2017). The nine field-based points shown here are given in Table 2 (Serial No. 1 to 9).

16 September was much closer to the field-based measured depth over the nine GPS points (Table 2). This suggestive model-based floodwater depth is quite similar to the field conditions during the flood with a mean difference of 0.25 m between modeled depth 16 September and field-based depth. In addition to the above, the field-based measured depth for GPS point 10 and 11 comprising gauge stations of CWC was also compared (Table 2). At the CWC gauge station (point 10), the model depth was 31.2 m on 16 September (above MSL) whereas field-based observation was 30.8 m. At point 11 CWC gauge station, the model depth was 25.1 m whereas field-based observation was 24.06 m.

4.5. Water level at various gauge stations of CWC

An overview of CWC water level sites in adversely affected districts has been shown in Table 4 and the corresponding units are above mean sea level (AMSL). These data indicate that the water level crossed the danger level (DL) by 23rd August 2017. Hayaghat gauge stations in Darbhanga district and Benibad gauge stations in Muzaffarpur district showed that the water levels crossed the DL (45.72 and 48.68 m), but remained within the HFL limit as 48.96 and 50.01 m, respectively. At Khagaria gauge stations in the Khagaria district, it was observed that the water level crossed the DL after the 23rd of August onwards due to excess rainfall in upstream regions. At Rosera gauge stations in Samastipur district, the water level crossed the DL after the 23rd Aug onwards but remained within the HFL limit of 46.35 m. These water levels data at different gauge stations revealed that the peak flood was attained by 23rd August 2017 and then receding of floodwater ensued after the 4th September 2017 and are consistent with the peak flood pattern discussed in Figure 3.

5. Discussion

The Kosi river basin (KRB) is well known for the utmost flood-affected basin of South Asia (Sinha et al. 2008). There were no such comprehensive studies available over the KRB, where the flood inundation and floodwater depth mapping have been performed. It is also not reported the variation of floodwater depth and its duration, which are important flooding characteristics for any regions to make flood risk assessment associated with infrastructure loss, agriculture loss, economy, among others. In this case study, the multi-temporal C-band (Sentinel-1A) SAR data (VH polarization) were employed to derive

Table 4. Station-wise water levels (m AMSL) during August and September 2017.

Stations/Districts	HFL	DL	18 Aug.	23 Aug.	4 Sept.	16 Sept.
Hayaghat/Darbhanga	48.96	45.72	45.14	46.07	45.60	42.12
Benibad/Muzaffarpur	50.01	48.68	49.48	49.25	49.18	48.61
Khagaria/Khagaria	39.22	36.58	36.42	36.91	36.51	34.00
Rosera/Samastipur	46.35	42.63	42.43	44.73	43.92	39.45

Note: The water levels were compared with Danger Level (DL) and Highest Flood Level (HFL). The bold indicates the water level above the DL (Data source: CWC).

floodwater distribution in inundated zones during August and September 2017 flood events and to assess the adverse effect of flood across the KRB. The FwDET model was employed to derive floodwater depth maps and subsequently, floodwater duration maps. As per the composite flood inundation map (Figure 8a), an inundated area of 4,108.16 km² (20.88%) was found flooded owing to monsoon rainfall and river overflow. The weekly variability of rainfall based on TMPA as well as IMD has been shown in Figure 2S that revealed heavy rainfall (> 100 mm) in the higher elevated upstream areas in the KRB during 1-7 August 2017. The intensity of rainfall again raised in the downstream areas during 8-14 August 2017. The variability of rainfall was reduced during 15-21 August 2017, but it again increased over upstream areas of KRB during 22-28 August 2017. The flood inundation pattern revealed that rainfall variability is the main factor of floods over the KRB in North Bihar. It was also observed that an increase in rainfall has a corresponding effect on increased water levels at various gauge stations of CWC as shown in Table 4. The spatial pattern of the inundation map as derived from SAR data was also comparable to BSDMA and FMISC which were prepared by the Bihar State government.

The estimated inundated area based on SAR data is comparable to previous studies that have estimated 3,968 km² area was inundated based on optical MODIS NRT data (Tripathi et al. 2019). The latest study reported that about 4,600 km² area was inundated due to flood over North Bihar using the multi-temporal satellite data during July-September 2017 (Rättich et al. 2020). The estimated inundated area is lower by 492 km² than the Rättich et al. (2020) which could be explained by the differences in composite inundation maps between the two studies. In other words, our composite map was prepared based on August-September whilst Rättich et al. (2020) prepared composite map data based on July-September.

The flood inundation impact on LULC classes was assessed using the composite flood inundation map (Table 5 and Figure 8a). The highest impact was found in the agricultural area (13.78%) followed by fallow land (5.15%) whilst land use classes such as Built-up, Forest, Water bodies, and barren land and sandy areas were inundated by less than 0.5% each. The barren land and sandy areas are kept under the other class. It was also evident that about 79 km² area was affected by floods over the urban area in North Bihar that account for 26% of the urban area.

The key findings indicate that by 23rd August, around 2,206.17 km² affected area out of a total inundated area of 3,348 km² (or 11.21% of KRB) had a water depth of < 1 m. Whereas, about 879.08 km² inundated area of KRB (or 4.47%) had a water depth of 1 to 2 m. The remaining 1.34% affected area had a water depth of 2 m. As per the composite floodwater depth map (Figure 8b), about 2,750 km² (or 14% of KRB) flooded domain area had a water depth of 0.1 to 1 m over the KRB. The calculated floodwater depths are quite comparable to the ground-based observations and water level gauge-based data. The calculated depth is based on 12.5 m ALOS DEM resolution and thereby, these calculations can be improved if high-resolution DEM is included in future studies. But, due to the lack of a high-resolution DEM dataset in India, we infer that these results are subjected to

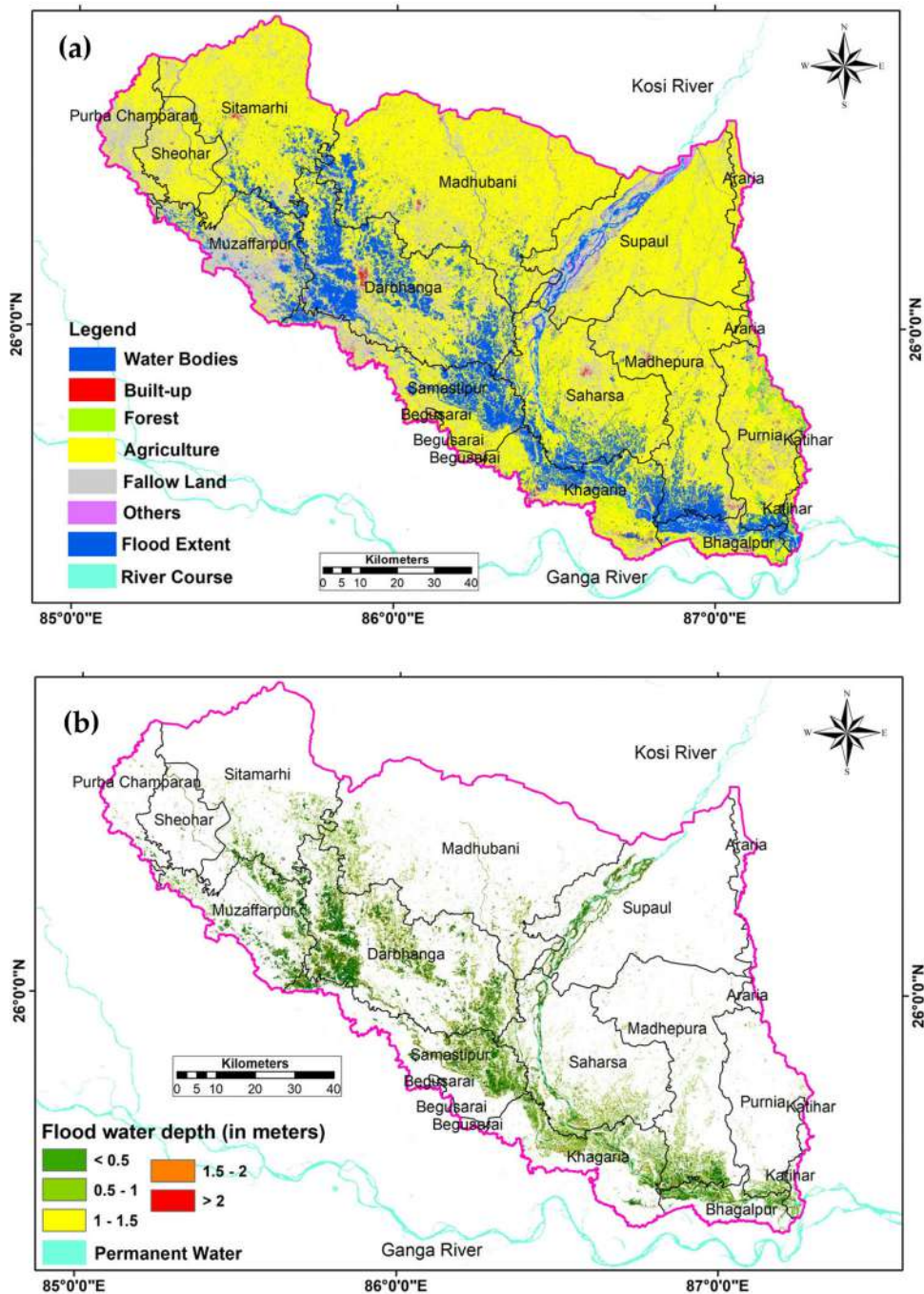


Figure 8. Composite flood inundation map overlaid on LULC map (a) and composite floodwater depth map (b) during August and September 2017.

improvement as there will be DEM errors for its vertical accuracy. In Asia, the FwDET model was employed in 2018 flooding Sri Lanka and in 2018 Philippine flooding (Cohen et al. 2019), which utilized 30 m DEM data and suggested that the method performed well for these flooding events. The FwDET model simulated floodwater depth accurately

Table 5. Statistics of the various LULC classes and flood inundation based on composite flood inundation map Figure (8a).

LULC classes	Area (km ²)	Inundated area (km ²)	Inundated area (%)
Built-up	302.67	79.18	0.40
Agriculture	13677.57	2711.62	13.78
Fallow land	4986.37	1013.72	5.15
Forest	228.60	113.78	0.58
Others	266.89	104.25	0.53
Water bodies	211.90	85.61	0.44
Total	19,674	4,108.16	20.48

Note: The inundated area (%) was with respect to a total area of 19,674 km².

against the hydrological models for a large flood event in 2016 in Brazos River, Texas, USA using a 10 m DEM (Cohen et al. 2018). However, an average difference of 0.3 to 0.5 m water depths was reported by the FwDET model against the 2D hydraulic model using a 10 m DEM (Cohen et al. 2018; Cohen et al. 2019). The differences of 0.5 m flood-water depth were also reported by RAPIDE with respect to the 2D hydraulic model (Scorzini et al. 2018). Nevertheless, the lack of high-resolution DEM data can pose a challenge to obtain accurate water depths using FwDET or RAPIDE model, and furthermore, the uncertainty may increase when applied in fragmented flood inundation domains.

The floodwater duration information is very important for disaster risk assessment and provides first-hand information to decision-makers. In this context, our key findings reveal that the floodwater stays up to 24 days over the 53.96 km² inundated area (0.27% of KRB). Most of the underlying areas with 24 days flood duration are over urban and agriculture and consequently the longer inundation can damage standing crops. In the context of floodwater duration, our results are quite similar to Rättich et al. (2020) that demonstrated the floodwater duration varied from 30-40 days (with a mean of 26 days) using multi-temporal and multi-sensor satellite data. The current study is useful for disaster mitigation and flood risk management in particular, for emergency, recovery, and preparedness. During the emergency, near real-time flood water extent, depth, and duration are the most essential information for policymakers to effectively mobilize relief resources to priority areas. During the recovery and preparedness, especially the floodwater duration map can be important inputs for insurance companies for managing the damage and rolling out claims and it can also be useful for land use and hydrological planning.

The limitation of the present studies is the use of coarse resolution (12.5 m) of DEM data for this hydrological application and the measured floodwater depth was taken after 24 days of peak flood and after 1 day from the receding phase of floodwater. It remained a challenge to collect data during the flood that needs actions from the state governments and Non-Governmental Organizations (NGOs). Due to a very large area of the KRB within North Bihar, it took more than 220 hrs to compute floodwater depth for a single date using the FwDET approach.

6. Conclusions

The satellite-based monitoring flood extent overcomes the limitations of hydrological model-based approaches. Various attempts have been made in the near past to map flood inundation over KRB from satellite images using optical sensors. This study employed multi-temporal Sentinel-1A SAR images to map floodwater inundation for the 2017 August floods in KRB. The results indicate that about 20.4% of the inundation area was due to the flooding and most of the area (~ 14%) had a floodwater depth up to 1 m water level. The floodwater depth has been computed using the FwDET 0 D model using 12.5 m

DEM. It can be acknowledged that the derived floodwater depth can be improved by simulating depth with high-resolution DEM data, albeit such data are sparse over India. Nevertheless, the model can be an effective tool to provide information on areas vulnerable to flooding and to identify flood hazard zonation layers for prioritizing flood mitigation measures. The adopted methodology is very useful in data-scarce environments, where the hydrological models cannot be employed owing to the high demand for hydro-meteorological inputs and model calibrations which are not readily available.

Acknowledgment

The authors gratefully acknowledge the support provided by Space Application Centre (SAC), Ahmedabad, Indian Space Research Organization (ISRO) for providing research grant under the NISAR Flood (Project code HYD-03). The authors wish to acknowledge the Alaska Satellite Facility for providing Sentinel-1A SAR satellite data free of cost.

Disclosure statement

No potential conflict of interest was reported by the author(s).

Funding information

This research was funded by SAC-ISRO under NISAR flood project (HYD 03).

ORCID

Bikash Ranjan Parida  <http://orcid.org/0000-0001-7444-573X>
 Gaurav Tripathi  <http://orcid.org/0000-0002-1114-7660>
 Arvind Chandra Pandey  <http://orcid.org/0000-0003-2796-0477>
 Amit Kumar  <http://orcid.org/0000-0002-4582-5677>

References

- Afshari S, Tavakoly AA, Rajib MA, Zheng X, Follum ML, Omranian E, Fekete BM. 2018. Comparison of new generation low-complexity flood inundation mapping tools with a hydrodynamic model. *J Hydrol.* 556:539–556.
- Agnihotri AK, Ohri A, Gaur S, Shivam Das N, Mishra S. 2019. Flood inundation mapping and monitoring using SAR data and its impact on Ramganga River in Ganga basin. *Environ Monit Assess.* 191(12): 760. <http://link.springer.com/10.1007/s10661-019-7903-4>.
- Ajadi O, Meyer F, Webley P. 2016. Change detection in synthetic aperture radar images using a multi-scale-driven approach. *Remote Sensing.* 8(6):482.
- Alfieri L, Cohen S, Galantowicz J, Schumann GJ-P, Trigg MA, Zsoter E, Prudhomme C, Kruczakiewicz A, Coughlan de Perez E, Flamig Z, et al. 2018. A global network for operational flood risk reduction. *Environ Sci Policy.* 84:149–158.
- Alsdorf DE, Rodríguez E, Lettenmaier DP. 2007. Measuring surface water from space. *Rev Geophys.* 45(2):1–24. <http://doi.wiley.com/10.1029/2006RG000197>.
- Aristizabal F, Judge J, Monsivais-Huertero A. 2020. High-resolution inundation mapping for heterogeneous land covers with synthetic aperture radar and terrain data. *Remote Sensing.* 12(6):900. <https://www.mdpi.com/2072-4292/12/6/900>.
- Bates PD, Wilson MD, Horritt MS, Mason DC, Holden N, Currie A. 2006. Reach scale floodplain inundation dynamics observed using airborne synthetic aperture radar imagery: Data analysis and modelling. *J Hydrol.* 328(1-2):306–318.
- Beven K, Gilman K, Newson M. 1979. Flow and flow routing in upland channel networks/L'écoulement et le calcul du cheminement de l'écoulement dans les réseaux des canaux montagneux. *Hydrol Sci Bull.* 24(3):303–325.

- Bovenga F, Belmonte A, Refice A, Pasquariello G, Nutricato R, Nitti D, Chiaradia M. 2018. Performance analysis of satellite missions for multi-temporal SAR interferometry. *Sensors*. 18(5):1359. <http://www.mdpi.com/1424-8220/18/5/1359>.

Brivio PA, Colombo R, Maggi M, Tomasoni R. 2002. Integration of remote sensing data and GIS for accurate mapping of flooded areas. *Int J Remote Sens*. 23(3):429–441.

Brunner GW. 1995. HEC-RAS River Analysis System. Hydraulic Reference Manual. Version 1.0.; Hydrologic Engineering Center: Davis, CA, USA.

Cao H, Zhang H, Wang C, Zhang B. 2019. Operational flood detection using Sentinel-1 SAR data over large areas. *Water*. 11(4):786. <https://www.mdpi.com/2073-4441/11/4/786>.

Chen H, Zamorano MF, Ivanoff D. 2010. Effect of flooding depth on growth, biomass, photosynthesis, and chlorophyll fluorescence of *typha domingensis*. *Wetlands*. 30(5):957–965.

Clement MA, Kilsby CG, Moore P. 2018. Multi-temporal synthetic aperture radar flood mapping using change detection: Multi-temporal SAR flood mapping using change detection. *J Flood Risk Management*. 11(2):152–168. <http://doi.wiley.com/10.1111/jfr3.12303>.

Cohen S, Brakenridge GR, Kettner A, Bates B, Nelson J, McDonald R, Huang Y-F, Munasinghe D, Zhang J. 2018. Estimating floodwater depths from flood inundation maps and topography. *J Am Water Resour Assoc*. 54(4):847–858.

Cohen S, Raney A, Munasinghe D, Loftis JD, Molthan A, Bell J, Rogers L, Galantowicz J, Brakenridge GR, Kettner AJ, et al. 2019. The Floodwater Depth Estimation Tool (FwDET v2.0) for improved remote sensing analysis of coastal flooding. *Nat Hazards Earth Syst Sci*. 19(9):2053–2065.

Conde FC, Muñoz MDM. 2019. Flood monitoring based on the study of Sentinel-1 SAR images: The Ebro river case study. *Water*. 11(12):2454. <https://www.mdpi.com/2073-4441/11/12/2454>.

Di Baldassarre G, Claps P. 2011. A hydraulic study on the applicability of flood rating curves. *Hydrology Research*. 42(1):10–19.

Dumitru CO, Cui S, Faur D, Datcu M. 2015. Data analytics for rapid mapping: case study of a flooding event in Germany and the Tsunami in Japan using very high resolution SAR images. *IEEE J Sel Top Appl Earth Observations Remote Sensing*. 8(1):114–129. <http://ieeexplore.ieee.org/document/6819782>.

Ezzine A, Saidi S, Hermassi T, Kammessi I, Darragi F, Rajhi H. 2020. Flood mapping using hydraulic modeling and Sentinel-1 image: Case study of Medjerda Basin, northern Tunisia. *The Egyptian Journal of Remote Sensing and Space Science*. S1110982318303752. 23(3):303–310. <https://linkinghub.elsevier.com/retrieve/pii/S1110982318303752>.

García-Pintado J, Neal JC, Mason DC, Dance SL, Bates PD. 2013. Scheduling satellite-based SAR acquisition for sequential assimilation of water level observations into flood modelling. *J Hydrol*. 495:252–266.

Garousi-Nejad I, Tarboton DG, Aboutalebi M, Torres-Rua AF. 2019. Terrain analysis enhancements to the height above nearest drainage flood inundation mapping method. *Water Resour Res*. 55(10):7983–8009.

Getahun YS, Gebre SL. 2015. Flood hazard assessment and mapping of flood inundation area of the Awash River Basin in Ethiopia using GIS and HEC-GEORAS/HEC-RAS Model. *J Civil Env Eng*. 5(4):1–12.

Hassan MM, Ash K, Abedin J, Paul BK, Southworth J. 2020. A quantitative framework for analyzing spatial dynamics of flood events: a case study of super cyclone Amphan. *Remote Sensing*. 12(20):3454. <https://www.mdpi.com/2072-4292/12/20/3454>.

Johnson JM, Munasinghe D, Eyelade D, Cohen S. 2019. An integrated evaluation of the National Water Model (NWM)–Height Above Nearest Drainage (HAND) flood mapping methodology. *Nat Hazards Earth Syst Sci*. 19(11):2405–2420.

Kent RJ, Johnson DE. 2001. Influence of flood depth and duration on growth of lowland rice weeds, Cote d'Ivoire. *Crop Prot*. 20(8):691–694.

Klemas V. 2015. Remote sensing of floods and flood-prone areas: an overview. *J Coast Res*. 314: 1005–1013. <http://www.bioone.org/doi/10.2112/COASTRES-D-14-00160.1>.

Kordelas G, Manakos I, Aragonés D, Díaz-Delgado R, Bustamante J. 2018. Fast and automatic data-driven thresholding for inundation mapping with Sentinel-2 Data. *Remote Sensing*. 10(6):910. <http://www.mdpi.com/2072-4292/10/6/910>.

Kumar R, Jain V, Prasad Babu G, Sinha R. 2014. Connectivity structure of the Kosi megalfan and role of rail-road transport network. *Geomorphology*. 227:73–86.

Lal P, Prakash A, Kumar A. 2020. Google Earth Engine for concurrent flood monitoring in the lower basin of Indo-Gangetic-Brahmaputra plains. *Nat Hazards*. 104(2):1947–1952. <http://link.springer.com/10.1007/s11069-020-04233-z>.

- Laur P, Bally P, Meadows P, Sanchez J, Schaettler B, Lopinto E, Esteban D. 2003. Derivation of the Backscattering coefficient in ESA ERS SAR PRI Products. https://earth.esa.int/documents/700255/1509236/ers_sar_calibration_issue2_5e.pdf. European Space Agency.
- Li J, Wang S. 2015. An automatic method for mapping inland surface waterbodies with Radarsat-2 imagery. *Int J Remote Sens.* 36(5):1367–1384. <https://www.tandfonline.com/doi/full/10.1080/01431161.2015.1009653>.
- Macchione F, Costabile P, Costanzo C, De Santis R. 2019. Moving to 3-D flood hazard maps for enhancing risk communication. *Environmental Modelling & Software*. 111:510–522.
- Manfreda S, Samela C. 2019. A digital elevation model based method for a rapid estimation of flood inundation depth. *J Flood Risk Management*. 12(S1):1–10. e12541):<https://onlinelibrary.wiley.com/doi/abs/10.1111/jfr3.12541>.
- Manjusree P, Prasanna Kumar L, Bhatt CM, Rao GS, Bhanumurthy V. 2012. Optimization of threshold ranges for rapid flood inundation mapping by evaluating backscatter profiles of high incidence angle SAR images. *Int J Disaster Risk Sci.* 3(2):113–122.
- Martinis S, Rieke C. 2015. Backscatter analysis using multi-temporal and multi-frequency SAR data in the context of flood mapping at River Saale, Germany. *Remote Sensing*. 7(6):7732–7752. <http://www.mdpi.com/2072-4292/7/6/7732>.
- Matgen P, Hostache R, Schumann G, Pfister L, Hoffmann L, Savenije HHG. 2011. Towards an automated SAR-based flood monitoring system: Lessons learned from two case studies. *Physics and Chemistry of the Earth, Parts A/B/C*. 36(7–8):241–252. <https://linkinghub.elsevier.com/retrieve/pii/S1474706510002160>.
- Matgen P, Schumann G, Pappenberger F, Pfister L. 2007. Sequential assimilation of remotely sensed water stages in flood inundation models. In: *Remote Sensing for Environmental Monitoring and Change Detection [Internet]*. Vol. 316. Perugia, Italy: IAHS Publication. <https://iahs.info/uploads/dms/14108.15-78-88-26-Matgen.pdf>.
- Moore ID, Grayson RB, Ladson AR. 1991. Digital terrain modelling: A review of hydrological, geomorphological, and biological applications. *Hydrol Process*. 5(1):3–30.
- Najibi N, Devineni N, Lu M. 2017. Hydroclimate drivers and atmospheric teleconnections of long duration floods: An application to large reservoirs in the Missouri River Basin. *Adv Water Resour.* 100: 153–167.
- NIDM 2018. Annual Report of National Institute of Disaster Management (NIDM) 2018-19, Ministry of Home Affairs, Government of India. New Delhi. https://nidm.gov.in/PDF/pubs/areport_18.pdf.
- Nobre AD, Cuartas LA, Momo MR, Severo DL, Pinheiro A, Nobre CA. 2016. HAND contour: a new proxy predictor of inundation extent: Mapping Flood Hazard Potential Using Topography. *Hydrol Process*. 30(2):320–333.
- Oberstädler R, Hönsch H, Huth D. 1997. Assessment of the mapping capabilities of ERS-1 SAR data for flood mapping: a case study in Germany. *Hydrol Process*. 11(10):1415–1425.
- Pandey AC, Singh SK, Nathawat MS. 2010. Waterlogging and flood hazards vulnerability and risk assessment in Indo Gangetic plain. *Nat Hazards*. 55(2):273–289.
- Parida BR, Behera S, Bakimchandra O, Pandey AC, Singh N. 2017. Evaluation of satellite-derived rainfall estimates for an extreme rainfall event over Uttarakhand, Western Himalayas. *Hydrology*. 4(2):22.
- Parida BR, Behera SN, Oinam B, Patel NR, Sahoo RN. 2018. Investigating the effects of episodic Super-cyclone 1999 and Phailin 2013 on hydro-meteorological parameters and agriculture: An application of remote sensing. *Remote Sens Appl: Soc Environ*. 10:128–137.
- Parker DJ. 2017. Flood Warning Systems and Their Performance. In: *Oxford Research Encyclopedia of Natural Hazard Science*. Oxford: Oxford University Press; [accessed 2020 Feb 17].
- Patel NR, Mukund A, Parida BR. 2019. Satellite-derived vegetation temperature condition index to infer root zone soil moisture in semi-arid province of Rajasthan, India. *Geocarto International*. 34:1–17.
- Rana VK, Suryanarayana TMV. 2019. Evaluation of SAR speckle filter technique for inundation mapping. *Remote Sens Appl: Soc Environ*. 16:100271. <https://linkinghub.elsevier.com/retrieve/pii/S2352938519302186>.
- Rättich M, Martinis S, Wieland M. 2020. Automatic flood duration estimation based on multi-sensor satellite data. *Remote Sensing*. 12(4):643. <https://www.mdpi.com/2072-4292/12/4/643>.
- Refsgaard JC, Havnø K, Ammentorp HC, Verwey A. 1988. Application of hydrological models for flood forecasting and flood control in India and Bangladesh. *Adv Water Resour.* 11(2):101–105.
- Rogers L, Borges D, Murray J, Molthan A, Bell J, Allen T, Bekaert D, Loftis JD, Wang H, Cohen S, et al. 2018. NASA's Mid-Atlantic Communities and Areas at Intensive Risk Demonstration: Translating Compounding Hazards to Societal Risk. In: *OCEANS 2018 MTS/IEEE Charleston*. Charleston, SC: IEEE; p. 1–5. <https://ieeexplore.ieee.org/document/8604797>.
- Sahana M, Patel PP. 2019. A comparison of frequency ratio and fuzzy logic models for flood susceptibility assessment of the lower Kosi River Basin in India. *Environ Earth Sci.* 78(10):289.

- Schlaffer S, Matgen P, Hollaus M, Wagner W. **2015**. Flood detection from multi-temporal SAR data using harmonic analysis and change detection. *Int J Appl Earth Obs Geoinf.* 38:15–24.
- Schumann G, Bates PD, Horritt MS, Matgen P, Pappenberger F. **2009**. Progress in integration of remote sensing-derived flood extent and stage data and hydraulic models. *Rev Geophys.* 47(4):1–20. <http://doi.wiley.com/10.1029/2008RG000274>.
- Schumann G, Matgen P, Hoffmann L, Hostache R, Pappenberger F, Pfister L. **2007**. Deriving distributed roughness values from satellite radar data for flood inundation modelling. *J Hydrol.* 344(1-2):96–111.
- Scorzini A, Radice A, Molinari D. **2018**. A new tool to estimate inundation depths by spatial interpolation (RAPIDE): design, application and impact on quantitative assessment of flood damages. *Water.* 10(12):1805. <http://www.mdpi.com/2073-4441/10/12/1805>.
- Sinha R, Baplu GV, Singh LK, Rath B. **2008**. Flood risk analysis in the Kosi river basin, north Bihar using multi-parametric approach of Analytical Hierarchy Process (AHP). *J Indian Soc Remote Sens.* 36(4):335–349.
- Small D. **2011**. Flattening gamma: radiometric terrain correction for SAR imagery. *IEEE Trans Geosci Remote Sensing.* 49(8):3081–3093.
- Smith LC. **1997**. Satellite remote sensing of river inundation area, stage, and discharge: a review. *Hydrol Process.* 11(10):1427–1439.
- Teng J, Jakeman AJ, Vaze J, Croke BFW, Dutta D, Kim S. **2017**. Flood inundation modelling: A review of methods, recent advances and uncertainty analysis. *Environmental Modelling & Software.* 90:201–216.
- Tesfaye K, Aggarwal P, Mequanint F, Shirasath P, Stirling C, Khatri-Chhetri A, Rahut D. **2017**. Climate variability and change in Bihar, India: challenges and opportunities for sustainable crop production. *Sustainability.* 9(11):1998. <http://www.mdpi.com/2071-1050/9/11/1998>.
- Tiwari V, Kumar V, Matin MA, Thapa A, Ellenburg WL, Gupta N, Thapa S. **2020**. Flood inundation mapping- Kerala 2018; Harnessing the power of SAR, automatic threshold detection method and Google Earth Engine. *PLoS One.* 15(8):e0237324. <https://dx.plos.org/10.1371/journal.pone.0237324>.
- Towfiqul Islam ARM, Talukdar S, Mahato S, Kundu S, Eibek KU, Pham QB, Kuriqi A, Linh NTT. **2021**. Flood susceptibility modelling using advanced ensemble machine learning models. *Geosci Front.* 12(3):101075.
- Townsend PA, Walsh SJ. **1998**. Modeling floodplain inundation using an integrated GIS with radar and optical remote sensing. *Geomorphology.* 21(3-4):295–312.
- Tripathi G, Pandey AC, Parida BR, Kumar A. **2020**. Flood inundation mapping and impact assessment using multi-temporal Optical and SAR satellite data: A case study of 2017 Flood in Darbhanga district, Bihar, India. *Water Resource Management.* 34: 1871–1892.
- Tripathi G, Parida BR, Pandey AC. **2019**. Spatio-Temporal Rainfall Variability and Flood Prognosis Analysis using Satellite Data over North Bihar during the August 2017 Flood. *Event. Hydrology.* 6(2):38.
- Tsyganskaya V, Martinis S, Marzahn P, Ludwig R. **2018**. SAR-based detection of flooded vegetation – a review of characteristics and approaches. *Int J Remote Sens.* 39(8):2255–2293.
- Twele A, Cao W, Plank S, Martinis S. **2016**. Sentinel-1-based flood mapping: a fully automated processing chain. *Int J Remote Sens.* 37(13):2990–3004.
- Vishnu CL, Sajinkumar KS, Oommen T, Coffman RA, Thrivikramji KP, Rani VR, Keerthy S. **2019**. Satellite-based assessment of the August 2018 flood in parts of Kerala. *India. Geomatics, Natural Hazards and Risk.* 10(1):758–767.
- Wan X, Yang Q, Jiang P, Zhong P. **2019**. A Hybrid model for real-time probabilistic flood forecasting using Elman neural network with heterogeneity of error distributions. *Water Resour Manage.* 33(11):4027–4050.
- Warwick NWM, Brock MA. **2003**. Plant reproduction in temporary wetlands: the effects of seasonal timing, depth, and duration of flooding. *Aquat Bot.* 77(2):153–167.
- Wolock DM, McCabe GJ. **1995**. Comparison of single and multiple flow direction algorithms for computing topographic parameters in TOPMODEL. *Water Resour Res.* 31(5):1315–1324.
- Zhang M, Chen F, Liang D, Tian B, Yang A. **2020**. Use of Sentinel-1 GRD SAR Images to Delineate Flood Extent in Pakistan. *Sustainability.* 12(14):5784. <https://www.mdpi.com/2071-1050/12/14/5784>.
- Zhang Q, Gu X, Singh VP, Shi P, Sun P. **2018**. More frequent flooding? Changes in flood frequency in the Pearl River basin, China, since 1951 and over the past 1000 years. *Hydrol Earth Syst Sci.* 22(5):2637–2653. <https://www.hydrol-earth-syst-sci.net/22/2637/2018/>.
- Zhou Q, Mikkelsen PS, Halsnaes K, Arnbjerg-Nielsen K. **2012**. Framework for economic pluvial flood risk assessment considering climate change effects and adaptation benefits. *J Hydrol.* 414-415:539–549.

Endorsement Certificate from the Mentor & Host Institute

This is to certify that:

- I. The applicant, Dr. Gaurav Tripathi, will assume full responsibility for implementing the project.
- II. The fellowship will start from the date on which the fellow joins University/Institute where he/she implements the fellowship. The mentor will send the joining report to the SERB. SERB will release the funds on receipt of the joining report.
- III. The applicant, if selected as SERB-N PDF, will be governed by the rules and regulations of the University/ Institute and will be under administrative control of the University/ Institute for the duration of the Fellowship.
- IV. The grant-in-aid by the Science & Engineering Research Board (SERB) will be used to meet the expenditure on the project and for the period for which the project has been sanctioned as indicated in the sanction letter/ order.
- V. No administrative or other liability will be attached to the Science & Engineering Research Board (SERB) at the end of the Fellowship.
- VI. The University/ Institute will provide basic infrastructure and other required facilities to the fellow for undertaking the research objectives.
- VII. The University/ Institute will take into its books all assets received under this sanction and its disposal would be at the discretion of Science & Engineering Research Board (SERB).
- VIII. University/ Institute assume to undertake the financial and other management responsibilities of the project.
- IX. The University/ Institute shall settle the financial accounts to the SERB as per the prescribed guidelines within three months from the date of termination of the Fellowship.

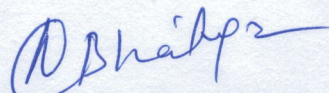
Dated: 09th Aug, 2023

Signature of the Mentor:



Name & Designation: Dr. Mahabendra Saharia, (Assistant Professor),
Civil Engg Dept, IIT Delhi.

Dated:



Signature of the Registrar of University/Head of Institute: नैरेश भटनागर

Prof. Naresh Bhatnagar

संकायाध्यक्ष (अनुसंधान एवं विकास)

Dean (Research & Development)

भारतीय प्रौद्योगिकी संस्थान दिल्ली

Indian Institute of Technology Delhi

हौज़ खास, नई दिल्ली-110016

Hauz Khas, New Delhi-110016

Seal of the Institution